PHOTOCHEMICAL MODIFICATION AND STABILIZATION OF ZWITTERIONIC POLYMER NETWORKS: MECHANISM, KINETICS, AND APPLICATIONS

by

QIAOHONG LIU

(Under the Direction of Jason Locklin)

ABSTRACT

This dissertation aims to both deepen and broaden our understanding of copolymer with pendent benzophenone (BP) in mechanism, kinetics and applications. Photo-activated of BP copolymers have been widely used in robust and efficiently functional polymer films combining with delicate nano- or micro- structures to achieve specialized interfacial properties of substrates. Herein, we focused on zwitterionic copolymer with pendent BP. A series of zwitterionic copolymers was synthesized with different hydrophilicity and polarity, and a linear decrease on crosslinking rate constant was observed with the increase of partition coefficient, logP. This linear correlation was confirmed valid for the zwitterionic copolymer with glass transition temperature lower than room temperature. However, for the zwitterionic polymer with high glass transition temperature, the chemical environment (polymer polarity) was not the dominated factor anymore, and the crosslinking rate decreased due to the restrict segment movement. The ring substituent also demonstrated great influence in BP kinetics for BP pendent copolymer. For the BP containing copolymer applications, a zwitterionic copolymer, 2-methacryloyloxyethyl phosphorylcholine-co-butyl methacrylate-co-benzophenone (BPMPC), was covalently crosslink to nitric oxide releasing substrates, and demonstrated excellent antifouling and antimicrobial properties. The protein

adsorption test results indicate a significant reduction (~84-93%) of protein adhesion on the test samples compared to the control samples. Test samples containing both NO donor and BPMPC show a 99.91 ± 0.06 % reduction of viable bacteria, *Staphylococcus aureus*, when compared to control samples. Another application, antifogging and self-cleaning polymer was immobilized on glass and plastic surface using a BP pendent copolymer that were prepared using free radical polymerization. The optical clarity of the substrates is not impacted by the polymer coating, and even slightly improved due to the lower refractive index of the polymer relative to glass. The coatings exhibit excellent chemical and mechanical resistance and maintain antifogging properties after abrasion testing in the presence of either chemical detergents or common household cleaners. In addition, the reason of contact angle increase for BPMPC under UV was explained. The mechanism of BPMPC demonstrate antifogging and antifouling properties with relatively poor hydrophilicity was also discussed.

INDEX WORDS: KINETICS, POLARITY, ZWITTERIONIC, ANTIFOULING, ANTIMICROBIAL, ANTIFOGGING, BENZOPHENONE, SURFACE FUNCTIONALITY, COVALENT BONDING.

PHOTOCHEMICAL MODIFICATION AND STABILIZATION OF ZWITTERIONIC POLYMER NETWORKS: MECHANISM, KINETICS, AND APPLICATIONS

by

QIAOHONG LIU

BS, University of Science and Technology of China, China, 2007

MS, University of Science and Technology of China, China, 2010

A Dissertation Submitted to the Graduate Faculty of The University of Georgia in Partial Fulfillment of the Requirements for the Degree

DOCTOR OF PHILOSOPHY

ATHENS, GEORGIA

2019

PHOTOCHEMICAL MODIFICATION AND STABILIZATION OF ZWITTERIONIC POLYMER NETWORKS: MECHANISM, KINETICS, AND APPLICATIONS

by

QIAOHONG LIU

Major Professor:	Jason Locklin
Committee:	Jin Xie
	Sergiy Minko

Electronic Version Approved:

Suzanne Barbour
Dean of the Graduate School
The University of Georgia
May 2019

DEDICATION

To my family. Thank you for your unconditional support and love. Specially for my husband, I could not finish this challenging and rewarding journal without your help and support, and I am forever grateful for all that you have done for me and all the love you have given me. You were there to help me become my best. For my mom, who always stand beside me, trust me on every decision, and proud of me for every accomplishment, no matter how little it is. I am so lucky to have such an amazing, hard-working, and loving mother.

ACKNOWLEDGEMENTS

I would want to thank my family for their support and caring throughout my PhD study. I really want to thank my dear husband, Zilong, who always give me valuable advice and unconditional support. I would not start and could not accomplish this without you. I also want to thank my parents, who encourage and comfort me when I feel frustrated and depressed, even from thousands of miles away. Thanks to my children, Yi and Lanlan. You guys are incredible and fantastical, and I will always feel grateful to have you. Also, thanks for making this journey even harder, which let me believe that I can overcome any difficulties and challenges in the future.

Secondly, I would like to thank my advisor, Dr. Jason Locklin. I have to say it is an incredible experience to working under your directing. Thanks for extremely patient and providing tons of help for the past five years. Your advice, mentorship, and guidance has shaped both my graduate school and professional career for better. Thank you for giving me confidence and recognition. I have learned so much from you, not just science. I hope that one day I will be as confident, energetic, dedicated, aspiring as you are. To my committee members, Dr. Minko and Dr. Xie, thank you for your time, advice, and knowledge in helping shape my projects to be the best I could produce.

In addition, I want to thank all my collaborators and lab mates. Priya Singha, who is an efficient and knowledgeable co-worker, has provided great help and made our cooperation successful. I want to thank Li for all the experiences we shared, from preparing seminars and prospectus to struggling in oral comprehensive and defense. It is so great to have a partner throughout the rough time in PhD study. I also want to thank Yutian for offering valuable advice

in synthesis, every time after my group meeting. Thank you Apisata for bringing me delicious meals, they are really good. And you might need to take my job on cutting the cake. My group members and friends, Jessica, Grant, Jess, Scott, DeMicheal, Tim, Caitlin, Shunli, Evan, and Madison, being in coworker and friends with you make working in lab great. Shunli have given me tons of ideas in job hunting. And Evan, who is so trustful, is always the person I ask for help whenever I face a problem. I could not thank enough. I really appreciate having all of you during my tough and incredible PhD journey.

TABLE OF CONTENTS

Page

ACKNOWLEDGEMENTS v

LIST OF TABLES x

LIST OF FIGURES xi

CHAPTER

1 Introduction and Literature Review 1

Functional Polymer Coatings 1

Methods of Immobilization 2

Benzophenone Photo-crosslinker 4

Objectives and Dissertation Outline 10

References 13

2 The Photo-crosslinking Kinetics Study of Benzophenone containing zwitterionic copolymer 21

Abstract 22

Introduction 23

Experiment Section 26

Results and Discussion 30

Conclusion 41

References 42

3 Covalent Grafting of Antifouling Phosphorylcholine-Based Copolymers with Antimicrobial Nitric Oxide Releasing Polymers to Enhance Infection-Resistant Properties of Medical Device Coatings....46
Abstract....47
Introduction....48
Materials and Methods....50
Results and Discussion....58
Conclusion....69
References....71
4 Transparent Grafted Zwitterionic Copolymer Coatings That Exhibit Both Antifogging and Self-cleaning Properties....78
Abstract....79
Introduction....80
Experiment Section....82
Results and Discussion....86
Conclusion....97
References....98
5 Self-association of Zwitterionic Polymer Coatings Bearing Benzophenone Crosslinker....104
Abstract....105
Introduction....106
Experiment Section....108
Results and Discussion....109

Conclusion 117

References 118

6 Conclusion and Future Outlook 122

Conclusions 122

Future Work 123

Final marks 124

APPENDICES

A NMR Spectra of Compounds 125

B DSC Spectra of Compounds 132

C UV-vis Spectra of Compounds 134

LIST OF TABLES

Page

Table 2.1: Synthetic results of BPMPC polymers 31

Table 2.2: The value of rate constant and logP of BPMPC polymer series.....34

Table 2.3: The synthetic results of MPC-Q polymers 37

Table 2.4: Rate constant (*k*) for MPC-Q polymers 38

Table 3.1: Comparison of nitric oxide release kinetics between control and coated samples 10% SNAP with only CarboSil topcoat.....64

Table 5.1: BPMPC and PMPBMA film thickness before and after UV irradiation.....113

Table 5.2: The CA of BPMPC coating under different temperature 115

LIST OF FIGURES

Page

Figure 1.1: PDRC polymer coating (A) under sunlight, (B) under thermo-camera. 2

Figure 1.2: *S*chematic illustration of different methods for immobilizing polymer chains on solid surface: physisorption, "grafting-to" and "grafting from" 3

Figure 1.3: Scheme of benzophenone (BP) crosslink.....5

Figure 1.4: Schematic illustration of poly (ethylene glycol) photographing-from polycarbonate urethane film 6

Figure 1.5: (A) Schematic detailing the fabrication of BP-photoinitiated films of PSt on (a) bare, (b) unexposed monolayer modified, and (c) UV exposed monolayer modified Au substrates. SEM images depicting PSt thin films after (B−D) thermal nanoimprint lithography and (E−G) wet etching. 6

Figure 1.6: Preparation of PEI multilayers using PAABp and PAH to create gradients of increasing Young's modulus. A7rS cells stained for actin (red) show increasing filament organization along the increasing gradient from (A) to (F) with the corresponding low magnification image in (G). 8

Figure 1.7: Jablonski diagram of BP excited states 9

Figure 1.8: Energy levels of p-aminobenzophenone isopropanol and in cyclohexane.....10

Figure 2.1: BPMPC photo-cross-linking kinetics study by UV-vis spectroscopy.....32

Figure 2.2: The relation of the rate constant with the percentage of BPMPC (blue line) and logP (red line) in BPMPC polymer 34

Figure 2.3: MPC-Q4~18 photo-cross-linking kinetics study by UV-vis spectroscopy 38

Figure 3.1: Nitric oxide chemiluminescence analyzer flowchart 55

Figure 3.2: UV-vis absorption spectrum of BPMPC drop-cast onto a quartz substrate as a function of photochemical irradiation time at 254 nm (6.5 mW cm^{-1} intensity).....60

Figure 3.3: ATR-FTIR spectra of BPMPC coating before (A) and after (B) UV exposure.....60

Figure 3.4: Contact angle measurement as a function of time for CarboSil coated with BPMPC and incubated in 37 ℃ in PBS under mild agitation.....61

Figure 3.5: (A) SNAP leaching measured using UV-vis over 2 weeks and (B) Nitric oxide release measured over 2 weeks (n = 3) using chemiluminescence 63

Figure 3.6: Thickness increase after incubation in (A) Fibrinogen solution and (B) in Lysozyme solution. 66

Figure 3.7: Fluorescence micrographs (magnification 10x) of uncoated films after (A) 90-minute incubation, (B) 1 day in BSA PBS solution before incubation, and (C) 7 days in BSA PBS solution before incubation in 2 mg/ml FITC-BSA solution. (D-F) are the coated film measured under the same experimental conditions.....67

Figure 3.8: Antimicrobial efficacy of NO-releasing BPMPC coated samples relative to controls (n=3) 69

Figure 4.1: Contact angle of pure glass, iBTS modified glass and BPMPC coated glass, and digital images of water droplet respectively (top).....87

Figure 4.2: (A) UV-vis spectra of bare glass and BPMPC polymer modified glass with different coating thickness, (B) optical photograph of BPMPC coated (left side) and bare (left side) safety glasses, (C) optical photograph of BPMPC coated (right side) and bare (left side) eyeglasses.....88

Figure 4.3: AFM topography images of (A) bare glass, (B) 60 nm, (C) 250 nm and (D) 300 nm BPMPC coatings 89

Figure 4.4: Photographs of glass slides over hot steaming water: (A) control uncoated, (B) iBTS modified and (C) BPMPC functionalized 90

Figure 4.5: Photographs of (A) polycarbonate safety glasses and (B) eyeglasses on hot boiling water (left sides with BPMPC coating).....91

Figure 4.6: Photographs of safety glasses exposed to ambient condition (temperature ~20℃, 50% relative humidity) right after being stored at -20 ℃ for 30 min 92

Figure 4.7: (A) Oil droplets on on iBTS modified glass (top), pure glass (middle), and BPMPC coated glass (bottom). (B) Corresponding slides after water rinse. (C) Photoshop enhanced image of (B), and the oil residues in the red box. (D)-(F) Water formation on different surfaces during the washing process, iBTS modified glass, pure glass, and BPMPC functionalized glass respectively. 94

Figure 4.8: (A) Fingerprint images before water application on iBTS modified glass (top), pure glass (middle), and BPMPC coated glass (bottom). (B) Corresponding fingerprints after stirring in water solution for 30 sec 95

Figure 4.9: Photographs of BPMPC coated glass slides after Windex wash on hot boiling water (A) without UV curing and (B) with UV curing. (C) Photograph of eyeglasses after cleaning with Expo on hot water, BPMPC coated (left) and control (right). 96

Figure 5.1: Thickness and contact angle of PMPCBMA and BPMPC coatings before and after UV irradiation 111

Figure 5.2: ATR-FTIR spectra of BPMPC and irradiated under UV (254 nm, 6.5 mW cm^{-2}) for 1, 3, 5, and 10 min, and FTIR of PMPCBMA 114

Figure 5.3: AFM topography (A-C) and DMT modulus data of BPMPC films irradiated with various time: no UV (A, D); 1 min (B, E); 5 min (C, F) 115
Figure 5.4: Water contact angle of BPMPC (after 1 min UV) and bare glass with time 116

CHAPTER 1

INTRODUCTION AND LITERATURE REVIEW

Functional Polymer Coatings

Coatings are used on surfaces of most products to offer decoration, protection, and special functions.[1] Coating science and technology is a developed field, which attracts constant attention due to increasing environmental protection laws and performance requirement. One trend for the development of coatings is the emergence of multifunctional or even smart coatings, that include self-cleaning coatings, self-healing coatings, sensory coatings, anti-icing coatings, antimicrobial coatings. These functions of coatings are not easily achieved by traditional synthesis methods and formulation techniques, but they can be possibly realized by the application of functional polymers. Functional polymers can be synthesized with specific surface properties including wettability, bondability, adhesion, friction, surface micro- and nano-structures and barrier properties. For instance, the researchers from Columbia Engineer has invented a high-performance polymer material using porous poly (vinylidene fluoride-co-hexafluoropropene) which demonstrated excellent passive daytime radiative cooling (PDRC) capability.[2] High, substrate-independent hemispherical solar reflectance (0.96 ± 0.03) and long-wave infrared emittances (0.97 ± 0.02) allow for sub-ambient temperature drops of ~ 6°C and cooling powers of ~ 96 watts per square meter ($W\ m^{-2}$) under solar intensities of 890 and 750 $W\ m^{-2}$, respectively. In addition, the polymer coating can be fabricated, dyed, and applied like paint to various surfaces, such as buildings, paper, and vehicles (Figure 1.1).

Figure 1.1. PDRC polymer coating (A) under sunlight, (B) under thermo-camera.[2]

Methods for Immobilizing Polymer Films.

Different methods can be utilized for surface modification, depending on the surface properties required. As depicted in Figure 1.2, the surface modification can be divided into two classes: physical and chemical methods.[3] Physical modification relies on intermolecular interactions, including electrostatic, hydrogen bonding, and van der Waals. A classic example is layer-by-layer assembly of polyelectrolyte multilayers based on the alternative adsorption of polyelectrolytes with complementary charges.[4, 5] This approach demonstrated the potential for modifying the surface properties of a biomaterial.[6, 7] The major disadvantage of physisorption is the weak stability under certain conditions of solvent and temperature, where surface immobilized functionalities are susceptible to degradation, delamination or dewetting. On the other hand, chemical modification is attractive due to the relative stability of the layers. The formation of covalent bonds between the polymer films and substrates are essential for the mechanical and chemical robustness. Surface-grafting via covalent attachment typically be classified according to the nature of the grafting strategy as either “grafting from” or “grafting to.”

The “grafting from” approach refers to the method of synthesis of a covalently attached polymer in situ on the solid substrate.[8-11] Almost all known mechanisms for polymer synthesis can be employed for “grafting from” approach, including atom transfer radical polymerization (ATRP),[12, 13] reversible addition-fragmentation chain transfer polymerization (RAFT),[14, 15] and nitroxide-mediated polymerization (NMP).[16, 17] Grafting density is determined by the initiator density which can be relatively high since the initiator is generally of a small size. However, “grafting from” generally require multiple steps in initiator synthesis, complicated substrates pretreatment, and the strict reaction conditions. Therefore, this method is difficult to apply to large-scale manufacture in industry.

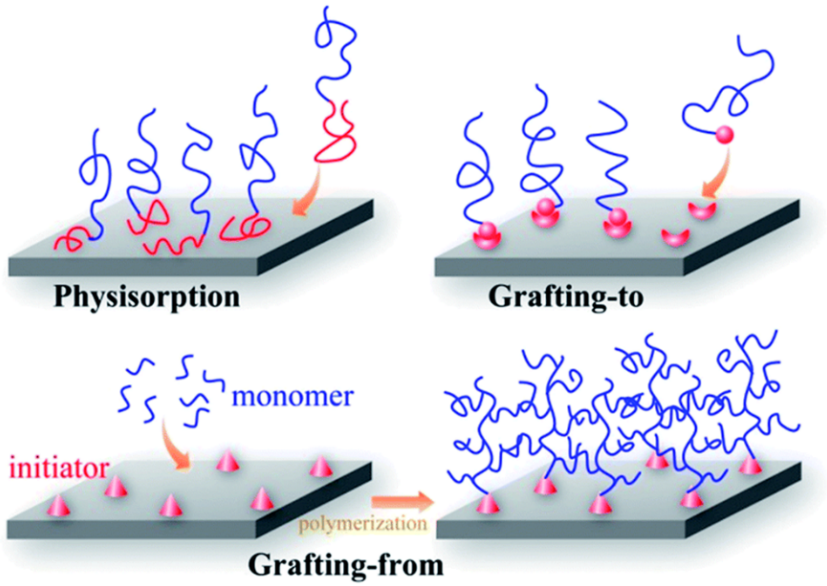

Figure 1.2. Schematic illustration of different methods for immobilizing polymer chains on a solid surface: physisorption, "grafting-to" and "grafting from."[3]

In the case of “grafting to,” an end-functionalized polymer is synthesized and subsequently adsorbed onto a substrate to form a chemical bond. Such end-functionalized polymers may be

formed via a variety of polymerization strategies. In contrast to "grafting from," it is difficult to achieve high graft density using "grafting to" due to the steric hinderance, particularly as the chain length increases. However, in the "grafting to" method, polymers can be conveniently characterized before grafting. Moreover, this method is more suitable for large-scale surface modification due to its relatively simpler synthetic pathway and reaction condition, which is appealing in industrial applications.

"Grafting to" surface modification relies on efficient conjugation reactions, such as thiol-ene chemistry,[18] Diels-Alder cycloaddition,[19, 20] azide-alkyne cycloaddition,[21, 22] and oxime formation.[23, 24] The compatibility of different conjugation chemistries with a wide range of functional groups allows for preparation of multifunctional patterned surface.[25, 26] The most notable "grafting to" strategy in which high graft chain density is typically achieved is self-assembled monolayers (SAMs), which are classified defined as ordered molecular assemblies that form spontaneously onto substrates.[27, 28] The choice of SAMs depends on the substrate materials. For instance, when preparing metal materials such as gold, silver and copper, alkane thiol (R-SH) and disulfide (R-S-S-R') can be used.[29-31] Alcohol (R-OH) groups are useful for attaching chins to iron oxide and silicon surfaces.[32-34] If the surface is rich in hydroxyl groups (e.g., silica and glass alumina), silane functionalized polymers may be effectively surface-grafted. For example, polymers containing an R-Si-X end group (which X is -Cl, -OCH, or -OCHCH) may be grafted to a hydroxylated surface.[35] In addition, acid and plasma treatments may be used to increase the concentration of hydroxyl groups on many substrates, including polymer substrates.[36-38]

Benzophenone Photo-crosslinker

Photochemical methods are some of the most versatile techniques for both synthetic and natural polymer modification. A number of photoreactive reagents have been used to functionalized surfaces for different applications. Including diazirines,[39] aryl azides,[40, 41] nitrobenzils,[42, 43] cyclic disulfides[44, 45] and benzophenone (BP).[46] BP is probably the most widely used and versatile photo-crosslinker in organic chemistry, bioorganic chemistry, and material science as a result of its unique photochemical properties, the commercial availability or the reagents, and the ease of use.[47-49] The hydrogen abstraction mechanism of BP has been discussed previously (Figure 1.3): upon n – π^* excitation at 365 nm, a biradicaloid triplets state is formed reversibly, which can abstract a hydrogen atom from accessible C-H bonds; the radicals subsequently recombine, creating a stable covalent C-C bond. This photo-reaction proceeds in diverse chemical environments with reasonable efficiency, and tolerance to oxygen. For these reasons, BP has been extensively used in various approaches for surface modification in polymer and material science.

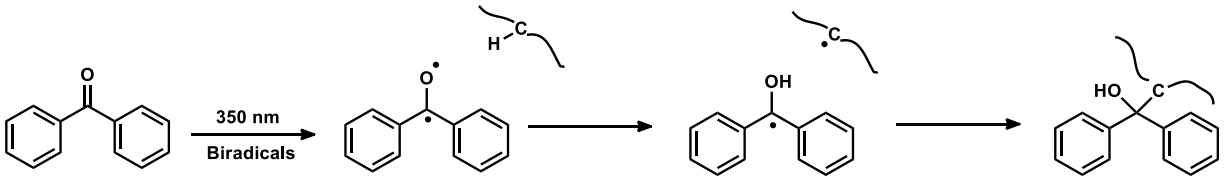

Figure 1.3. Scheme of benzophenone (BP) crosslink.

The utilizing of BP can be dividedly in three ways. First BP is used as a photoinitiator in the presence of UV light to start the polymerization of vinyl, acrylate, methylate monomers form surfaces with high efficiency in a "grafting from" fashion. Feng *et al.* have reported BP molecules

onto carbonate urethane surfaces and induced the polymerization of poly (ethylene glycol) into different molecular weight by using UV light (Figure 1.4).[50] BP has also been used in grafting poly (acrylic acid) onto the polydimethylsiloxane microfluidic devices with complex geometry.[51]

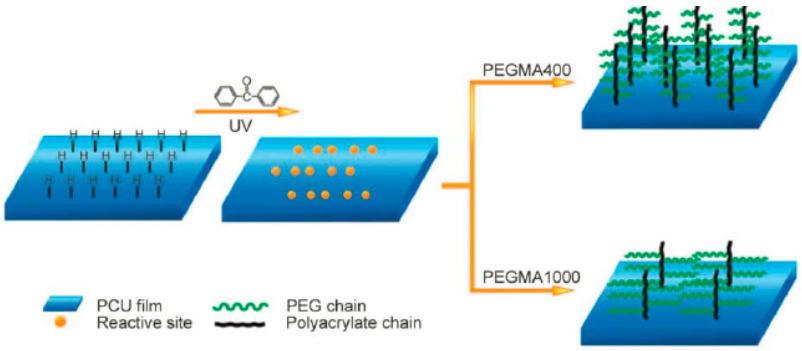

Figure 1.4. Schematic illustration of poly (ethylene glycol) photographing-from polycarbonate urethane film.[50]

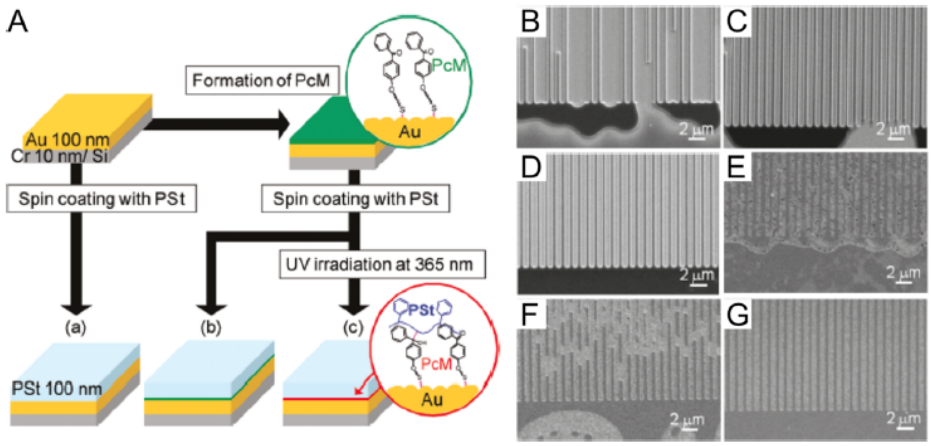

Figure 1.5. (A) Schematic detailing the fabrication of BP-photoinitiated films of PSt on (a) bare, (b) unexposed monolayer modified, and (c) UV exposed monolayer modified Au substrates. SEM images depicting PSt thin films after (B−D) thermal nanoimprint lithography and (E−G) wet etching.[52]

Second, BP can be attached and employed as a photosensitizer on the surface, resulting in the covalent attachment of polymer chains. Incorporation into the polymer as an anchoring group to activate the immobilization of the polymers to surfaces in a "grafting to" manner. For example, Oda *et al.* reported a patterning strategy to photo-graft polystyrene thin films to monolayers of BP-terminated alkane thiolates on Au substrates using UV activation (Figure 1.5).[52] Third, BP was incorporated into the polymers as an anchoring, or as a monomer in the copolymers, to immobilize polymer films to substrates. A small antimicrobial molecule that comprised a long hydrocarbon chain substituted quaternary ammonium connected to a BP tethering head. This molecule can be covalently attached to surfaces and forms a cross-linked polymeric network under mild irradiation.[53, 54] The modified surfaces demonstrated excellent contact-active, non-leaching antimicrobial activity toward Gram-positive (*Staphylococcus aureus*) and Gram-negative (*Escherichia coli*) bacteria. In addition, the activated UV range (350-360) for BP does not damage cells, proteins, and antibodies, which makes BP an optimal photophore for photo-grafting of small and large biomolecules in the preparation of biocompatible materials, devices, and sensors.[55] As a result, BP has been utilized for the photo-cross-linking of polymers and photo-immobilization of peptides and proteins in creating cell adhesive bio-interfaces in defined patterns[56-58] and gradients[59-61] for probing cellular dynamics, such as adhesion, polarization, neurite outgrowth and growth cone collapse, and migration.[60, 62-64] Martinez *et al*. investigated the behaviors of rat aortic smooth muscle (A7r5) and human osteosarcoma (U2OS) cells on photo-cross-linked polyelectrolyte multilayers (PEMUs) with uniform, or gradients of, moduli (Figure 1.6).[60] The PEMUs were built layer-by-layer with the polycation poly(allylamine hydrochloride) (PAH) and a polyanion poly(acrylic acid) (PAA) that was modified with photoreactive 4-(2-hydroxyethoxy) benzophenone (PAABp). The results demonstrated the utility of photo-cross-linked PEMUs to

direct vascular and osteoblast cell behavior, a potential application for PEMU coatings on biomedical implants.

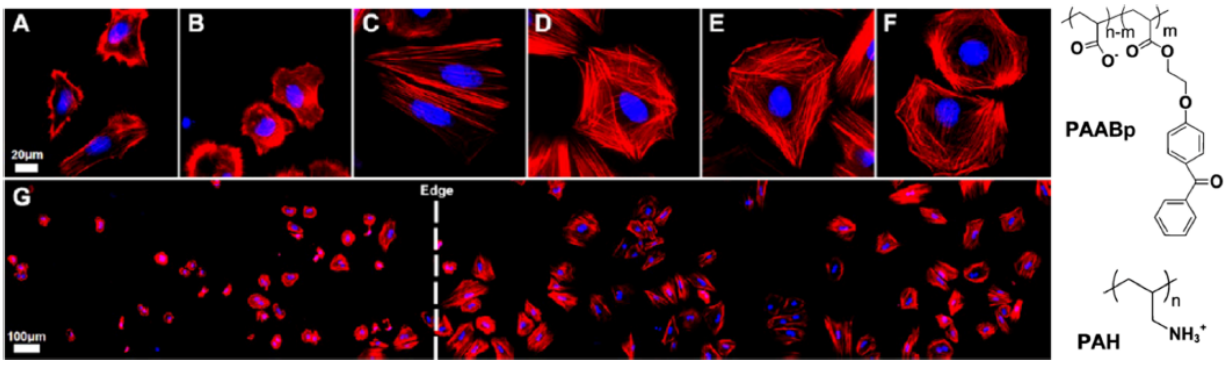

Figure 1.6. Preparation of PEI multilayers using PAABp and PAH to create gradients of increasing Young's modulus. A7rS cells stained for actin (red) show increasing filament organization along the increasing gradient from (A) to (F) with the corresponding low magnification image in (G). [60]

In order to design BP related polymers that can be efficiently and rapidly grafted on different surfaces, the mechanism and other factors that affect the reactivity and kinetics of BP photochemistry need to be carefully considered. In principle, when UV irradiated, ground state BP (S_0) is excited to a singlet state (S_1) that rapidly and efficiently undergoes intersystem crossing (ISC) to yield the lowest energy reactive triplet (Figure 1.7). The n-π^* triplet (T_1), which can be represented as a diradical, is well known to abstract aliphatic hydrogens with extremely high reactivity. However, the π-π^* charge transfer (CT) is much less reactive than n-π^*. Any change in energy level of n-π^* and π-π^* would affect the crosslinking speed.

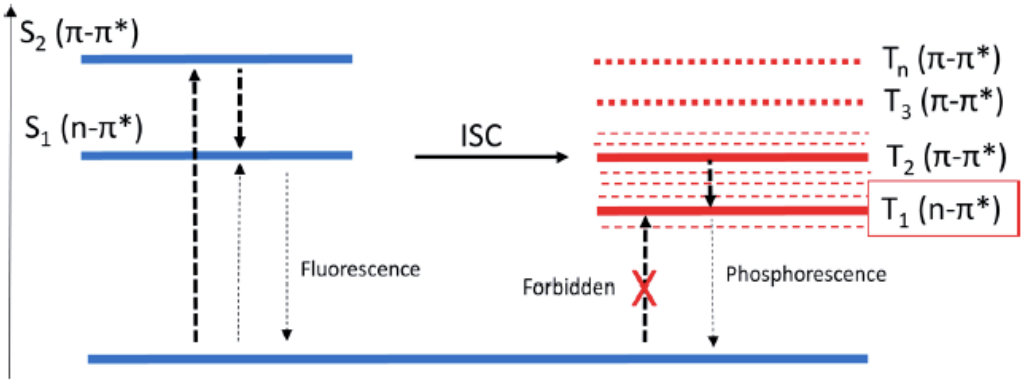

Figure 1.7. Jablonski diagram of BP excited states.

Substituent Effect

The reactivity of BP depends on the lowest energy triplet state in the given material, where the n-π^* triplet is the most reactive and π-π^* charge transfer (CT) is the least reactive. Although BP without substituent possesses a lowest energy n-π^* triplet, the substituent functional groups would change the energy levels. The unreactive CT states would be the lower state than n-π^* triplet under the effects of certain substituents. An electron donating group (i.e., amino, dimethylamino, hydroxy, etc.) at the meta or para position would help stabilized the CT stated of BP, which will invert their energy levels. Demeter *et al.* reported the energy profiles of substituted BPs using density functional theory (DFT) quantum chemical calculations.[65] The photoreduction rate coefficients demonstrate a strong dependence on ring substitution with a determining factor of the stability of aromatic ketyl radical formation. The trifluoromethyl-substituted ketyl radicals are much more stable than those containing electron donor substituents, and accordingly, their photochemical reactions are faster.

Solvent Effect

The reactivity of BP is also affected by the solvent condition, as the solvent polarity will influence the relative energy levels of BP derivatives, even inverting the CT and n-π^* states when they are close in energy. Porter has reported that for p-aminobenzophenone the π-π^* CT state is the lowest triplet in isopropanol, a polar solvent; while n-π^* is the lower energy state in cyclohexane, a nonpolar solvent (Figure 1.8).[66] Generally, the excited state energy will decrease in polar solvent if its polarity is higher than that of the ground state. Increasing the solvent polarity can shift the n-π^* triplet to the π-π^* or CT state, which prevents reactions of some BP derivatives in a polar solvent. However, even when the lowest energy triplet is the π-π^* or CT state, some extent of reactivity will be observed as thermal (vibrational) fluctuation to an n-π^* triplet.

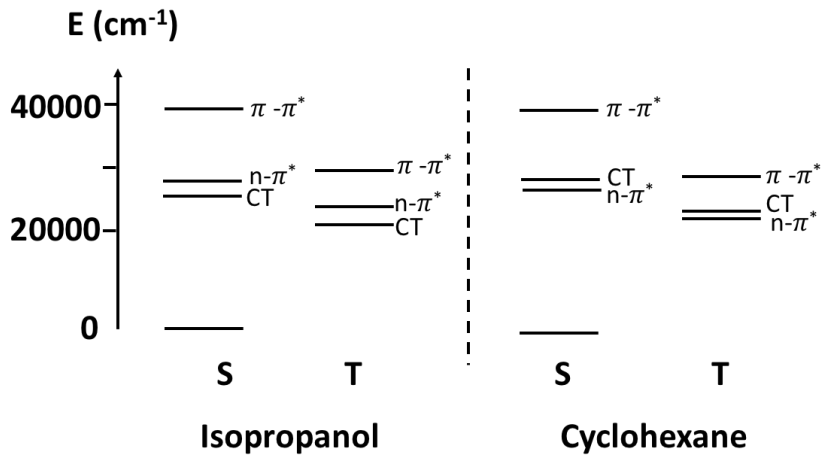

Figure. 1.8. Energy levels of p-aminobenzophenone isopropanol and in cyclohexane.[66]

Objectives and Dissertation Outline

The objective of this dissertation are as follows: (1) design an antifouling coating which can be combined with antimicrobial material to achieve the purpose of simultaneous bacterial

killing and repelling at the same time; (2) synthesis of a transparent antifogging and self-cleaning coatings, which can be applied in a broad selection of materials, including eyeglasses, safety goggles and windows; (3) investigate the effects of polymer environment to the BP crosslinking rate when BP as a pendent side chain, which can provide guidance in BP copolymer design; and (4) inspect the mechanism of contact angle increasing for BP containing polymer under UV irradiation.

The rest of the dissertation is organized in four chapters. Chapter 2 investigated the kinetics of BP containing zwitterionic copolymers. The kinetics BP and derivatives have been well studied in solvent and in polymer as a small molecule. In this chapter, we discussed the factors that can affect the rate of crosslinking when BP is incorporated into the copolymer as a side chain. The polarity of the polymer was estimated by partition coefficient logP, and the rate constant demonstrated a linear relationship with logP. This linear correlation was only valid for the zwitterionic polymer with a T_g lower or close to room temperature, in which the chemical environment was the determinant. The substituent effects also work in BP pendent copolymers as BP derivatives in solvent and in polymer matrix.

Chapter 3 is focused on an antifouling zwitterionic terpolymer, 2-methacryloyloxyethyl phosphorylcholine-co-butyl methacrylate-co-benzophenone (BPMPC), which is covalently grafted to a nitric oxide (NO) releasing antimicrobial biomedical grade copolymer of silicone-polycarbonate-urethane, CarboSil, to significantly enhance the biocompatibility, non-specific protein repulsion, and infection-resistant properties. Protein adsorption was tested on the material using fibrinogen and lysozyme, and significant decrease was observed in BPMPC coated substrates. The NO-releasing and leaching profile were monitored for two weeks, and no difference was observed. BPMPC even slightly increase the leaching of NO due to its

hydrophilicity. In addition, the antimicrobial efficiency was examined using *S. aureus*. This chapter is published in *Langmuir*, 2017, 33 (45), 13105-13113.

Chapter 4 demonstrates a transparent and robust zwitterionic polymer coating presenting both antifogging and self-cleaning properties. According to the UV spectra, the transparency was increased slightly due to the lower reflective index of the coating, which formed an anti-reflecting film on the substrates. The antifogging performance was examined using hot-vapor and freeze-warm approaches. Tetradecane oil and fingerprint removing tests were conducted on the polymer films to demonstrate self-cleaning ability. Moreover, the robustness is confirmed by the household chemical cleaning materials. This chapter is published in *ACS Omega*, 2018, 3 (12), 17743-17750.

Chapter 5 explained the mechanism of the unusual phenomena of BPMPC, the increasing of hydrophobicity under UV irradiation. Due to the crosslinking that occurs inside the polymer matrix, the possibility of zwitterionic side chain self-association significantly improve, which results in the contact angle increase, film thickness decreases, and Young's modulus increase. Additionally, the reason why BPMPC demonstrates antifouling and antifogging properties with poor hydrophilicity is described. Penetration into the polymer matrix and the un-association of zwitterionic components in a high dielectric constant solvent likely work together to contribute to the outstanding performance.

Finally, chapter 6 provides a general summary of the work completed for this dissertation, as well as the future direction for this research.

References

1. Wu, L. M.; Baghdachi, J., FUNCTIONAL POLYMER COATINGS Principles, Methods, and Applications Preface. *Wiley Ser Polym Eng* **2015**, Xiii-Xiv.

2. Mandal, J.; Fu, Y. K.; Overvig, A. C.; Jia, M. X.; Sun, K. R.; Shi, N. N.; Zhou, H.; Xiao, X. H.; Yu, N. F.; Yang, Y., Hierarchically porous polymer coatings for highly efficient passive daytime radiative cooling. *Science* **2018,** *362* (6412), 315-318.

3. Li, D.; Zheng, Q.; Wang, Y. W.; Chen, H., Combining surface topography with polymer chemistry: exploring new interfacial biological phenomena. *Polym Chem-Uk* **2014,** *5* (1), 14-24.

4. Han, L. L.; Mao, Z. W.; Wu, J. D.; Guo, Y.; Ren, T. C.; Gao, C. Y., Unidirectional migration of single smooth muscle cells under the synergetic effects of gradient swelling cue and parallel groove patterns. *Colloid Surface B* **2013,** *111*, 1-6.

5. Han, L. L.; Mao, Z. W.; Wu, J. D.; Guo, Y.; Ren, T. C.; Gao, C. Y., Directional cell migration through cell-cell interaction on polyelectrolyte multilayers with swelling gradients. *Biomaterials* **2013,** *34* (4), 975-984.

6. Fu, J. H.; Ji, J.; Yuan, W. Y.; Shen, J. C., Construction of anti-adhesive and antibacterial multilayer films via layer-by-layer assembly of heparin and chitosan. *Biomaterials* **2005,** *26* (33), 6684-6692.

7. Tang, Z. Y.; Wang, Y.; Podsiadlo, P.; Kotov, N. A., Biomedical applications of layer-by-layer assembly: From biomimetics to tissue engineering. *Adv Mater* **2006,** *18* (24), 3203-3224.

8. Zhao, B.; Brittain, W. J., Polymer brushes: surface-immobilized macromolecules. *Prog Polym Sci* **2000,** *25* (5), 677-710.

9. Ruhe, J.; Knoll, N., Functional polymer brushes (Reprinted from Supramolecular Polymers, pg 565-613, 2000). *J Macromol Sci-Pol R* **2002,** *C42* (1), 91-138.

10. Advincula, R. C., Surface initiated polymerization from nanoparticle surfaces. *J Disper Sci Technol* **2003,** *24* (3-4), 343-361.

11. Jennings, G. K.; Brantley, E. L., Physicochemical properties of surface-initiated polymer films in the modification and processing of materials. *Adv Mater* **2004,** *16* (22), 1983-1994.

12. Matyjaszewski, K.; Gobelt, B.; Paik, H. J.; Horwitz, C. P., Tridentate nitrogen-based ligands in Cu-based ATRP: A structure-activity study. *Macromolecules* **2001,** *34* (3), 430-440.

13. Nanda, A. K.; Matyjaszewski, K., Effect of [PMDETA]/[Cu(I)] ratio, monomer, solvent, counterion, ligand, and alkyl bromide on the activation rate constants in atom transfer radical polymerization. *Macromolecules* **2003,** *36* (5), 1487-1493.

14. Baum, M.; Brittain, W. J., Synthesis of polymer brushes on silicate substrates via reversible addition fragmentation chain transfer technique. *Macromolecules* **2002,** *35* (3), 610-615.

15. Yu, W. H.; Kang, E. T.; Neoh, K. G., Functionalization of hydrogen-terminated Si(100) substrate by surface-initiated RAFT polymerization of 4-vinylbenzyl chloride and subsequent derivatization for photoinduced metallization. *Ind Eng Chem Res* **2004,** *43* (17), 5194-5202.

16. Husseman, M.; Malmstrom, E. E.; McNamara, M.; Mate, M.; Mecerreyes, D.; Benoit, D. G.; Hedrick, J. L.; Mansky, P.; Huang, E.; Russell, T. P.; Hawker, C. J., Controlled synthesis of polymer brushes by "Living" free radical polymerization techniques. *Macromolecules* **1999,** *32* (5), 1424-1431.

17. Matsuno, R.; Yamamoto, K.; Otsuka, H.; Takahara, A., Polystyrene- and poly(3-vinylpyridine)-grafted magnetite nanoparticles prepared through surface-initiated nitroxide-mediated radical polymerization. *Macromolecules* **2004,** *37* (6), 2203-2209.

18. Zhao, G. L.; Hafren, J.; Deiana, L.; Cordova, A., Heterogeneous "Organoclick" Derivatization of Polysaccharides: Photochemical Thiol-ene Click Modification of Solid Cellulose. *Macromol Rapid Comm* **2010,** *31* (8), 740-744.

19. Houseman, B. T.; Mrksich, M., Carbohydrate arrays for the evaluation of protein binding and enzymatic modification. *Chem Biol* **2002,** *9* (4), 443-454.

20. Arumugam, S.; Popik, V. V., Patterned Surface Derivatization Using Diels-Alder Photoclick Reaction. *J Am Chem Soc* **2011,** *133* (39), 15730-15736.

21. Pearson, D.; Downard, A. J.; Muscroft-Taylor, A.; Abell, A. D., Reversible photoregulation of binding of alpha-chymotrypsin to a gold surface. *J Am Chem Soc* **2007,** *129* (48), 14862-+.

22. Lummerstorfer, T.; Hoffmann, H., Click chemistry on surfaces: 1,3-dipolar cycloaddition reactions of azide-terminated monolayers on silica. *J Phys Chem B* **2004,** *108* (13), 3963-3966.

23. Chan, E. W. L.; Yousaf, M. N., Immobilization of ligands with precise control of density to electroactive surfaces. *J Am Chem Soc* **2006,** *128* (48), 15542-15546.

24. Chan, E. W. L.; Yousaf, M. N., A photo-electroactive surface strategy for immobilizing ligands in patterns and gradients for studies of cell polarization. *Mol Biosyst* **2008,** *4* (7), 746-753.

25. Christman, K. L.; Schopf, E.; Broyer, R. M.; Li, R. C.; Chen, Y.; Maynard, H. D., Positioning Multiple Proteins at the Nanoscale with Electron Beam Cross-Linked Functional Polymers. *J Am Chem Soc* **2009,** *131* (2), 521-527.

26. Im, S. G.; Bong, K. W.; Kim, B. S.; Baxamusa, S. H.; Hammond, P. T.; Doyle, P. S.; Gleason, K. K., Patterning Nanodomains with Orthogonal Functionalities: Solventless Synthesis of Self-Sorting Surfaces. *J Am Chem Soc* **2008,** *130* (44), 14424-+.

27. Vericat, C.; Vela, M. E.; Salvarezza, R. C., Self-assembled monolayers of alkanethiols on Au(111): surface structures, defects and dynamics. *Phys Chem Chem Phys* **2005,** *7* (18), 3258-3268.

28. Love, J. C.; Estroff, L. A.; Kriebel, J. K.; Nuzzo, R. G.; Whitesides, G. M., Self-assembled monolayers of thiolates on metals as a form of nanotechnology. *Chem Rev* **2005,** *105* (4), 1103-1169.

29. Laibinis, P. E.; Whitesides, G. M.; Allara, D. L.; Tao, Y. T.; Parikh, A. N.; Nuzzo, R. G., Comparison of the Structures and Wetting Properties of Self-Assembled Monolayers of Normal-Alkanethiols on the Coinage Metal-Surfaces, Cu, Ag, Au. *J Am Chem Soc* **1991,** *113* (19), 7152-7167.

30. Motte, L.; Pileni, M. P., Influence of length of alkyl chains used to passivate silver sulfide nanoparticles on two- and three-dimensional self-organization. *J Phys Chem B* **1998,** *102* (21), 4104-4109.

31. Shon, Y. S.; Dawson, G. B.; Porter, M.; Murray, R. W., Monolayer-protected bimetal cluster synthesis by core metal galvanic exchange reaction. *Langmuir* **2002,** *18* (10), 3880-3885.

32. Boal, A. K.; Das, K.; Gray, M.; Rotello, V. M., Monolayer exchange chemistry of gamma-Fe2O3 nanoparticles. *Chem Mater* **2002,** *14* (6), 2628-2636.

33. Zharnikov, M.; Kuller, A.; Shaporenko, A.; Schmidt, E.; Eck, W., Aromatic self-assembled monolayers on hydrogenated silicon. *Langmuir* **2003,** *19* (11), 4682-4687.

34. Niederhauser, T. L.; Lua, Y. Y.; Jiang, G. L.; Davis, S. D.; Matheson, R.; Hess, D. A.; Mowat, I. A.; Linford, M. R., Arrays of chemomechanically patterned patches of homogeneous and mixed monolayers of 1-alkenes and alcohols on single silicon surfaces. *Angew Chem Int Edit* **2002,** *41* (13), 2353-2356.

35. Ratner, B. D., Hoffman, A. S., *Physicochemical Surface Modification of Materials Used in Medicine, in Biomaterials Science: An Introduction to Materials in Medicine,*. Elsevier Academic Press: New York, 2004; p 201-218.

36. Murthy, R.; Shell, C. E.; Grunlan, M. A., The influence of poly(ethylene oxide) grafting via siloxane tethers on protein adsorption. *Biomaterials* **2009,** *30* (13), 2433-2439.

37. Krishnan, S.; Wang, N.; Ober, C. K.; Finlay, J. A.; Callow, M. E.; Callow, J. A.; Hexemer, A.; Sohn, K. E.; Kramer, E. J.; Fischer, D. A., Comparison of the fouling release properties of hydrophobic fluorinated and hydrophilic PEGylated block copolymer surfaces: Attachment strength of the diatom Navicula and the green alga Ulva. *Biomacromolecules* **2006,** *7* (5), 1449-1462.

38. Owen, M. J.; Smith, P. J., Plasma Treatment of Polydimethylsiloxane. *J Adhes Sci Technol* **1994,** *8* (10), 1063-1075.

39. Sinz, A., Chemical cross-linking and mass spectrometry to map three-dimensional protein structures and protein-protein interactions. *Mass Spectrom Rev* **2006,** *25* (4), 663-682.

40. Tanaka, Y.; Bond, M. R.; Kohler, J. J., Photocrosslinkers illuminate interactions in living cells. *Mol Biosyst* **2008,** *4* (6), 473-480.

41. Pham, N. D.; Parker, R. B.; Kohler, J. J., Photocrosslinking approaches to interactome mapping. *Curr Opin Chem Biol* **2013,** *17* (1), 90-101.

42. Nam, C. Y.; Qin, Y.; Park, Y. S.; Hlaing, H.; Lu, X. H.; Ocko, B. M.; Black, C. T.; Grubbs, R. B., Photo-Cross-Linkable Azide-Functionalized Polythiophene for Thermally Stable Bulk Heterojunction Solar Cells. *Macromolecules* **2012,** *45* (5), 2338-2347.

43. Yoo, M.; Kim, S.; Lim, J.; Kramer, E. J.; Hawker, C. J.; Kim, B. J.; Bang, J., Facile Synthesis of Thermally Stable Core-Shell Gold Nanoparticles via Photo-Cross-Linkable Polymeric Ligands. *Macromolecules* **2010,** *43* (7), 3570-3575.

44. Guo, L. W.; Grant, J. E.; Hajipour, A. R.; Muradov, H.; Arbabian, M.; Artemyev, N. O.; Ruoho, A. E., Asymmetric interaction between rod cyclic GMP phosphodiesterase gamma subunits and alpha beta subunits. *J Biol Chem* **2005,** *280* (13), 12585-12592.

45. Suga, T.; Konishi, H.; Nishide, H., Photocrosslinked nitroxide polymer cathode-active materials for application in an organic-based paper battery. *Chem Commun* **2007,** (17), 1730-1732.

46. Dankbar, D. M.; Gauglitz, G., A study on photolinkers used for biomolecule attachment to polymer surfaces. *Anal Bioanal Chem* **2006,** *386* (7-8), 1967-1974.

47. Dorman, G.; Prestwich, G. D., Benzophenone Photophores in Biochemistry. *Biochemistry-Us* **1994,** *33* (19), 5661-5673.

48. Horie, K.; Ando, H.; Mita, I., Photochemistry in Polymer Solids .8. Mechanism of Photoreaction of Benzophenone in Polyvinyl-Alcohol). *Macromolecules* **1987,** *20* (1), 54-58.

49. Brauchle, C.; Burland, D. M.; Bjorklund, G. C., Hydrogen Abstraction by Benzophenone Studied by Holographic Photochemistry. *J Phys Chem-Us* **1981,** *85* (2), 123-127.

50. Feng, Y. K.; Zhao, H. Y.; Behl, M.; Lendlein, A.; Guo, J. T.; Yang, D. Z., Grafting of poly(ethylene glycol) monoacrylates on polycarbonateurethane by UV initiated polymerization for improving hemocompatibility. *J Mater Sci-Mater M* **2013,** *24* (1), 61-70.

51. Schneider, M. H.; Willaime, H.; Tran, Y.; Rezgui, F.; Tabeling, P., Wettability Patterning by UV-Initiated Graft Polymerization of Poly(acrylic acid) in Closed Microfluidic Systems of Complex Geometry. *Anal Chem* **2010,** *82* (21), 8848-8855.

52. Oda, H.; Ohtake, T.; Takaoka, T.; Nakagawa, M., Photoreactive Chemisorbed Monolayer Suppressing Polymer Dewetting in Thermal Nanoimprint Lithography. *Langmuir* **2009,** *25* (12), 6604-6606.

53. Gao, J.; Martin, A.; Yatvin, J.; White, E.; Locklin, J., Permanently grafted icephobic nanocomposites with high abrasion resistance. *J Mater Chem A* **2016,** *4* (30), 11719-11728.

54. Yatvin, J.; Gao, J.; Locklin, J., Durable defense: robust and varied attachment of non-leaching poly"-onium" bactericidal coatings to reactive and inert surfaces. *Chem Commun* **2014,** *50* (67), 9433-9442.

55. Dorman, G.; Nakannura, H.; Pulsipher, A.; Prestwich, G. D., The Life of Pi Star: Exploring the Exciting and Forbidden Worlds of the Benzophenone Photophore. *Chem Rev* **2016,** *116* (24), 15284-15398.

56. Larsen, E. K. U.; Mikkelsen, M. B. L.; Larsen, N. B., Protein and cell patterning in closed polymer channels by photoimmobilizing proteins on photografted poly(ethylene glycol) diacrylate. *Biomicrofluidics* **2014,** *8* (6).

57. Larsen, E. K. U.; Mikkelsen, M. B. L.; Larsen, N. B., Facile Photoimmobilization of Proteins onto Low-Binding PEG-Coated Polymer Surfaces. *Biomacromolecules* **2014,** *15* (3), 894-899.

58. Fink, J.; Thery, M.; Azioune, A.; Dupont, R.; Chatelain, F.; Bornens, M.; Piel, M., Comparative study and improvement of current cell micro-patterning techniques. *Lab Chip* **2007,** *7* (6), 672-680.

59. Martin, T. A.; Herman, C. T.; Limpoco, F. T.; Michael, M. C.; Potts, G. K.; Bailey, R. C., Quantitative Photochemical Immobilization of Biomolecules on Planar and Corrugated Substrates:

A Versatile Strategy for Creating Functional Biointerfaces. *Acs Appl Mater Inter* **2011,** *3* (9), 3762-3771.

60. Martinez, J. S.; Lehaf, A. M.; Schlenoff, J. B.; Keller, T. C. S., Cell Durotaxis on Polyelectrolyte Multilayers with Photogenerated Gradients of Modulus. *Biomacromolecules* **2013,** *14* (5), 1311-1320.

61. Toh, C. R.; Fraterman, T. A.; Walker, D. A.; Bailey, R. C., Direct Biophotolithographic Method for Generating Substrates with Multiple Overlapping Biomolecular Patterns and Gradients. *Langmuir* **2009,** *25* (16), 8894-8898.

62. Adams, D. N.; Kao, E. Y. C.; Hypolite, C. L.; Distefano, M. D.; Hu, W. S.; Letourneau, P. C., Growth cones turn and migrate up an immobilized gradient of the laminin IKVAV peptide. *J Neurobiol* **2005,** *62* (1), 134-147.

63. Baek, N. S.; Kim, Y. H.; Han, Y. H.; Offenhausser, A.; Chung, M. A.; Jung, S. D., Fine neurite patterns from photocrosslinking of cell-repellent benzophenone copolymer. *J Neurosci Meth* **2012,** *210* (2), 161-168.

64. Herman, C. T.; Potts, G. K.; Michael, M. C.; Tolan, N. V.; Bailey, R. C., Probing dynamic cell-substrate interactions using photochemically generated surface-immobilized gradients: application to selectin-mediated leukocyte rolling. *Integr Biol-Uk* **2011,** *3* (7), 779-791.

65. Demeter, A.; Horvath, K.; Boor, K.; Molnar, L.; Soos, T.; Lendvay, G., Substituent Effect on the Photoreduction Kinetics of Benzophenone. *J Phys Chem A* **2013,** *117* (40), 10196-10210.

66. Porter, G.; Suppan, P., Primary Photochemical Processes in Aromatic Molecules .12. Excited States of Benzophenone Derivatives. *T Faraday Soc* **1965,** *61* (512p), 1664-&.

CHAPTER 2

THE PHOTOCROSSLINKING KINETICS STUDY OF BENZOPHENONE CONTAINNING ZWITTERIONIC COPOLYMER[1]

[1]Liu, Q. Locklin, J; To be submitted to [Langmuir]

Abstract

The kinetics of benzophenone and its small molecule derivatives have been widely studied in different solvents by nanosecond laser flash photolysis, as well as diffusing in polymer matrix. In this work, BP pendent zwitterionic copolymer kinetics was investigated using UV-vis for the first time. Due to the high hydrophilicity of zwitterionic molecule, the influence of polarity of polymer matrix on the crosslinking rate was observed. With increasing zwitterionic percentage in copolymer, the polarity of the copolymer increases and the BP reactivity decreases. A linear relationship between rate constant and partial coefficient logP was observed. Moreover, the thermal property is also an important factor affecting the BP reactivity. In the polymers with high T_g, the reactivity was not dominated by chemical environment, such as polarity, and the restricted segment movement reduces the crosslinking rate. Additionally, the ring substituent effects plays the same important role in BP pendent copolymers as with small molecules. Electron-withdrawing groups help to stabilize the BP triplet radical and facilitate crosslinking, while electron-donating groups work oppositely. Polarity, thermal properties, and substituents should be taken in consideration when designing BP containing functional polymers used to modify surfaces.

Introduction

Benzophenone (BP) and its derivatives are perhaps the most widely used photoinitiators and have been studied extensively, both as additives[1-5] and pendent chromophores incorporated into functional polymer side chains.[6-7] Ciamician et al. explored the basic photochemical features of benzophenone-ethanol system. BP like other ketones, when irradiated in solution, undergoes photodecomposition by reaction with solvent. The excited triplet stated produces a high yield of ketyl radical in alkyl solvent by hydrogen abstraction, according to the following reaction sequence (Scheme 2.1): (1) formation of triplet during the (20 ns) laser pulse; (2a) the first order phosphorescence; (2b) intersystem crossing (ISC); (2c) second-order triplet-triplet annihilation reaction; (3) the hydrogen abstraction and production of an equal amount of the aliphatic and aromatic ketyl radicals; (4) recombination of alphatic and aromatic radical to form new C-C bond; (5, 6) second order self-termination; (7) the secondary reduction of the aromatic ketone by aliphatic ketyl radicals formed in the primary atom transfer.[8-10]

Scheme 2.1.

$$\mathrm{Ph_2CO} \xrightarrow{\mathrm{hv}} {}^1\mathrm{Ph_2CO^*} \rightarrow {}^3\mathrm{Ph_2CO^*} \quad (1)$$

$${}^3\mathrm{Ph_2CO} \rightarrow {}^1\mathrm{Ph_2}CO + hv' \quad (2a)$$

$${}^3\mathrm{Ph_2}C\mathit{O} \rightarrow \mathrm{Ph_2CO} \quad (2b)$$

$$2\ {}^3\mathrm{Ph_2CO} \rightarrow (2-\alpha)\mathrm{Ph_2CO} + \alpha\ {}^3\mathrm{Ph_2CO} \quad (2c)$$

$${}^3\mathrm{Ph_2CO} + \mathrm{RH_2} \rightarrow \mathrm{Ph_2\dot{C}OH} + \dot{\mathrm{R}}\mathrm{H} \quad (3)$$

$$\mathrm{Ph_2\dot{C}OH} + \dot{\mathrm{R}}\mathrm{H} \rightarrow \mathrm{Ph_2(OH)C} - \mathrm{RH} \quad (4)$$

$$2\dot{\mathrm{R}}\mathrm{H} \rightarrow \mathrm{HR} - \mathrm{RH} \quad (5)$$

$$2\ \mathrm{Ph_2\dot{C}OH} \rightarrow \mathrm{Ph_2(OH)C(OH)CPh_2} \quad (6)$$

$$Ph_2CO + \dot{R}H \rightarrow Ph_2\dot{C}OH + R \quad (7)$$

The kinetics of BP derivatives also have well also studied in various conditions. The hydrogen abstraction of benzophenone triplet was investigated using nanosecond flash photolysis measurements and activation energy in different solvent systems. Increasing the solvent polarity can shift the n-π* triplet to the π-π* or charge transition state (CT), which will decrease the reactivity.[11-14] The relationship between the spectroscopic and photochemical properties also have studied in detail in substituted benzophenones. Electron donors increase the electron density at the carbonyl, making it less electrophilic and therefore less reactive, inhibiting H-abstraction. Electron withdrawing groups on BPs have an opposite effect, increase the reactivity of the n-π* radical.[11, 15-16] Other factors that affect the kinetics of BP including stereoelectronic control, regioselectivity and heterologous. [17-19]

Reactions in polymer solids greatly differ from those in solution mainly because the mobility of the reactants is far more suppressed in the former than in the later.[20-22] Another important difference in is that reactions in polymer solids frequently proceed in a heterogeneous fashion, owing to the aggregation or the free volume distribution.[20, 22-23] In the case of Norrish type II photolysis, the quantum yield in solid films above T_g is the same as that in solution, but it follows diffusion mechanism between T_g > T > T_β.[24-25] Other factors that influence reactions in polymer solids also include crosslinking, chain scission, excited energy transfer and migration and electron transfer.[26] BP kinetics in poly(methyl methacrylate) (PMMA), poly(isopropyl methacrylate) (PIPMA) and poly(methyl acrylate) (PMA) was studied at different temperature. The decay process of triplet ^{3}BP* in polymer matrices is as followed:[27]

Scheme 2.2

$$^3BP^* \xrightarrow{k_0} BP \tag{8}$$

$$^3BP^* + [Q] \xrightarrow{k_q} BP + [Q] \tag{9}$$

Where k_0 is the rate constant for spontaneous deactivation of the BP triplet, and [Q] is the concentration of ester, phenyl, or phenylene groups in the matrix polymer. The bimolecular rate coefficient k_q is expressed by eq. (2.1):

$$k_q = \frac{4\pi RDN}{1 + \frac{4\pi RDN}{k}}\left[1 + \frac{R}{\left(1 + \frac{4\pi RDN}{k}\right)\sqrt{\pi DT}}\right] \tag{2.1}$$

where D is the sum of the diffusion coefficient for the carbonyl group in BP that for ester carbonyl group, R is the reaction radius between the two groups, k is the intrinsic (chemical) rate constant that would pertain if the equilibrium concentration of the quenching group were maintained, and N is the Avogadro number divided by 10^3. The decay of BP triplet in all three polymers is nonexponential for the temperature range $T_\beta < T < T_g$, which controlled by both diffusion and chemical steps.

The BP kinetics studies previous are focused on small molecules, either in solution or a polymer matrix. Recently, the development of BP is in the polymer community has focused on BP pendent copolymers, which provide more straightforward synthesis and application. Antifogging,[28] antimicrobial,[29] anti-icing,[30] antifouling[31] surfaces all have been synthesized and stabilized using BP as a monomer component. More functional polymers can be covalently attached to alkyl substrates by incorporation a BP component. However, the kinetics of BP pendent polymer has not yet been investigated.

We investigate the kinetics of BP as a monomer moiety in the zwitterionic copolymer. The ratio of polymer components has significant influence on the rate of BP crosslinking. We

hypothesized the polarity of the polymer matrix would affect the energy level and the reactivity of the BP pendent groups, just like the polarity of solvent to BP derivatives. A series of copolymers have been synthesized by radical polymerization, and the polarity of each polymer has been evaluated by the partition coefficienct, logP. The linear relationship between logP and rate constant of BP was evaluated by zwitterionic polymers with different T_g, and its application range was described. Additionally, BP with different substituent was also incorporated into the polymer chain, and the kinetics was investigated using UV-vis.

Experiment Section

Materials.

2-Methacryloyloxyethyl phosphorylcholine (MPC), diisopropylethylamine, *N, N'*-diisopropylcarbodiimide (DIC), pyrene and 2-(dimethylamino) ethyl methacrylate (DMAEMA) were purchased from Sigma Aldrich, 2,2'-azobis(2-methylpropionitrile) (AIBN), 1-bromobutane (C4), 1-bromododecane (C12), allyl alcohol, 1-bromooctadecane (C18) and n-butyl methacrylate (BMA) were bought from Alfa-Aesar. Isobutyltrichlorosilane (iBTS), 4-hydroxybenzophenone, 4-dimethylaminopyridine (DMAP) were purchased from Tokyo Chemical Industry. Acryloyl chloride was purchased from Beantown. 4-vinyl benzophenone (BP),[30] 4-benzoylbenzoic acid[32] were synthesized according to literature procedures.

Synthesis of 4-acryloylbenzophenone (ABP)

4-hydroxybenzophenone (20 g, 0.1 mol), diisopropylethylamine (19.3 mL, 0.1110 mol), and dichloromethane (80 mL) were added into a round-bottom flask, and the solution was stirred in an ice bath. Acryloyl chloride (9.02 mL, 0.111 mol) solution in dichloromethane (20 mL) was

added to the reaction dropwise. The reaction was carried out at 0 ℃ for 3 h, then room temperature for 5 h. The methylene chloride was removed by rotary evaporation, and the residue was washed with 20% HCl, saturated $NaHCO_3$, then dried over sodium sulfate. The white crystal product was generated by recrystallized in n-hexane with a yield of 91%. The structure of ABP was confirmed by ^{1}H NMR (Figure A1): δ: 7.88 (*m*, 2H); 7.80 (*m*, 2H); 7.60 (*m*, 1H); 7.49 (*m*, 2H); 7.27 (*m*, 2H); 6.65 (*d*, *J*=6.66, 1H); 6.35 (*dd*, *J*=6.35, 9.07, 1H,), 6.07 (*d*, *J*=6.07, 1H).

Synthesis of Prop-2-enyl 4-benzoylbenzonate (PBB)

A mixture of 4-benzoylbenzoic acid (2.5 g, 11 mmol), DIC (2.5 ml, 16 mmol), DMAP (0.1 g, 0.8 mmol), and dry CH_2Cl_2 (25 ml) was stirred for 2 h at 20 ℃ (dimmed light). Allyl alcohol (10 ml) was added, and the mixture stirred at 20 ℃ for 24 h. The mixture was evaporated, the residue taken up in CH_2Cl_2, then the solution was washed with saturated $NaHCO_3$ solution and H_2O. The residue was purified by fast chromatography. ^{1}H NMR (Figure A2): δ: 8.20-8.14 (*m*, 2H); 7.85-7.79 (*m*, 4H); 7.61(*m*, 1H); 7.49 (*m*, 2H), 6.05(*m*, 1H); 5.44 (*ddd*, *J*=17.2, 2.9, 1.0, 1H); 5,32 (*dd*, *J*=10.1, 2.2, 1.0, 1H); 4.86 (*dt*, ^3J=5.3, ^4J=1.0, 2H).

BPMPC Polymer Series Synthesis.

All BPMPC polymers were synthesized by radical polymerization. Appropriate amounts of MPC, BMA, and BP were dissolved in pure EtOH (total monomer concentration: 1mmol mL^{-1}) with initiator AIBN (0.01 mmol mL^{-1}), and the solutions were degassed under argon for 30 min. The polymerization reactions were carried under N_2 flow at 60 ℃ for 16 h. The reactions were stopped by exposing the solution to air, cooled to room temperature. The polymers were

precipitated in ether and dried under vacuum for 12 h to get the white solid products. The structure and monomer ratio are confirmed by ^{1}H NMR in DMSO-d6 (Figure A3).

Quaternary DMAEMA (QDMAEMA) synthesize.

3.37 mL DMAEMA and appropriate bromoalkane (mole ratio: 1:1.2) were added to 15 mL EtOH, and the solution was reflux under 60 ℃ for 1 h then at 68 ℃ for 3 h. The solvent was removed by rotavapor. The solution was cooled to room temperature before adding diethyl ether (35 mL). The crystallized monomer was filtered out, washed with diethyl ether for 3 times, and dried in a vacuum oven at room temperature overnight. The product chemical structure of QDMAEMA was confirmed by ^{1}H NMR (Figure A4). DMAEMA-C_4H_9 (Q4) yield: 72%, δ (DMSO-d6): 6.06 (s, 1H), 5.75 (s, 1H), 4.49 (t, 2H), 3.67 (t, 2H), 3.07(s, 6H), 3.03 (2H), 1.89 (3H), 1.64 (2H), 1.27(2H), 0.91 (3H). DMAEMA-$C_{12}H_{25}$ (Q12) yield, 58%, δ (DMSO-d6): 6.06 (1H), 5.75 (1H), 4.50 (2H), 3.67 (2H), 3.07(6H), 3.03 (2H), 1.89 (3H), 1.65 (2H), 1.27(18H), 0.84 (3H). DMAEMA-$C_{18}H_{37}$ (Q12) yield, 58%, δ ($CDCl_3$): 6.16 (1H), 5.70 (1H), 4.65 (2H), 3.67 (2H), 3.07(6H), 3.03 (2H), 1.96 (3H), 1.65 (2H), 1.26(30H), 0.88 (3H).

MPC- QDMAEMA polymers synthesis.

MPC, QDMAEMA, and BP (mole ratio 3:6:1) were dissolved in EtOH (total monomer concentration: 1 mmol mL^{-1}) with initiator AIBN (0.02 mmol mL^{-1}). The solution was degassed under Argon for 30 min, then polymerized under N_2 flow for 16 h under 60 ^{0}C. The polymer was collected by precipitating in THF, then vacuum at room temperature overnight. White product was received, and ^{1}H NMR was taken to confirm the composition (Figure A5).

Polymer Characterization.

The cross-linking kinetics of all polymers were investigated by UV-vis spectroscopy iBTS functionalized quartz substrates. The quartz slides were sonicated in DI water, iso-propanol, and acetone for 5 min each, followed by plasma (Harrick Plasma PDC-32G) cleaning and treatment with iBTS in toluene (10 mmol) overnight before modification with the polymer. The polymer solution (10 µL, 10 mg mL^{-1}) was cast on alkylated quartz and the solvent allowed to evaporate. The UV-vis spectroscopy was performed on a Cary Bio spectrophotometer (Varian). The UV light sources were a Compact UV lamp (UVP) and FB-UVXL-1000 UV Crosslinker (Fisher Scientific) with bulbs of a wavelength at 254 nm. The substrates were held a certain distance from the light source during irradiation to obtain the power of 6.5 mW cm^{-2}.

The glass transition temperature (T_g) of the copolymer was measured by using a differential scanning calorimeter DSC 250 (TA Instruments). Data was stored and manipulated using the software TRIOS v4.4 (TA Instruments). Samples were scanned at a rate of 10 °C min^{-1}, and the second-heat-scan curves were used for analysis.

The value of logP for each monomer was estimated using the Molinspiration online property calculation toolkit (http://www.molinspiration.com), which based on group contributions and correction factors. The method is very robust and is able to process practically organic, and most organometallic molecules. The copolymer logP was estimated based on the weight average (mole percentage) of each component, eq. (2.2).

$$\log \quad \mathrm{P(copolymer)} = \sum \mathrm{mol\%_i log\ P_i} \tag{2.2}$$

Results and Discussion

The zwitterionic polymers (BPMPC37, BPMPC55, BPMPC73, and BPMPC91, Table 2.1) were synthesized by radical polymerization (Scheme 2.1), and the polymer composition was confirmed by ^{1}H NMR spectroscopy (Figure A3). The monomer unit composition was confirmed based on the following analysis: 3.25 ppm (-N(CH_3)$_3$, 9H) for MPC unit, 1.45-1.63 ppm (-CH_2-, 4H) for the BMA unit, and 6.80-7.85 ppm (benzophenone-H, 9H) for the BP unit. The monomer units in the polymer chain were randomly distributed, with a total composition approximately equal to that of the monomer feeding ratio (Table 2.1).

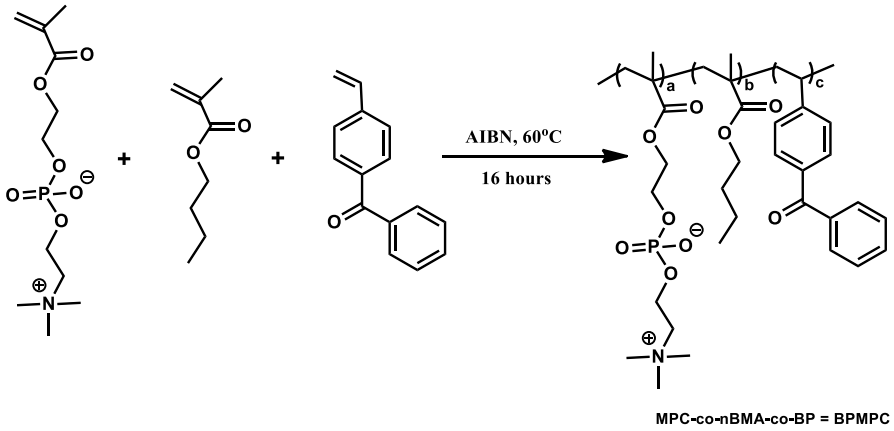

Scheme 2.1. Synthesis of 2-methacryloyloxyethyl phosphorylcholine-co-butyl methacrylate-co-benzophenone (BPMPC).

Table 2.1. Synthetic Results of BPMPC polymers.

	Composition (mol/%) in feed MPC/BMA/BP	Initiator (mmol/ml)	Composition (mol%) in copolymer MPC/BMA/BP	Yield (%)
BPMPC37	3/7/0.5	0.02	27.1/70.6/2.2	88.7
BPMPC55	5/5/0.5	0.02	48.9/48.6/2.5	82.4
BPMPC73	7/3/0.5	0.02	66.7/30.7/2.6	75.6
BPMPC91	9/1/0.5	0.02	76.9/20.0/3	79.1

BP kinetics calculation was based on the intensity of the carbonyl group in the UV-vis spectra. In the context of hydrogen abstraction, the carbonyl group of BP converts to the hydroxide group (Scheme 2.1.3) and the intensity of the absorption peak decrease accordingly. Figure C1 demonstrated the UV-vis spectra of BPMPC37, BPMPC55, BPMPC 73 and BPMPC91 respectively, where the decreasing absorbance of the BP group at 255 nm occurs with increased irradiation time. For BPMPC 37, the absorbance peak completely disappeared in less than 1 min; while for BPMPC 91, the absorbance intensity maintained a small amount even after 10 min irradiation. The decrease of crosslinking rate with the increase of the concentration of MPC can be observed from the UV-vis spectra. Further comparing the kinetics difference between all of the polymers, the conversion of cross-linking reactions was depicted by plotting the decay of absorbance of BP moiety as a function of irradiation time (Figure 2.1). As shown in Figure 2.1, with the increase of MPC percentage in the copolymer, the reactivity of BP crosslinking decreases. As discussed above, the triplet decay and hydrogen abstraction of BP deriviatives in the polymer are affected by temperature and molecular motion of the matrix, free volume distribution (diffusion), and size and shape of the reaction groups. However, BP is a side chain to the polymer

and nearly impossible to diffuse through the polymer matrix in this study. Therefore, the molecule diffusion, size, and shape of the reactive groups are negligible under this senario.

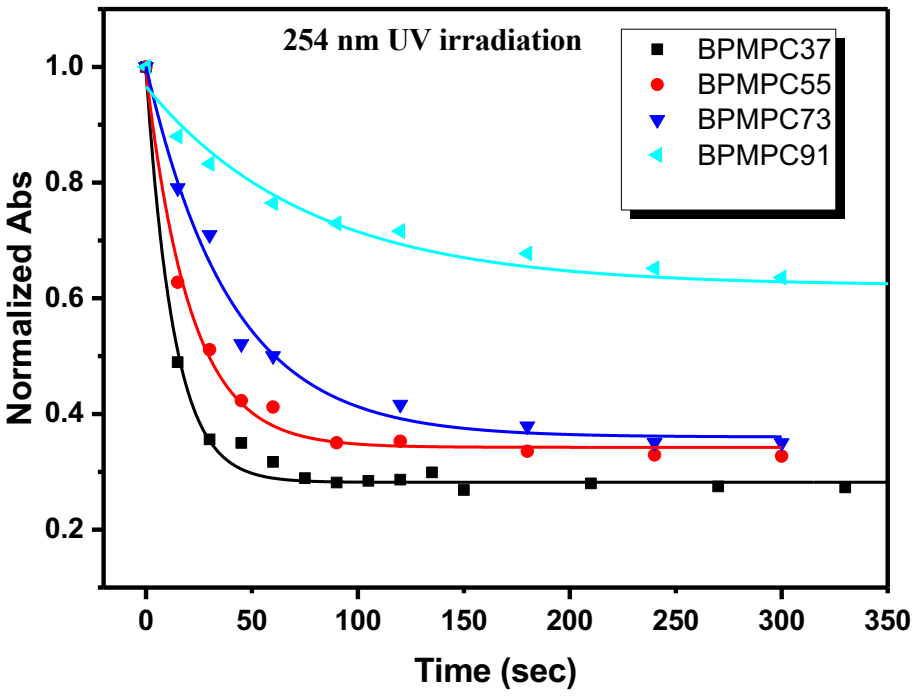

Figure 2.1. BPMPC photo-cross-linking kinetics study by UV-vis spectroscopy.

The thermal properties of BPMPC polymer series were examined by DSC from -60 °C to 180 °C (Figure B1). Previous studies suggested that the glass transition temperature (T_g) of polymer would affect the cross-linking rate of BP derivatives. When the irradiation temperature higher than T_g, the polymer would have sufficient free-volume to encounter surrounding C-H groups in the solid states. On the contrast, when the irradiation temperature lower than T_g, the segment motion would limit which lead to the slow of hydrogen abstraction. Based on DSC results,

the T_g of BPMPC37, BPMPC55, BPMPC73, and BPMPC91 are 53.61 °C, -0.98 °C, 19.58 °C, and 18.65 °C respectively. The UV curing experiments were carried out under room temperature ~ 25℃, and the temperature at the irradiation spot is 49.2°C, which was measured by infrared thermometer. The T_g for all BPMPC polymers are lower or close to the irradiation temperature under continuous UV irradiation, which indicated the polymer side chains have sufficient segmental movement. Literature suggested that the photolysis in polymer film follows a chemically-controlled mechanism for T > T_g as in solution. In all BPMPC polymers, the monomer components are the same, and the only difference is the concentration of each component.

As the concentration of MPC in the polymer matrix increase, the hydrophilicity and polarity of the polymer would increase according. From the past studies, solvent conditions are known as an important parameter to affect the reactivity of BP derivatives. Increasing the solvent polarity can shift the n- π* triplet to the π- π* or CT state, which has a lower reactivity compare to former one. As the π- π* CT state is more polar than the n- π* triplet, its stabilization in polar media is greater, preventing reaction of some BP derivatives in polar solvents. However, some extent of reactivity can be maintained as thermal (vibrational) fluctuation to an n- π* triplet, even if the lowest energy triplet is the π- π* or CT state. The results observed in BPMPC polymers have similarity to BP derivatives in the solvent system. More hydrophilicity of the polymer results in less reactivity of BP crosslinking. Therefore, a hypothesis arises that the hydrophlicity/polarity of polymer matrix would affect cross-linking kinetics of BP pendent copolymer in the similar way as the solvent to BP derivatives.

To calculate the kinetics constant for each polymer, the initial absorbance was normalized to 1 for all polymers, and the data was described by single-exponential decay.

$$A_{normal} = e^{-kt} + A_{\infty} \tag{2.3}$$

Where k is the reaction rate constant, t is the irradiation time, and A_∞ is the constant absorbance in infinite time. According to the kinetics curves, the reaction constant, k, was calculated as showed in Table 2.2. A significant decrease in the value of rate constant can be observed as the increase of MPC percentage. Figure 2.2 (bottom X axis, blue line) exhibited the relation of the percentage of MPC and the kinetics constant, and a deceasing linear correlation can be observed.

Table 2.2. The value of rate constant and logP of BPMPC polymer series.

Polymer	BPMPC37	BPMPC55	BPMPC73	BPMPC91
k (10^{-2} s^{-1})	7.653	4.16	2.502	1.303
log P	0.63542	-1.12982	-2.57553	-3.50188

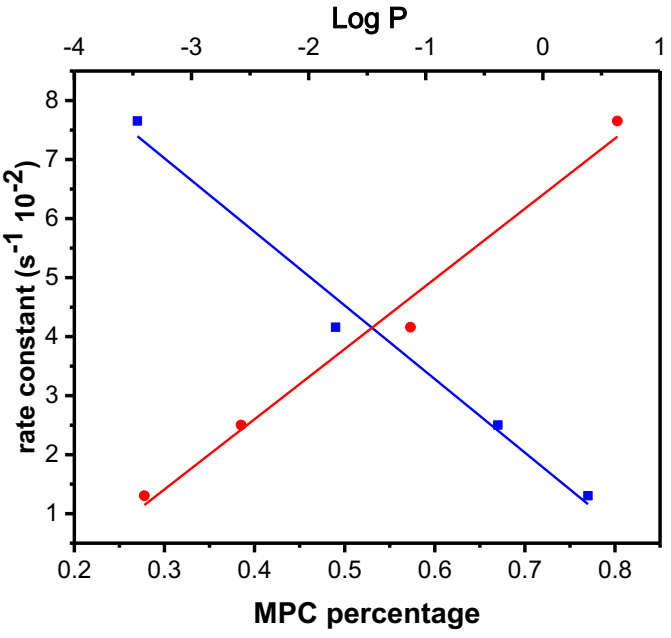

Figure 2.2. The relation of the rate constant with the percentage of MPC (blue line) and logP (red line) in BPMPC polymer.

To further investigate the relationship between polymer polarity and BP kinetics, octanol-water partition coefficients (P) were introduced. Polarity is a complex factor and encompasses a range of non-covalent interactions including dipolarity/polarizability and hydrogen bonding. The polymer polarity was determinated the polarity of the monomers, polymer composition, conformation and configurations. Contact angle measurements were generally used for the investigation of surface polarity (hydrophilic-hydrophobic property) and the polarity of polymer microenvironment can be estimated by the polymer solubility in a binary solvent. Herein, partition coefficients, **P**, were used to estimate the polymer polarity. **P** is a measurement of the different solubility of compound in two immiscible solvents and provides a useful quantitative parameter for representing the lipophilic/hydrophilic nature of the substance. The most commonly used solvent system is octanol/water (Eq. 2.4). A negative value of logP means the compound has a higher affinity for the aqueous phase, and a positive value of logP indicates the compound is more lipophilic. LogP is used in quantitative structure-activity relationship (QSAR) studies and rational drug design as a measure of molecular hydrophobicity and has become a key parameter in studies of the environmental fate of chemicals.[96]

$$\boldsymbol{P} = \frac{[Compond]_{octanol}}{[Compond]_{water}} \tag{2.4}$$

The value of logP for MPC, BMA, and BP is -5.32, 2.81, and 4.24 respectively, and the value of logP for each polymer was calculated based on Eq. 2.2 and listed in Table 2.2. The relationship between logP and rate constant can be described as a linear correction (Figure 2.2, top axis, red line) with a slope of 1.546 and intercept of 6.406 (Eq. 2.5), with a R^2 of 0.98.

$$k = 1.546 \times logP + 6.404 \tag{2.5}$$

In polymer environment, the side chain length is also an important element that can influence a number of physical and chemical properties. To test the validation of the relationship between logP and kinetics coefficient, a zwitterionic copolymer with different side chain length was investigated. A series of quaternized DMAEMA was synthesized by reflux DMAEMA with bromoalkane (Scheme 2.3A). Different length of carbon chain was selected, including C4, C12, and C18. The chemical structure of Q4, Q12, and Q18 were confirmed by ^{1}H NMR. Radical polymerization was also used in the synthesis of a series of MPC-Q polymers (Scheme 2.3B). The ratio of each monomer in MPC-Q was calculated based on the following analysis: 0.8-1.0 ppm (-CH_3, 3H) for QDMAEMA unit; -3.34 ppm (-$N(CH_3)_3$, 9H and -$N(CH_3)_2$, 6H) for MPC and QDMAEMA units, and 6.80-7.85 ppm (benzophenone-H, 9H) for the BP unit. The monomer feed ratios of MPC, QDMAEMA, and BP are fixed as 30%, 60%, and 10% respectively. The resulting ratio in the polymer is slightly different from the input (Table 2.3).

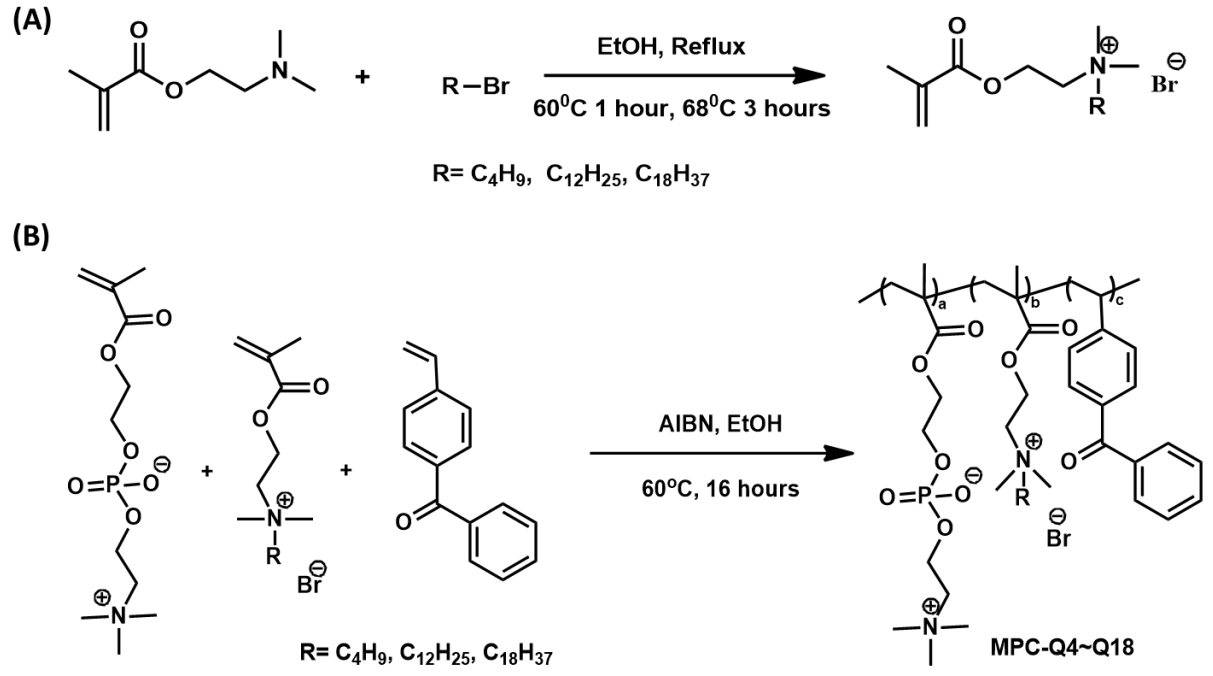

Scheme 2.2. (A) Quaternization of DMAEMA, (B) Polymerization of MPC-QDMAEMA-BP.

Table 2.3. The synthetic results of MPC-Q polymer

	Composition (mol/%) in feed MPC/QDMAEMA/BP	Initiator (mmol/ml)	Composition (mol/%) In copolymer MPC/QDMAEMA/BP	Yield (%)
MPC-Q4	3/6/1	0.02	27.5/66.8/5.7	75.6
MPC-Q12	3/6/1	0.02	26.0/68.8/5.2	67.8
MPC-Q18	3/6/1	0.02	27.5/64.9/7.6	72.3

Kinetics of all MPC-Q polymer was also recorded by UV-vis (Figure C2), and the conversion of crosslinking is calculated by the decreasing of BP absorbance peak as a function of irradiation time (Figure 2.3). MPC-Q18 has the fastest crosslinking rate, the second is MPC-Q12, and MPC-Q4 has the slowest rate. The same single-exponential decay model was used to calculate the kinetics constant (k) for MPC-Q polymer series and the same equation was used for the calculation of logP (Table 2.4). The logP value for Q4, Q12, and Q18 are -1.14, 2.90, and 5.93 respectively.

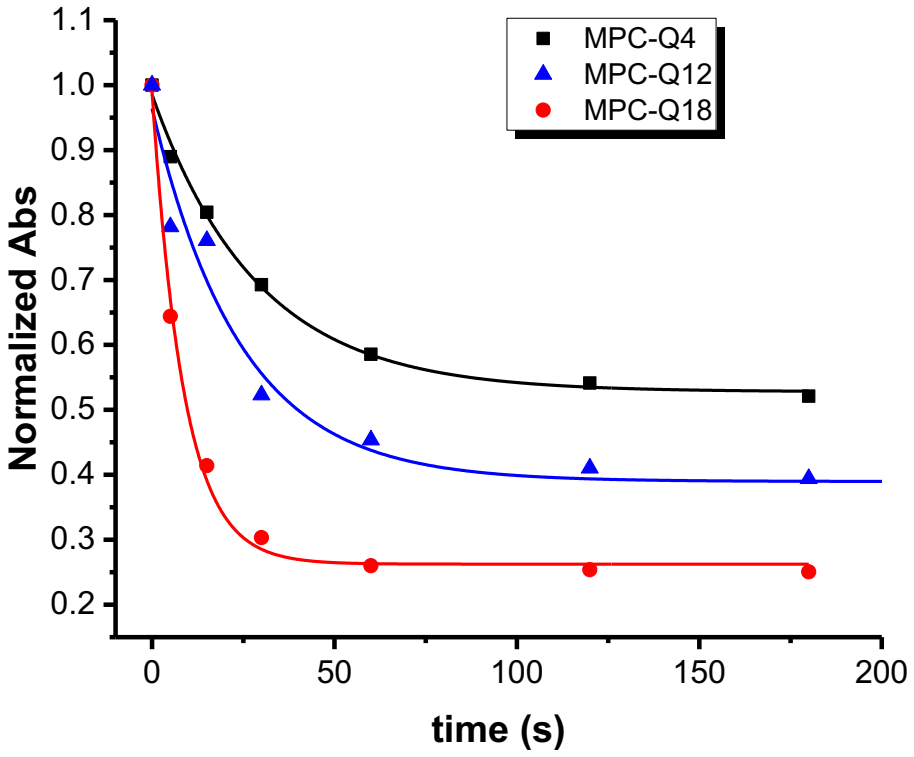

Figure 2.3. MPC-Q4~18 photo-cross-linking kinetics study by UV-vis spectroscopy

$k_{calc.}$ was generated by the Eq. 2.5 using the logP of the polymer and demonstrated outstanding predication in MPC-Q4 and MPC-Q18. However, the value of $k_{calc.}$(MPC-Q8) is about twice that ovserved in the experimental data.

Table 2.4. Rate constant (k) for MPC-Q polymers

Polymer	MPC-Q4	MPC-Q12	MPC-Q18
logP	-1.98	0.83	2.71
$\boldsymbol{k_{calc.}}$ **(10^{-2} s^{-1})**	3.34	7.69	10.59
$\boldsymbol{k}$ **(10^{-2} s^{-1})**	3.475	4.131	11.517

To explain these results, the thermal properties of MPC-Q polymers were investigated by DSC. According to DSC traces, the T_g , T_c and T_m for MPC-Q4 are -1 °C ,88°C and 133 °C respectively; T_g for MPC-Q12 is 121 °C; and the T_m for MPC-Q18 is 12 °C (Figure B2). Though the T_g for MPC-Q18 was not detected during the measuring range (-60 °C to 180 °C), a very low T_g can be anticipated based on the value of T_m. MPC-Q4 and MPC-Q18 have a T_g lower than room temperature, which is similar to the situation of BPMPC discussed above. When T > T_g, the crosslinking rate was mainly controlled by the chemical environment. Therefore, the equation demonstrated a good fit for MPC-Q4 and MPC-Q18, and the rate constants calculated ($k_{calc.}$) based on logP was very close to the experimental values. However, the T_g of MPC-Q12 is 121.28 °C, which is much higher than room temperature and the temperature at irradiation spot. As a result, the chain segment movement in MPC-Q12 was restricted, and the BP photoreaction would not proceed like that found in solution. Hence, the actual rate constant of MPC-Q12 (k) was only half of the calculated value, due to the molecular motion in the polymer matrix. The linear correlation between logP and k is only effective for the zwitterionic copolymer with relatively low T_g, in which the kinetics was dominated by the polarity of polymer matrix.

Substituent effects also play a significant role in influence the kinetics of BP derivatives. Generally, electron-withdrawing groups increase the reactivity of n-π* radicals, while electron-donating groups have the opposite effect, inhibiting H-abstraction. To exam the influence of BP ring substitution in the zwitterionic copolymer, BPA and PBB were synthesized with opposite effect substituent (Scheme 2.3A-B). Poly(MPC-BMA-ABP) (ABPMPC), and poly(MPC-BMA-PBB) (PBBMPC) were produced using the same procedure as BPMPC73. The MPC percentage

was fixed as 70% in three polymers and the only difference is the substituent group on BP rings (Scheme 2.3 C).

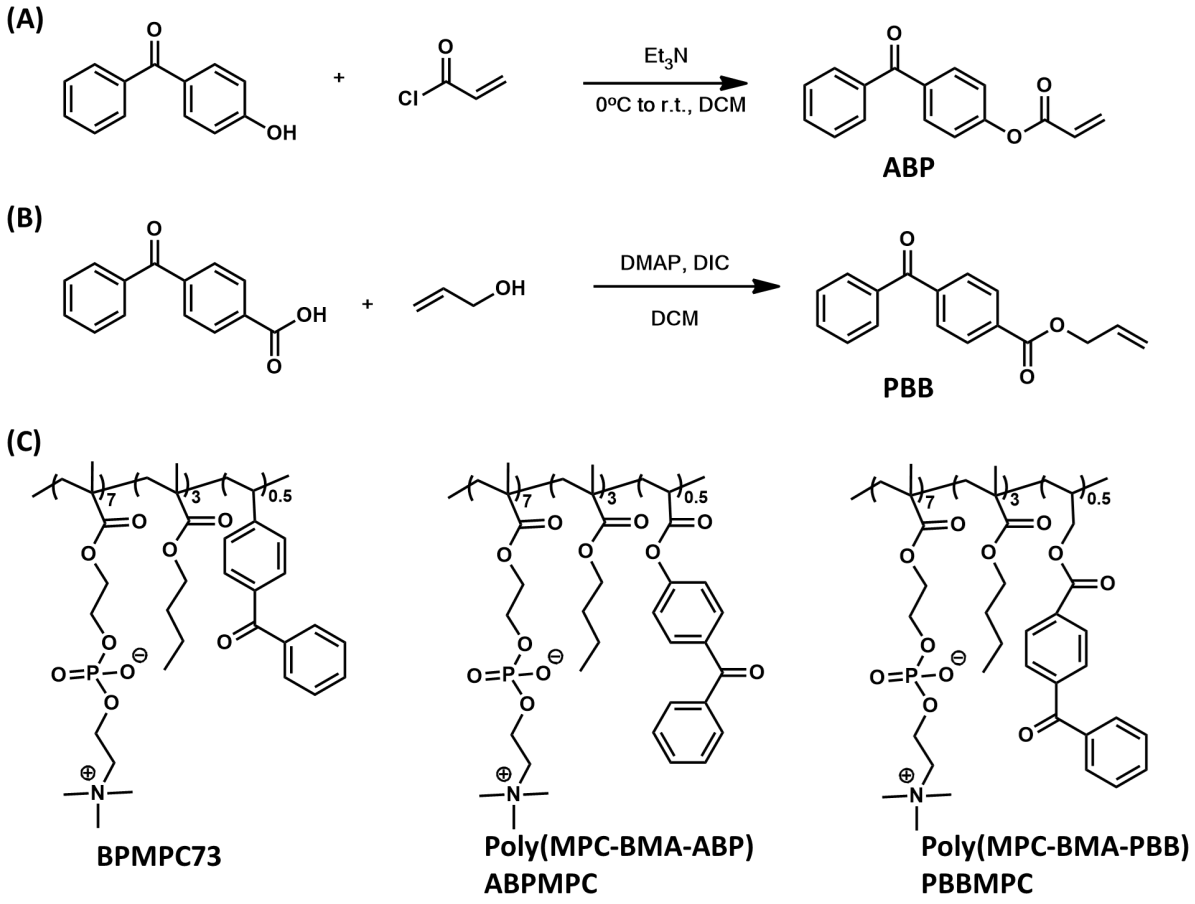

Scheme 2.3. (A) synthesis of 4-acryloylbenzophenone (ABP); (B) Synthesis of Prop-2-enyl 4-benzoylbenzonate (PBB); (C) chemical structures of polymers BPMPC73, poly(MPC-BMA-ABP) (ABPMPC), and poly(MPC-BMA-PBB) (PBBMPC).

UV-vis spectra were recorded to demonstrate the influence of substituent group on BP to crosslinking kinetics (Figure C3), in which ABPMPC with an electron donating group demonstrated slower crosslinking rate than BPMPC73, and PBBMPC exhibited higher reactivity

than BPMPC73 with an electron withdrawing group. These results indicated the substituent effects for BP kinetics is still effective for BP pendent copolymer and should be taken into consideration for polymer designing.

Conclusion

The BP crosslinking kinetics in BP pendent zwitterionic copolymers was investigated, and the factors that affect the reactivity were discussed in this chapter. The polarity of the polymer matrix significantly influences the BP crosslinking rate similar to that of BP deriviatives in the solvent systems. The rate constant follows a linear relation with the value of polymer polarity for a specific condition, in which the zwitterionic polymer has a T_g lower or close to the temperature of irradiation spot. Under these circumstances, the chemical environment dominates the BP reactivity. However, for the zwitterionic polymer with a higher T_g, the segmental movement was restricted, and the thermal properties control the BP kinetics. Additionally, the substituents on BP demonstrates the same effects in polymer side chains as in small molecules in solution.

References

1. Allen, N. S.; Marin, M. C.; Edge, M.; Davies, D. W.; Garrett, J.; Jones, F.; Navaratnam, S.; Parsons, B. J., Photochemistry and photoinduced chemical crosslinking activity of type I & II co-reactive photoinitiators in acrylated prepolymers. *J Photoch Photobio A* **1999,** *126* (1-3), 135-149.

2. Carroll, G. T.; Sojka, M. E.; Lei, X. G.; Turro, N. J.; Koberstein, J. T., Photoactive additives for cross-linking polymer films: Inhibition of dewetting in thin polymer films. *Langmuir* **2006,** *22* (18), 7748-7754.

3. Doytcheva, M.; Dotcheva, D.; Stamenova, R.; Orahovats, A.; Tsvetanov, C.; Leder, J., Ultraviolet-induced crosslinking of solid poly(ethylene oxide). *J Appl Polym Sci* **1997,** *64* (12), 2299-2307.

4. Pappas, S. P.; Fischer, R. M., Photochemistry of Pigments - Studies on Mechanism of Chalking. *J Paint Technol* **1974,** *46* (599), 65-72.

5. Qu, B. J.; Xu, Y. H.; Ding, L. H.; Ranby, B., A new mechanism of benzophenone photoreduction in photoinitiated crosslinking of polyethylene and its model compounds. *J Polym Sci Pol Chem* **2000,** *38* (6), 999-1005.

6. Ruhe, J.; Madge, D., Grafting of polymers to solid surfaces using self-assembled monolayers with polymerizable groups. *Abstr Pap Am Chem S* **2003,** *225*, U684-U684.

7. Ruhe, J.; Seidel, K.; Toomey, R., Surface-attached polymer networks: Synthesis and swelling behavior. *Abstr Pap Am Chem S* **2004,** *227*, U861-U861.

8. Demeter, A.; Berces, T., Study of the Long-Lived Intermediate Formed in the Photoreduction of Benzophenone by Isopropyl-Alcohol. *J Photoch Photobio A* **1989,** *46* (1), 27-40.

9. Demeter, A.; Berces, T., Direct Kinetic-Study of Radical Transformation Reaction Me2coh + Ph2co-]Me2co + Ph2coh. *J Phys Chem-Us* **1991,** *95* (3), 1228-1232.

10. Demeter, A.; Laszlo, B.; Berces, T., Kinetics of Ketyl Radical Reactions Occurring in the Photoreduction of Benzophenone by Isopropyl-Alcohol. *Ber Bunsen Phys Chem* **1988,** *92* (12), 1478-1485.

11. Porter, G.; Suppan, P., Primary Photochemical Processes in Aromatic Molecules .12. Excited States of Benzophenone Derivatives. *T Faraday Soc* **1965,** *61* (512p), 1664-&.

12. Bhasikuttan, A. C.; Singh, A. K.; Palit, D. K.; Sapre, A. V.; Mittal, J. P., Laser flash photolysis studies on the monohydroxy derivatives of benzophenone. *J Phys Chem A* **1998,** *102* (20), 3470-3480.

13. Singh, A. K.; Bhasikuttan, A. C.; Palit, D. K.; Mittal, J. P., Excited-state dynamics and photophysical properties of para-aminobenzophenone. *J Phys Chem A* **2000,** *104* (30), 7002-7009.

14. Ghoneim, N.; Monbelli, A.; Pilloud, D.; Suppan, P., Photochemical reactivity of para-aminobenzophenone in polar and non-polar solvents. *J Photoch Photobio A* **1996,** *94* (2-3), 145-148.

15. Li, W.; Xue, J. D.; Cheng, S. C.; Du, Y.; Phillips, D. L., Influence of the chloro substituent position on the triplet reactivity of benzophenone derivatives: a time-resolved resonance Raman and density functional theory study. *J Raman Spectrosc* **2012,** *43* (6), 774-780.

16. Aspari, P.; Ghoneim, N.; Haselbach, E.; vonRaumer, M.; Suppan, P.; Vauthey, E., Photoinduced electron transfer between triethylamine and aromatic carbonyl compounds: The role of the nature of the lowest triplet state. *J Chem Soc Faraday T* **1996,** *92* (10), 1689-1691.

17. Turro, N. J. R., V.; Scaiano, J. C., *Principles of Molecular Photochemistry: an Introduction*. University Science Books: Herndan, VA, 2009.

18. Sergentu, D. C.; Maurice, R.; Havenith, R. W. A.; Broer, R.; Roca-Sanjuan, D., Computational determination of the dominant triplet population mechanism in photoexcited benzophenone. *Phys Chem Chem Phys* **2014,** *16* (46), 25393-25403.

19. Dorman, G.; Nakannura, H.; Pulsipher, A.; Prestwich, G. D., The Life of Pi Star: Exploring the Exciting and Forbidden Worlds of the Benzophenone Photophore. *Chem Rev* **2016,** *116* (24), 15284-15398.

20. Katchalsky, A.; Kunzle, O.; Kuhn, W., Behavior of Polyvalent Polymeric Ions in Solution. *J Polym Sci* **1950,** *5* (3), 283-300.

21. Kuhn, W.; Kunzle, O.; Katchalsky, A., *Denouement De Molecules En Chaines Polyvalentes Par Des Charges Electriques En Solution. *B Soc Chim Belg* **1948,** *57* (10-1), 421-431.

22. Kunzle, O., Einfluss Mittlerer Ionenkonzentrationen Auf Die Elektrostatische Energie Von Fadenmolekulionen in Losung. *Recl Trav Chim Pay B* **1949,** *68* (9-10), 699-716.

23. Kuhn, W.; Hargitay, B.; Katchalsky, A.; Eisenberg, H., Reversible Dilation and Contraction by Changing the State of Ionization of High-Polymer Acid Networks. *Nature* **1950,** *165* (4196), 514-516.

24. Eisenbach, C. D., Cis-Trans Isomerization of Aromatic Azo-Compounds Built in the Polyester Segment of Poly(Ester Urethanes). *Polym Bull* **1979,** *1* (7), 517-522.

25. Menju, A.; Hayashi, K.; Irie, M., Photoresponsive Polymers .3. Reversible Solution Viscosity Change of Poly(Methacrylic Acid) Having Spirobenzopyran Pendant Groups in Methanol. *Macromolecules* **1981,** *14* (3), 755-758.

26. Horie, K.; Mita, I., Reactions and Photodynamics in Polymer Solids. *Adv Polym Sci* **1989,** *88*, 77-128.

27. Horie, K.; Morishita, K.; Mita, I., Photochemistry in Polymer Solids .3. Kinetics for Nonexponential Decay of Benzophenone Phosphorescence in Acrylic and Methacrylic Polymers. *Macromolecules* **1984,** *17* (9), 1746-1750.

28. Liu, Q. H.; Locklin, J., Transparent Grafted Zwitterionic Copolymer Coatings That Exhibit Both Antifogging and Self-Cleaning Properties. *Acs Omega* **2018,** *3* (12), 17743-17750.

29. Gao, J.; Huddleston, N. E.; White, E. M.; Pant, J.; Handa, H.; Locklin, J., Surface Grafted Antimicrobial Polymer Networks with High Abrasion Resistance. *Acs Biomater Sci Eng* **2016,** *2* (7), 1169-1179.

30. Gao, J.; Martin, A.; Yatvin, J.; White, E.; Locklin, J., Permanently grafted icephobic nanocomposites with high abrasion resistance. *J Mater Chem A* **2016,** *4* (30), 11719-11728.

31. Liu, Q. H.; Singha, P.; Handa, H.; Locklin, J., Covalent Grafting of Antifouling Phosphorylcholine-Based Copolymers with Antimicrobial Nitric Oxide Releasing Polymers to Enhance Infection-Resistant Properties of Medical Device Coatings. *Langmuir* **2017,** *33* (45), 13105-13113.

32. Chen, H. S.; Kuo, S. C.; Teng, C. M.; Lee, F. Y.; Wang, J. P.; Lee, Y. C.; Kuo, C. W.; Huang, C. C.; Wu, C. C.; Huang, L. J., Synthesis and antiplatelet activity of ethyl 4-(1-benzyl-1H-indazol-3-yl)benzoate (YD-3) derivatives. *Bioorgan Med Chem* **2008,** *16* (3), 1262-1278.

33. Sangster, J., Octanol-Water Partition-Coefficients of Simple Organic-Compounds. *J Phys Chem Ref Data* **1989,** *18* (3), 1111-1229.

CHAPTER 3

COVALENT GRAFTING OF ANTIFOULING PHOSPHORYLCHOLINE-BASED COPOLYMERS WITH ANTIMICROBIAL NITRIC OXIDE RELEASING POLYMERS TO ENHANCE INFECTION-RESISTANT PROPERTIES OF MEDICAL DEVICE COATINGS[1]

[1]Accepted by [Liu, Q.; Singha, P.; Handa, H.; Locklin, J.; "Covalent Grafting of Antifouling Phosphorylcholine-Based Copolymers with Antimicrobial Nitric Oxide Releasing Polymers to Enhance Infection-Resistant Properties of Medical Device Coatings" Langmuir, 2017, 33 (45), 13105-13113]. Reprinted here with permission of publisher.

Abstract

Medical device coatings that resist protein adhesion and bacterial contamination are highly desirable in the healthcare industry. In this work, an antifouling zwitterionic terpolymer, 2-methacryloyloxyethyl phosphorylcholine-co-butyl methacrylate-co-benzophenone (BPMPC), is covalently grafted to a nitric oxide (NO) releasing antimicrobial biomedical grade copolymer of silicone-polycarbonate-urethane, CarboSil, to significantly enhance the biocompatibility, non-specific protein repulsion and infection-resistant properties. The NO donor embedded into CarboSil is S-nitroso-N-acetylpenicillamine (SNAP) and covalent grafting of the BPMPC is achieved through rapid UV-crosslinking, providing a stable, hydrophilic coating that has excellent durability over a period of several weeks under physiological conditions. The protein adsorption test results indicate a significant reduction (~84-93%) of protein adhesion on the test samples compared to the control samples. Bacteria tests were also performed using the common nosocomial pathogen, Staphylococcus aureus. Test samples containing both NO donor and BPMPC show a 99.91 ± 0.06 % reduction of viable bacteria when compared to control samples. This work demonstrates a synergistic combination of both antimicrobial and antifouling properties in medical devices using NO donors and zwitterionic copolymers that can be covalently grafted to any polymer surface.

Introduction

The non-specific adsorption of proteins has long been considered a grand challenge in many biomedical applications such as implants, contact lenses, catheters, and biosensors. In addition to medical device failure, the consequences of protein adsorption include thrombus formation, innate immune response, and bacterial infection.[1-2] Preventing direct microbial contamination is also highly desired characteristic of medical devices, implants, and hospital equipment.[3-6] Although significant progress has been made in understanding and reducing adsorption and contamination, the Centers for Disease Control and Prevention (CDC) still reported that, in 2011, there were an estimated 722,000 healthcare-associated infections (HAIs) in U.S. acute care hospitals. Additionally, about 75,000 patients with HAIs died during their hospitalization.[7] On any given day, approximately 1 out of every 25 patients in the U.S. contracts at least one infection during their hospital care. Therefore, materials demonstrating antifouling and antimicrobial effects are highly desirable.

In recent years, zwitterionic polymers have attracted attention due to their biomimetic nature, which provides excellent biocompatibility and antifouling properties compared to traditional materials like poly(ethylene glycol) (PEG).[8-10] Zwitterionic polymers, in which both cationic and anionic groups are on the same monomer residue, have a strong hydration ability which accounts for their ultra-low fouling properties.[11-16] The dipole arrangement of water molecules in the hydration shell formed via electrostatic interactions with the charged groups of the zwitterion are closer to free water than the directional arrangement of water molecules in the hydration shell formed via hydrogen bonds in case of PEG.[17] The excellent hydrophilicity of zwitterionic polymers, however, provides a difficult challenge in coating hydrophobic materials,

where coating delamination under physiological conditions has so far limited practical application.[18]

To explore the covalent grafting of zwitterionic polymers to various substrates ranging from hydrophilic to hydrophobic, we incorporated the benzophenone (BP) chromophore, a photoactive tethering reagent, into the polymeric backbone.[19-24] The BP group can produce a diradical under low-intensity UV irradiation (350-365 nm) that abstracts an aliphatic hydrogen from a neighboring C-H bond to form a new C-C bond, without intensive UV oxidative damage to the polymer or substrates.[20] Through this process, network polymer films can be grafted with excellent durability to a broad selection of C-H containing materials and surfaces, and has been used for many applications such as microfluidics,[25-26] organic semiconductors,[27] redox polymers,[28-29] anti-icing polymers,[30] and biosensors.[31-32]

Nitric oxide (NO) is known as a potent and nonspecific bactericidal agent due to its natural broad-spectrum antimicrobial properties with low risk for promoting bacterial resistance.[33-35] NO utilizes several antimicrobial mechanisms including nitrosation of amines and thiols, lipid peroxidation, tyrosine nitration and DNA cleavage.[36] Major classes of current NO donors include organic nitrates, metal-NO complexes, N-nitrosamines, and S-nitrosothiols,[37] S-nitroso-N-acetylpenicillamine (SNAP), a commonly studied NO donor, exhibits significant antimicrobial and antithrombotic effects.[38-39] In our previous studies, SNAP has been successfully doped into CarboSil polymer films, and these SNAP-doped polyurethane-based materials can release NO for extended periods (20 days) with very low levels of leaching.[38, 40-41]

In this work, we synthesized zwitterionic terpolymers (2-methacryloyloxyethyl phosphorylcholine-co-butyl methacrylate-co-benzophenone, BPMPC) that can be covalently grafted to antimicrobial, NO-releasing CarboSil (silicone-polycarbonate-urethane thermoplastic)

upon UV-irradiation. The polymer-coated surfaces are characterized in detail and the zwitterionic stability is assessed under physiological conditions. The protein repellency properties of these coatings are evaluated. At the same time, no SNAP degradation was observed during coating or UV irradiation, and the release profile remained above the physiological level for 2 weeks with the zwitterionic top-coat. Moreover, enhanced antimicrobial activity was demonstrated with bacteria testing.

Materials and Methods

Materials.

4-vinylbenzophenone (BP) was synthesized according to a previously reported method.[30] 2-Methacryloyloxyethyl phosphorylcholine (MPC), albumin from bovine serum (BSA), fluorescein isothiocyanate labeled bovine serum albumin (FTIC-BSA), N-acetyl-D-penicillamine (NAP), sodium nitrite ($NaNO_2$), concentrated sulfuric acid (conc. H_2SO_4), tetrahydrofuran (THF), sodium phosphate monobasic (NaH_2PO_4), sodium phosphate dibasic (Na_2HPO_4), potassium chloride, sodium chloride, and ethylenediamine tetraacetic acid (EDTA) were purchased from Sigma Aldrich (St. Louis, MO). 2,2'-azobis(2-methylpropionitrile) (AIBN) and n-butyl methacrylate (BMA) were bought from Alfa-Aesar (Haverhill, MA). Isobutyltrichlorosilane was purchased from Tokyo Chemical Industry (Portland, OR). Concentrated hydrochloric acid (conc. HCl), sodium hydroxide (NaOH), and methanol were bought from Fisher-Scientific (Hampton, NH). Potassium phosphate monobasic (KH_2PO_4) and lysozyme from egg white were purchased from BDH Chemicals - VWR International (West Chester, PA). CarboSilTM 20 80A UR STPU (referred to as CarboSil hereon) was acquired from DSM Biomedical Inc. (Berkeley, CA). Milli-Q filter was used to obtain de-ionized (DI) water for all the aqueous solution preparations. Nitrogen

and oxygen gas cylinders were purchased from Airgas (Kennesaw, GA). Staphylococcus aureus (ATCC 6538, *S. aureus*) was used for the bacterial experiments. LB Agar (LA), Miller and Luria broth (LB), Lennox were purchased from Fischer BioReagents (Fair Lawn, NJ). All the chemicals were used without further purification.

In brief, CarboSil polymers with 10 wt % SNAP (test samples) and no SNAP content (control samples) were prepared using solvent evaporation and/or spin coating method. These samples were then coated with a zwitterionic copolymer (referred to as BPMPC) which was covalently bonded to the CarboSil base polymers by UV-crosslinking. Surface analysis was performed on the films pre- and post- UV radiation to understand the crosslinking behavior of the polyzwitterionic system. Test and control samples with the BPMPC coating were analyzed for their NO release behavior. The samples were then tested for protein adhesion for 14 days in physiological conditions (37°C in PBS) to evaluate antifouling properties of the topcoat. Finally, antimicrobial assay of the samples was done using a modified version of ASTM E2180 protocol.

Synthesis of NO donor, SNAP. S-nitroso-N-acetylpenicillamine was synthesized using a revised approach for a method previously reported.[38] 1M H_2SO_4 and 1M HCl were mixed with an equimolar amount of NAP, methanol and $NaNO_2$ aqueous solution. This reaction mixture was stirred for 20 minutes and then cooled for 7 hours with a constant flow of air on the mixture. After evaporation of the unreacted portion of the reaction mixture, precipitated green crystals of SNAP were filtered, collected and dried in a covered vacuum desiccator. Dried crystals of SNAP were used for all experiments.

Synthesis of CarboSil Films Doped with SNAP.

CarboSil films containing 10 wt % SNAP were prepared using solvent evaporation method. 700 mg of CarboSil was dissolved in 10 mL of THF to make the polymer solutions. 77 mg of SNAP was added to this solution for a final concentration of 10 wt % of SNAP. This polymer-SNAP blend was stirred in dark conditions until the SNAP crystals dissolved completely. The blend was then transferred into Teflon molds and allowed to let the solvent evaporate overnight in fume hood. The overnight dried films were then cut into circular shapes of 0.8 cm diameter each. Each sample was immersed into a CarboSil solution without SNAP (40 mg mL-1 of polymer concentration in THF) to coat it (this was repeated thrice for each sample). The samples were dried overnight and then dried under vacuum for an additional 24 hours. This added drying time was included to eliminate any remaining THF which can affect any following studies. Weight of each film was recorded before the topcoat application for all SNAP leaching behavior tests. The formulated samples were stored in the freezer (-18°C) in the dark between experiments to prevent escape of SNAP or consequent loss of NO. These SNAP-incorporated films were used for NO release, SNAP leaching and bacterial cell viability analyses. All samples used for the tests were less than a week old to ensure integrity of studies.

Synthesis of Zwitterionic Copolymer (BPMPC).

The polymer was synthesized by free radical polymerization. MPC (0.546 g, 1.85 mmol), n-BMA (0.105 mL, 0.66 mmol) and BP (0.027 g, 0.132 mmol) were dissolved in 5.3 mL ethanol (total monomer concentration 1.0 mmol mL^{-1}) with initiator AIBN (0.01 mmol mL^{-1}) and the solution was poured into polymerization tube. After degassed with argon for 30 minutes, the polymerization reaction was carried out under nitrogen flow at 60℃ for 16 h. The reaction was

stopped by exposing the solution to air, cooled to room temperature, and poured into ethyl ether to precipitate the polymer. The white solid was collected by vacuum filtration and dried under vacuum for 12 h. Yield: 0.552 g, 83%. ^{1}H NMR (D_2O) was taken to confirm the polymer composition (Figure A6).

Crosslinking of BPMPC with Substrates.

Silicon substrates were cut into 2.4cm×2.4cm pieces and sonicated with deionized water, isopropanol, and acetone for 5 min each then dried under nitrogen, followed by plasma (Harrick Plasma PDC-32G) clean and treated with iBTS in toluene overnight before modification with the polymer. CarboSil substrates were coated with polymer without pretreatment.

Two coating method were utilized when applying BPMPC on substrates: spin coating and spray coating. For spin coating, polymer modified film was developed on functionalized silicon substrate by using 0.5 mL BPMPC/ethanol solution (10 mg mL^{-1}) at 1000 rpm for 30 seconds. Spray coating was applied for CarboSil films with and without SNAP. BPMPC/ethanol solution (2 mg mL^{-1}) was sprayed using a spray gun from a distance of 10 cm onto vertically placed substrates to achieve uniform coating upon drying. We used spin coating in the protein adsorption experiments, and spray coating in SNAP/NO release and bacterial experiments, based on method that afforded the smoothest, pin-hole free coating on different forms of substrate. Then the BPMPC substrates were irradiated with UV light (UVP, 254 nm, 6.5 mW cm^{-2}) for 1 min to covalently bond the BPMPC to the surface. The substrates were rinsed with abundant ethanol to remove unattached BPMPC then dried under nitrogen.

Characterization of the polymer coatings.

The surface wettability was characterized by measuring the static water contact angle, which obtained from a DSA 100 drop shape analysis system (KRŰSS) with a computer-controlled liquid dispensing system. 1 μL DI water droplets were deposited onto substrate surfaces, and the water contact angles were measured within 10 seconds through the analysis of photographic images. The cross-linking kinetics of BPMPC coating was investigated by a UV-vis spectroscopy (Varian) with 254 nm UV light. The thickness of the spin-coated polymer layer on the silicon substrates and CarboSil substrates were measured by M-2000V Spectroscopic Ellipsometer (J.A. Woollam co., INC.) with a white light source at three incident angles (65°, 70°, and 75°). The thickness of the modified layer was measured and calculated using a Cauchy layer model. Infrared spectroscopy studies of polymer coated films were done using a Thermo-Nicolet model 6700 spectrometer equipped with a variable angle grazing angle attenuated total reflection (GATR-ATR) accessory (Harrick Scientific).

SNAP Leaching Study and NO-Release Profile.

The percentage of SNAP discharged from the samples were quantified by noting the absorbance of the PBS solutions (used to soak the samples) at 340 nm (characteristic absorbance maxima of S-NO group of SNAP). Each sample was weighed before coating with non-SNAP polymer solutions to determine the initial amount of SNAP in each film. The films were then immersed in vials containing PBS (pH 7.4 with 100 μM EDTA to prevent catalysis of NO release by metal ions) and stored at 37°C. A UV-vis spectrophotometer (Thermoscientific Genesys 10S UV-vis) was utilized to quantify the absorbance of the buffer solutions in the required time intervals. The readings were converted to wt % of SNAP in the buffer utilizing the initial amount

of SNAP present in each sample. 1 mL aliquots of the PBS solution in which the samples were soaked was used for each sample absorbance measurement to avoid any inconsistent readings and three replicates were utilized for each quantification. The calibration graph with known amounts of SNAP in PBS (with EDTA) was used to interpolate the absorbance quantifications recorded from the study and convert them to concentrations of SNAP in the quantified sample.

SNAP incorporated in the polymers release NO in physiological conditions and this release was measured and recorded in real time for the study using Sievers chemiluminescence NO analyzers® (NOA 280i, GE Analytical, Boulder, CO, USA). The sample holder maintained dark conditions for the samples to prevent catalysis of the NO production by any light source. It was filled with 5 mL of PBS (pH 7.4 with 100µM of EDTA) to soak the samples. EDTA acted as a chelating agent to prevent catalysis of NO production by metal ions in the PBS. This buffer solution was maintained at 37°C by a temperature-regulated water jacket placed around the sample holder. Once a baseline of NO flux without the sample (prepared according to section 2.4.) is established, the sample is then placed in the sample holder. Nitric oxide released by the sample in the sample holder was pushed and purged towards the analyzer by a continuous supply of nitrogen gas maintained at a constant flowrate of 200 mL min-1 through the sweep and bubble flows. The NO released by the sample is pushed towards the chemiluminescence detection chamber where the reactions shown on Figure 3.1 take place.

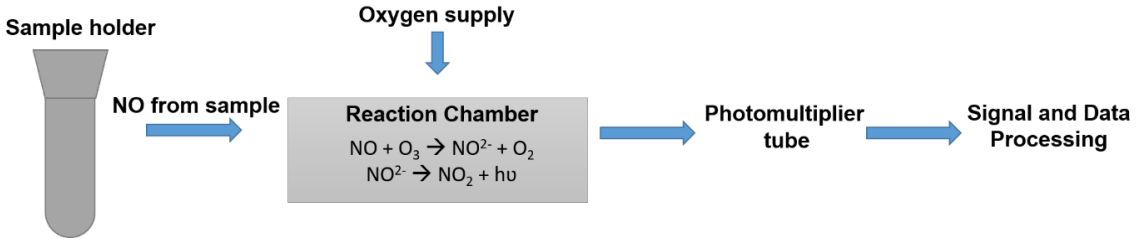

Figure 3.1. Nitric oxide chemiluminescence analyzer flowchart

The voltage signal produced is converted to concentration of NO and displayed on the analyzer's screen. Using the raw data in ppb form and NOA constant (mol ppb^{-1} s^{-1}), the data in ppb is normalized for surface area of the sample and converted to NO flux units (x 10^{-10} mol cm^{-2} min^{-1}). Data was collected in the time intervals mentioned and samples were stored in a PBS (with EDTA) solution at 37°C in dark conditions between measurements. The PBS was replaced daily to avoid any accumulation of SNAP leached or NO released during the storage time. The instrument operating parameters were a cell pressure of 7.4 Torr, a supply pressure of 6.1 psig and a temperature of −12 °C. Three replicates were used for each measurement.

Protein Adhesion Assay.

Protein adsorption test is a significant important method for evaluating the blood adhesion. Therefore, the thickness change of substrates before and after incubation in protein solutions was monitored, as an indication of protein adsorption. Coated substrates were incubated in fibrinogen (1 mg mL^{-1}) and lysozyme (1 mg mL^{-1}) in PBS (pH 7.4, 0.01 M) solutions up to 14 days, followed by thickness measurement every day.

In the second approach, fluorescein isothiocyanate-bovine serum albumin (FITC-BSA, 2 mg mL^{-1}) in PBS solution was used to evaluate the protein adsorption behavior on the surface of CarboSil substrate modified by BPMPC.[42-43] Substrates were immersed in FITC-BSA solution for one and half hour at 37℃, then rinsed with distilled water and dried with nitrogen. The substrates with protein then analyzed by Nikon Eclipse NI-U fluorescence microscope (Nikon Instruments, Inc.), using a 5x objective lens, with filter set (Ex/Em 470/525nm). To confirm the long-term

resistance to protein adsorption, the substrates were incubated in BSA (1 mg ml^{-1}) PBS solution for up to 7 days at 37℃ before putting in FITC-BSA solution.

Bacterial Assay.

Bacterial adhesion for each of the samples was calculated in terms of the bacterial cell viability using serial dilution after an incubation period of 24 hours. The method used to perform this assay was based on a modified version of the American Society for Testing and Materials E2180 protocol. S. aureus was used for antimicrobial evaluation of the samples. Bacteria were cultured in LB Broth (Lennox) at 37°C and grown to ~10^6 colony-forming units (CFU) per mL as measured by optical density. The resulting overnight culture was collected by centrifugation (2500 g, 7 min) and resuspended in PBS. This resuspended bacterial suspension was used for incubation of polymer samples for 24 hours.

After incubation with the bacterial solution, samples were washed gently with PBS to remove any unbound bacteria. The samples were then placed in 1 mL of PBS and homogenized for 1 minute each to transfer any adhered bacteria to this new PBS solution. After homogenization, homogenate samples were serially diluted and plated onto LB Agar nutrient plates (37°C). Bacterial viability was determined by counting the colonies on each plate manually. Calculation of bacterial adhesion was done by counting number of colonies per cm^2 of each sample.

Statistical Analysis.

All data are quantified as mean ± standard deviation with an $n \geqslant 3$ for all trials. The results between the control and test films were analyzed by a comparison of means using student's t-test. Values of p were obtained for the data analyzed and $p < 0.05$ was considered significant.

Results and Discussion

The zwitterionic polymer (BPMPC) was synthesized by radical polymerization in ethanol (Scheme 3.1A). The copolymer composition was confirmed by ^{1}H NMR spectroscopy (Figure A6), and consisted of 74:18:8 (MPC:nBMA:BP), which roughly matched the monomer feed ratio. This ratio provided the optimal anti-fouling result (discussed below) along with the most uniform coating on both hydrophobic and hydrophilic substrates. The polymer synthesis is simple and straightforward, no further purification is required besides precipitation, which makes large-scale production feasible. BPMPC is a hydrophilic polymer due to the high concentration of MPC and has a high solubility in aqueous and alcohol solutions. The butyl methacrylate component in the terpolymer aids in uniformity and substrate wetting (both hydrophobic and hydrophilic), along with providing additional photochemical cross-linking sites. As described above, the benzophenone component of BPMPC acts as a cross-linker between the hydrophilic polymer and any organic substrate through C-H activation.

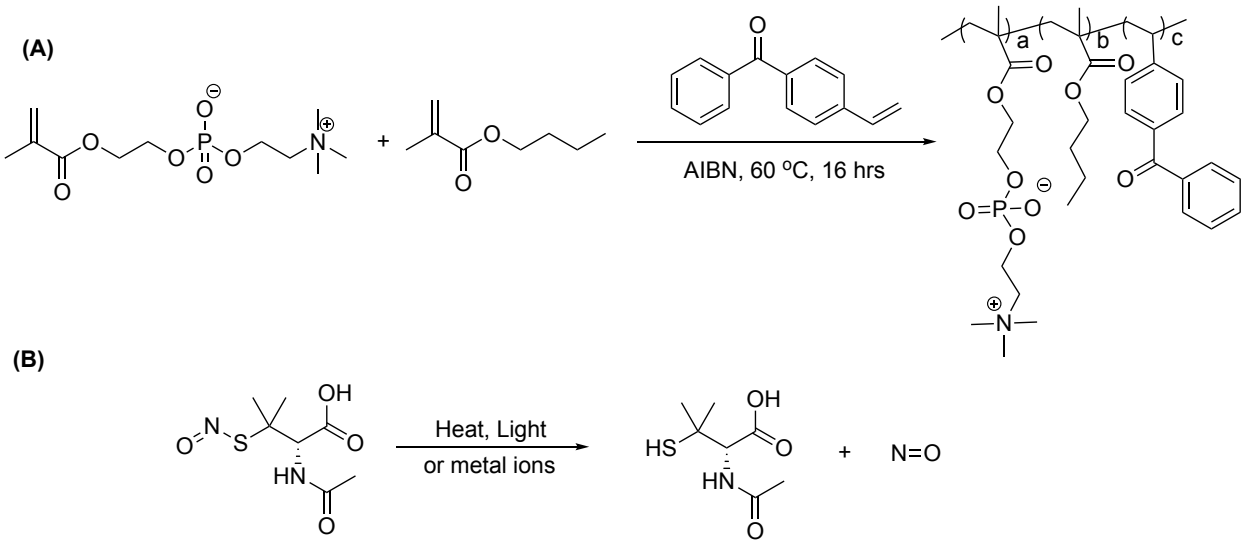

Scheme 3.1. A. Synthesis of the BPMPC copolymer. B. Chemical structure of SNAP and NO decomposition along with innocuous N-acetylpenicillamine byproduct.

The cross-linking kinetics of BPMPC was investigated by UV-vis spectroscopy on isobutyltrichlorosilane (iBTS) functionalized quartz substrates. The polymer solution (10 μL, 10 mg mL^{-1}) was drop cast on alkylated quartz and the solvent allowed to evaporate. The UV crosslinking reaction was monitored by UV-vis, where the decreasing absorbance of the BP group at 255 nm occurs with increased irradiation time. Figure 3.2 shows the UV-vis spectra, where the absorbance maxima at 255 nm decreased dramatically from 0 to 120 s, and after 240 s, no further absorbance change was observed, even after prolonged irradiation. This result demonstrates that BPMPC crosslinking occurs with rapid kinetics, and only a few seconds are needed to covalently bond BPMPC to a variety of different substrates.

To further confirm the deposition and cross-linking of the BPMPC polymer, FTIR was conducted on coated substrates. In the IR spectra (Figure 3.3), absorption peaks of the carbonyl (1720 cm^{-1}) and PC groups (1240, 1080, and 970 cm^{-1}) were observed and assigned to the MPC units. The peak at (1650 cm^{-1}) represents the C=O stretch of BP ketone. A significant reduction of this peak after irradiation further supports the formation of a network polymer of covalent linkage between BP and substrate.

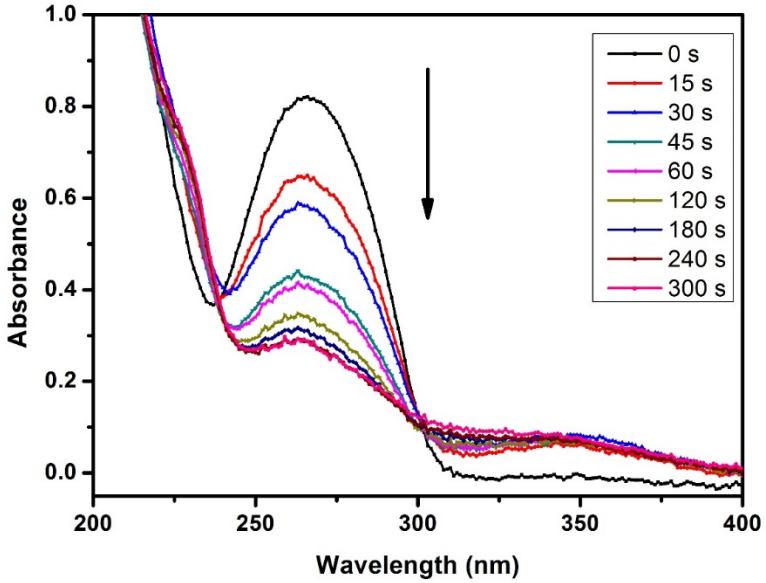

Figure 3.2. UV-vis absorption spectrum of BPMPC drop-cast onto a quartz substrate as a function of photochemical irradiation time at 254 nm (6.5 mW cm^{-2} intensity).

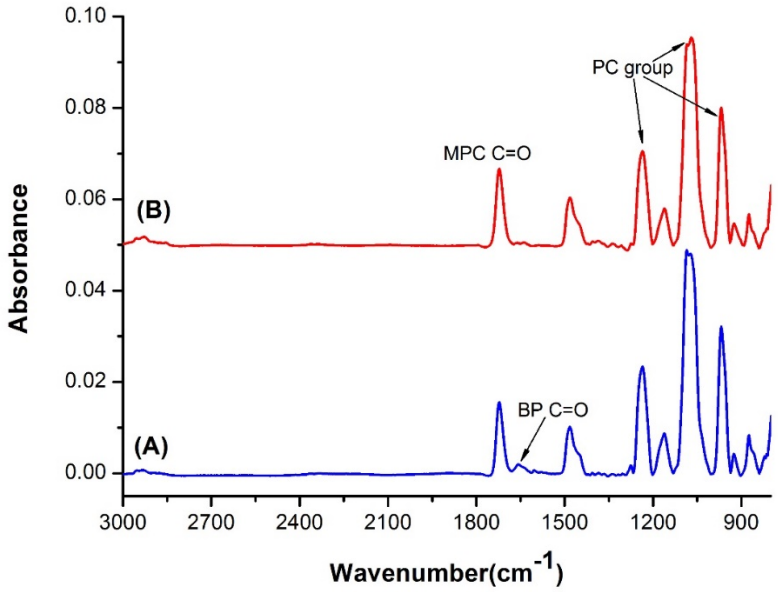

Figure 3.3. ATR-FTIR spectra of BPMPC coatings before (A) and after (B) UV exposure.

To test the stability and durability of the coating, we monitored the water contact angle of the BPMPC coated silicon samples up to 14 days. The coated substrates were immersed in PBS solution and stirred in an incubator at 37°C, subsequently rinsed with H_2O and dried with nitrogen before measuring the water contact angle (Figure 3.4). The initial static contact angle for the bare CarboSil substrate is about 110°. A significant decrease in contact angle was observed after coating with BPMPC, from 110° to 50°, and this value of contact angle was maintained over a period of 14 days immersed in an agitated PBS solution, which suggests the BPMPC coating was covalent bonded to the substrates and does not delaminate under physiological conditions.

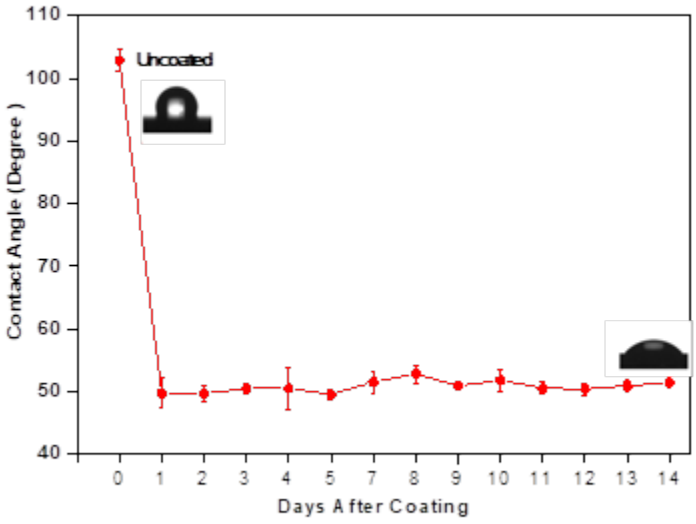

Figure 3.4. Contact angle measurement as a function of time for CarboSil coated with BPMPC and incubated at 37℃ in PBS under mild agitation.

The control samples used to test NO release behavior were coated only with CarboSil (the same polymer used to incorporate SNAP) while the test samples were coated with CarboSil and

BPMPC. The samples were tested in lightly agitated conditions to simulate physiological conditions. The samples were tested for a period of two weeks to demonstrate sustainable release of NO from the combination of hydrophobic and hydrophilic polymers.

A SNAP leaching study was conducted first to measure the retention of SNAP in the control and test polymer films during the course of the study. Measurements were recorded every other day for 2 weeks of soaking in PBS (Figure 3.5A). A high amount of SNAP retention in the polymers ensures sustained release of NO from the polymer matrix and minimizes the risks (if any) associated with SNAP leaching.44 As seen in Figure 3.5A, for the initial measurement (Day 0 on graph of Figure 3.5A) of leaching after one hour of storage in 37°C in PBS, a loss of 0.39 ± 0.06 % and 0.47 ± 0.26 % was recorded for the control and BPMPC-coated substrate, respectively. This initial higher leaching for the BPMPC-coated substrate is likely due to the hydrophilicity of the surface. However, SNAP leaching is almost identical between the control and test samples as supported by the data from 1 and 3 days of storage in 37°C for BPMPC-coated test films (0.96 ± 0.26 % and 1.44 ± 0.26 % for day 1 and day 3, respectively) and control films (0.96 ± 0.05 % and 1.55 ± 0.07 % for day 1 and day 3, respectively).

This trend of lower leaching of the SNAP molecules from the test films was observed over a 14-day period. It is also to be noted that at no point during the 14-day period were the samples kept at a temperature below 37°C or in dry conditions. This was done to closely simulate physiological conditions for a continuous duration. The leaching for both the control and test samples remained very low (<3.5 %) over the experiment duration but it is worth noting here that despite the expectation that the hydrophilic coating could cause a higher leaching of SNAP molecules from the NO donor containing polymer by attracting water molecules to the polymer

surface, this was not the case. This is likely due to the ultrathin nature of the coating, which influences the aqueous interface, but not the bulk of the polymer film.

NO release measurements of the control and test samples were also carried out for a period of 14 days (Figure 3.5B). Measurements with a Sievers chemiluminescence NO analyzer is the standard characterization methodology accepted for polymers that release NO.[45-47] It measures NO release in real time via the measurement of voltage produced by the photons on the reaction of NO with ozone. In this study, samples were stored at a constant temperature of 37°C and in PBS to simulate physiological conditions.

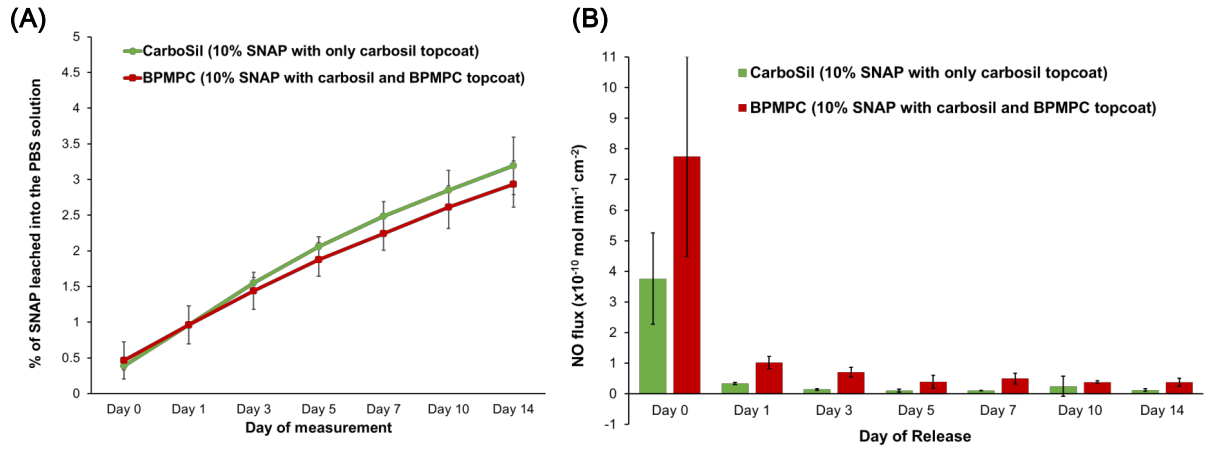

Figure 3.5. (A) SNAP leaching measured using UV-vis over 2 weeks and (B) Nitric oxide release measured over 2 weeks (n = 3) using chemiluminescence.

The results indicated a general trend of higher NO release from the test samples (SNAP-containing material coated with CarboSil and BPMPC) compared to the control samples (SNAP-containing material coated with only CarboSil). Day 0 measurements indicate that the test samples had a flux of 7.75 ± 3.26 (x 10^{-10}) mol cm-2 min-1 while control samples had 3.76 ± 1.50 (x 10^{-10}) mol cm^{-2} min^{-1} (Table 1). This burst of NO release from test samples results from the hydrophilicity

of the topcoat which attracts water molecules to the sample surface. Water molecules on the surface can accommodate release of NO as SNAP is more soluble (and prone to S-N=O bond cleavage) in aqueous conditions. After a day of storage, the control samples show a sharp decrease in NO flux ($0.34 \pm .03 \times 10^{-10}$ mol cm^{-2} min^{-1}). This is seen because of the initial loss in SNAP molecules on day 0 and but inability to maintain a hydrated state for day 1. In contrast, BPMPC-coated substrates show three times the NO flux at $1.02 \pm 0.02 \times 10^{-10}$ mol cm^{-2} min^{-1}. This difference in NO flux can result from the hydrophilic topcoat of test samples that maintains a hydrated surface layer, which facilitates the release of more NO. This trend of higher NO flux from test samples when compared to control samples can be seen through the 14-day study in Table 1 and the graph in Figure 3.5B.

Table 3.1 Comparison of nitric oxide release kinetics between control and coated samples

10% SNAP with only CarboSil topcoat

	10% SNAP with only CarboSil topcoat (NO flux ($x10^{-10}$ mol min^{-1} cm^{-2})	10% SNAP with CarboSil and BPMPC topcoat (NO flux ($x10^{-10}$ mol min^{-1} cm^{-2})
Day 0	3.759 ± 1.491	7.746 ± 3.263
Day 1	0.335 ± 0.032	1.016 ± 0.198
Day 3	0.141 ± 0.023	0.706 ± 0.157
Day 5	0.110 ± 0.045	0.395 ± 0.208
Day 7	0.105 ± 0.008	0.498 ± 0.173
Day 10	0.247 ± 0.324	0.383 ± 0.040
Day 14	0.127 ± 0.035	0.380 ± 0.125

At the end of the 14-day study, test samples (0.38 ± 0.13 (x 10^{-10}) mol cm^{-2} min^{-1}) still release three times the NO flux compared to the control samples (0.13 ± 0.03 (x 10^{-10}) mol cm^{-2} min^{-1}). This propensity of higher release of NO from CarboSil top-coated with BPMPC along with the reduction in leaching of SNAP is very beneficial and combines the material properties of CarboSil (low SNAP leaching) with a higher, sustained release of NO due to the hydrophilic BPMPC topcoat.

As mentioned earlier, the BPMPC coating has excellent hydrophilicity, which helps inhibit the adsorption of proteins from solution. Fibrinogen and lysozyme were used as model proteins to evaluate the antifouling properties of the BPMPC coatings. Fibrinogen is a large (340 kD, pI = 6.0) protein, and a key biomacromolecule in the coagulation cascade that rapidly adsorbs to foreign surfaces and binds to and activates platelets. Lysozyme is a small protein (14 kD, pI = 12) that is positively charged under physiological pH. Figure 3.6A shows the adsorption thickness increase of Fibrinogen on CarboSil, CarboSil with 10% SNAP, BPMPC coated CarboSil, and BPMPC coated CarboSil with 10% SNAP substrates respectively. On the bare CarboSil films used as a control, the thickness increased about 3 nm after incubation for 24 hours and increased to over 30 nm after 2 weeks. The similar phenomenon was observed for CarboSil with 10% SNAP films, which indicated a high amount of protein adsorption on surface, and protein accumulation over time. On the other hand, for the CarboSil films coated with BPMPC, the adsorption amount is significantly lower, only a 2 nm increase was observed after incubation for 2 weeks. The large difference in adsorption thickness confirmed that BPMPC coating has an excellent protein resistance properties, even after UV activation. As expected, the BPMPC coated CarboSil with 10% SNAP films also shows low adsorption for Fibrinogen. Moreover, similar behavior was observed when films were subjected to lysozyme solution (Figure 3.6B). The thickness increase

in control group was over 14 nm, while the coated group was less than 3 nm. The protein adsorption results indicate that the hydrophilic BPMPC surface layer provides excellent protein-resistant properties.

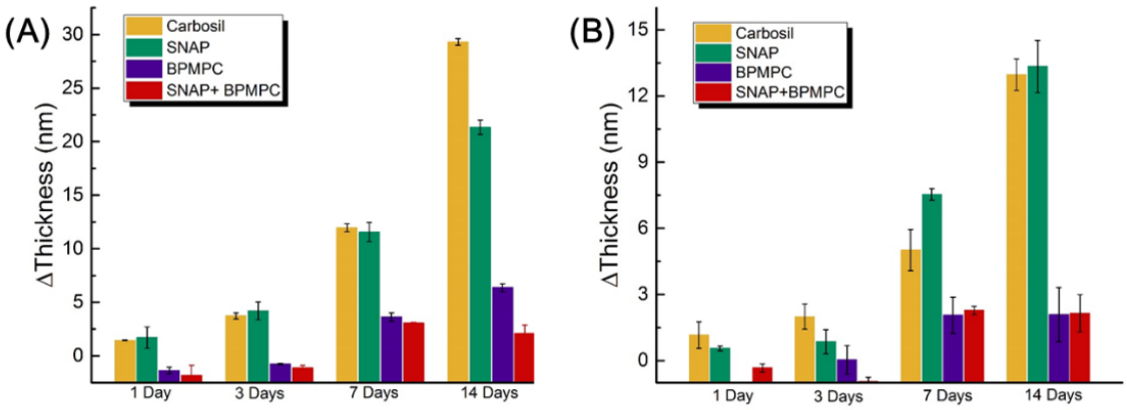

Figure 3.6. Thickness increase after incubation in (A) Fibrinogen solution and (B) in Lysozyme solution.

To further confirm the antifouling effectiveness of the durable BPMPC coating, fluorescence microscopy was utilized to evaluate the protein adsorption on the uncoated and coated CarboSil films using FITC labeled BSA protein. The fouling levels were compared between uncoated and BPMPC coated CarboSil films using the same excitation light intensity and exposure time. Figure 3.7A indicates protein adsorption on the control samples, and enhanced fluorescent signal (Figure 3.7B-C) was observed in the samples pretreated with BSA PBS solution. These results demonstrate that after incubation in protein solution, a large amount of BSA was attached to the CarboSil samples, which facilitate the aggregation of FITC-BSA. On the contrary, protein adhesion to the surface of BPMPC modified samples was not observed (Figure 3.7D-F), even after

incubation in BSA solution for 7 days. From all of these results collectively, the control films demonstrate large amounts of protein adsorption, while the BPMPC coated films display excellent antifouling properties.

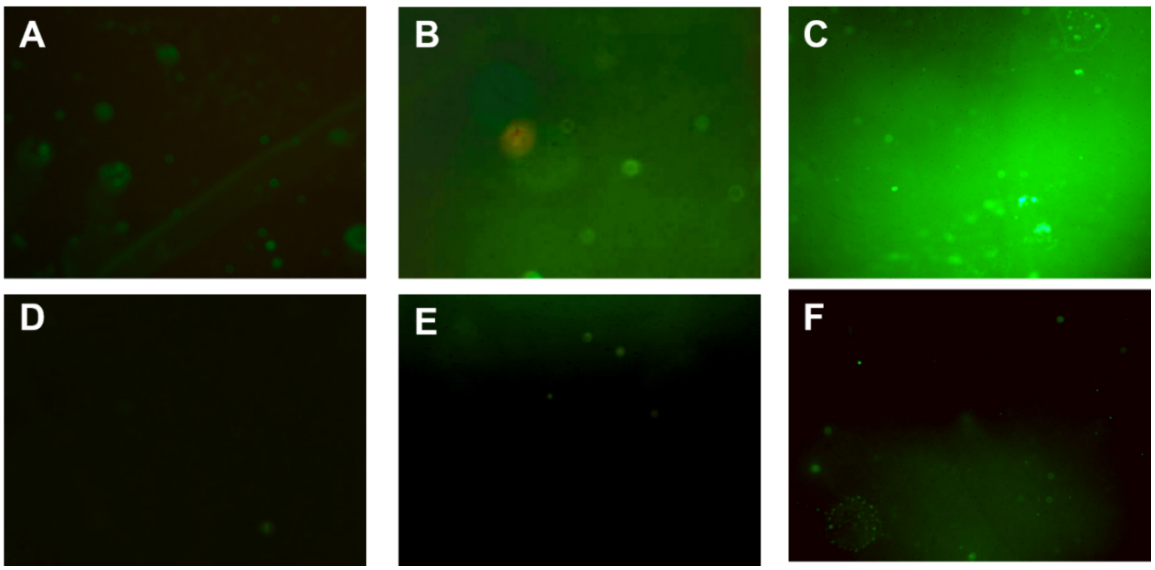

Figure 3.7. Fluorescence micrographs (magnification 10x) of uncoated films after (A) 90-minute incubation, (B) 1 day in BSA PBS solution before incubation, and (C) 7 days in BSA PBS solution before incubation in 2 mg/ml FITC-BSA solution. (D-F) are the coated film measured under the same experimental conditions.

Bacterial adhesion, which often results in biofilm formation, is a prevalent issue in moist and humid environments, including implanted devices. The basic nutrients important for bacterial growth may be resourced from the device material, bodily proteins that attach post-implantation, or other bodily macromolecular contaminants that adhere to the surface of the device. Antimicrobial efficacy of the designed test samples was compared to the control samples to confirm their superior bactericidal and bacterial repulsion properties.

The samples were soaked in bacterial solutions containing ~10^6 CFU/mL of *S. aureus*. *S. aureus* is a commonly found nosocomial infection bacteria. It has been increasingly linked with healthcare-associated infections in the last two decades.[48] They are most commonly associated with cardiac devices, intravascular catheters and urinary catheters, among other prosthetic devices. This high prevalence of *S. aureus* along with its known affinity to proteins [49-50] that foul medical devices has made it a very important pathogen used to evaluate the antimicrobial efficacy of medical device materials. For these reasons, bacterial adhesion study of the antifouling-biocide releasing polymer developed was done with S. aureus.

As mentioned in the introduction, the NO molecules liberated by the decomposition of SNAP actively kill bacteria while the zwitterion topcoat repels protein adsorption, leading to enhanced antimicrobial efficacy. After 24-hours of incubation, the antimicrobial effect of the test samples was clearly observed. NO releasing polymers with a top-coat of BPMPC showed a bactericidal efficiency of 99.91 ± 0.06 % (~3 log reduction, Figure 3.8) compared to the control samples where a growth of ~106 CFU/cm^2 was observed. This reduction is greater compared to films with only a BPMPC topcoat (70.15 ± 14.13 %) and also films with only NO-releasing moieties (98.88 ± 0.54 %). It can also be concluded from the results that BPMPC alone only reduces bacteria adhesion. However, because NO is not a contact active antimicrobial but a diffusing biocide, the SNAP-loaded samples also reduce bacterial adhesion significantly.

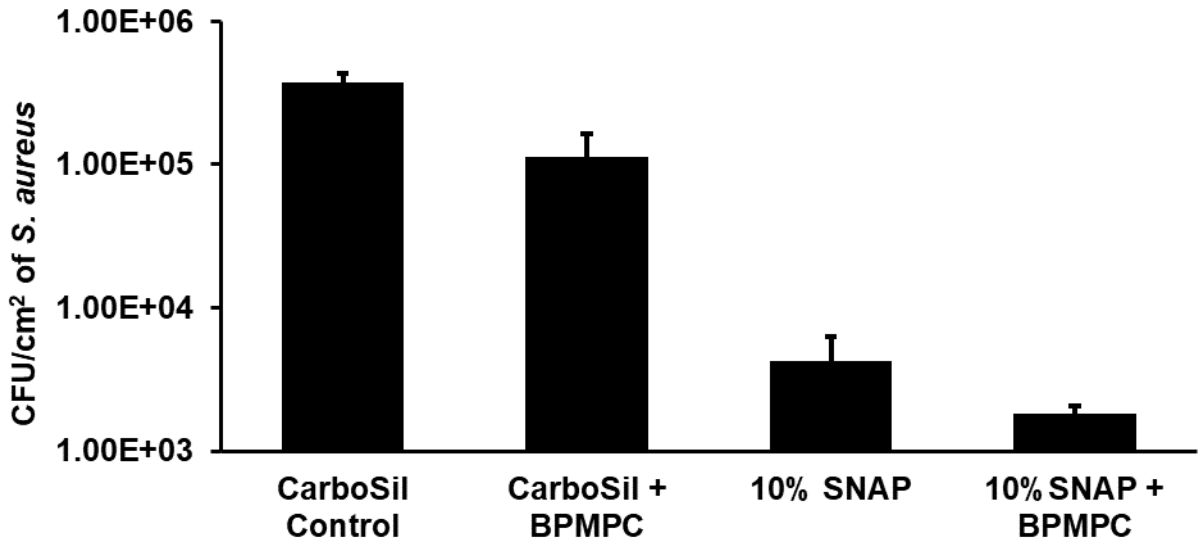

Figure 3.8. Antimicrobial efficacy of NO-releasing BPMPC coated samples relative to controls (n=3).

These results are consistent with the theoretical expectations underlying the surface chemistry of BPMPC and bactericidal properties of NO. In summary, the synergistic effect of the modifiable NO-release kinetics from CarboSil's surface and prevention of protein and/or bacterial adhesion due to BPMPC's surface chemistry will significantly reduce undesired clinical consequences for implanted medical devices.

Conclusion

In conclusion, we have demonstrated a combination of NO release and BPMPC can produce a material with antimicrobial ability and excellent antifouling properties. The formation of the covalent polymer network is rapid (less than 1 min) under mild UV conditions, and can be applied to various substrates, from hydrophilic to hydrophobic. More importantly, even though

the BPMPC coating is around 50 nm, it resists moderate abrasion for over a week with retention of its antifouling property. Moreover, the NO release profile indicated a higher NO release form the BPMPC coated sample when compared to the control, with lower leaching of SNAP. The coatings were also challenged with protein adsorption tests for an extended time (up to 2 weeks), where antifouling properties remain. It is noteworthy that, the high killing efficiency of SNAP to S. aureus is enhanced by BPMPC coating. This one step photochemical attachment process of an antifouling coating to NO-releasing antimicrobial polyurethanes is a simple and scalable process that has application in both medical devices and other and industrial applications where antifouling and antimicrobial properties are desired.

References

1. Cho, W. K., B. K., Choi, I. S., High Wfficient Non-biofouling Coating of Zwitterionic Polymer: Poly((3-(methacryloylamino)propyl)-dimethyl(3-sulfopropyl)ammonium hydroxide). *Langmuir* **2007**, 23, 5678.

2. Nguyen, A. T.; Baggerman, J.; Paulusse, J. M.; van Rijn, C. J.; Zuilhof, H., Stable Protein-repellent Zwitterionic Polymer Brushes Grafted from Silicon Nitride. *Langmuir* **2011**, 27, 2587-94.

3. Kenawy el, R.; Worley, S. D.; Broughton, R., The Chemistry and Applications of Antimicrobial Polymers: A State-of-the-art Review. *Biomacromolecules* **2007**, 8, 1359-84.

4. Dastjerdi, R.; Montazer, M., A Review on the Application of Inorganic Nano-structured Materials in the Modification of Textiles: Focus on Anti-microbial Properties. *Colloids Surf. B Biointerfaces* **2010**, 79, 5-18.

5. Hetrick, E. M.; Schoenfisch, M. H., Reducing Implant-related Infections: Active Release Strategies. *Chem. Soc. Rev.* **2006**, 35, 780-9.

6. Yatvin, J.; Gao, J.; Locklin, J., Durable defense: Robust and Varied Attachment of Non-leaching Poly"-onium" Bactericidal Coatings to Reactive and Inert Surfaces. *Chem. Comm. (Camb)* **2014**, 50, 9433-42.

7. Magill, S. S.; Edwards, J. R.; Bamberg, W.; Beldavs, Z. G.; Dumyati, G.; Kainer, M. A.; Lynfield, R.; Maloney, M.; McAllister-Hollod, L.; Nadle, J.; Ray, S. M.; Thompson, D. L.; Wilson, L. E.; Fridkin, S. K.; Emerging Infections Program Healthcare-Associated, I.; Antimicrobial Use Prevalence Survey, T., Multistate Point-prevalence Survey of Health Care-associated Infections. *N. Engl. J. Med.* **2014**, 370, 1198-208.

8. Lowe, S.; O'Brien-Simpson, N. M.; Connal, L. A., Antibiofouling Polymer Interfaces: Poly(ethylene glycol) and Other Promising Candidates. *Polym. Chem.* **2015**, 6, 198-212.

9. Jiang, S.; Cao, Z., Ultralow-fouling, Functionalizable, and Hydrolyzable Zwitterionic Materials and their Derivatives for Biological Applications. *Adv. Mater.* **2010**, 22, 920-32.

10. Wayne R. Gombotx, W. G., Thomas A. Horbett, Allan S. Hoffman, Protein Adsorption to Poly(ethylene oxide) Surfaces. *J. Biomed. Mater. Res.* **1991**, 25, 1547-1562.

11. Shao, Q.; Jiang, S., Molecular Understanding and Design of Zwitterionic Materials. *Adv. Mater.* **2015**, 27, 15-26.

12. Zhang, Z.; Chao, T.; Chen, S. F.; Jiang, S. Y., Superlow Fouling Sulfobetaine and Carboxybetaine Polymers on Glass Slides. *Langmuir* **2006**, 22, 10072-10077.

13. Hucknall, A.; Rangarajan, S.; Chilkoti, A., In Pursuit of Zero: Polymer Brushes that Resist the Adsorption of Proteins. *Adv. Mater.* **2009**, 21, 2441-2446.

14. Ladd, J.; Zhang, Z.; Chen, S.; Hower, J. C.; Jiang, S., Zwitterionic Polymers Exhibiting High Resistance to Nonspecific Protein Adsorption from Human Serum and Plasma. *Biomacromolecules* **2008**, 9, 1357-1361.

15. Holmlin, R. E.; Chen, X. X.; Chapman, R. G.; Takayama, S.; Whitesides, G. M., Zwitterionic SAMs that Resist Nonspecific Adsorption of Protein from Aqueous Buffer. *Langmuir* **2001**, 17, 2841-2850.

16. He, Y.; Hower, J.; Chen, S. F.; Bernards, M. T.; Chang, Y.; Jiang, S. Y., Molecular Simulation Studies of Protein Interactions with Zwitterionic Phosphorylcholine Self-assembled Monolayers in the Presence of Water. *Langmuir* **2008**, 24, 10358-10364.

17. Singha, P.; Locklin, J.; Handa, H., A review of the recent advances in antimicrobial coatings for urinary catheters. *Acta Biomater.* **2017**, 50, 20-40.

18. Ren, P. F.; Yang, H. C.; Liang, H. Q.; Xu, X. L.; Wan, L. S.; Xu, Z. K., Highly Stable, Protein-Resistant Surfaces via the Layer-by-Layer Assembly of Poly(sulfobetaine methacrylate) and Tannic Acid. *Langmuir* **2015**, 31, 5851-8.

19. Turro, N. J., Modern Molecular Photochemistry. Benjamin/Cummings Pub Co.: Menlo Park, CA, 1978.

20. Lin, A. A.; Sastri, V. R.; Tesoro, G.; Reiser, A.; Eachus, R., On the Crosslinking Mechanism of Benzophenone-containing Polyimides. *Macromolecules* **1988**, 21, 1165-1169.

21. Park, M.-K.; Deng, S.; Advincula, R. C., pH-Sensitive Bipolar Ion-Permselective Ultrathin Films. J. of the American Chemical Society **2004**, 126, 13723-13731.

22. Higuchi, H.; Yamashita, T.; Horie, K.; Mita, I., Photo-cross-linking Reaction of Benzophenone-containing Polyimide and Its Model Compounds. Chemistry of Materials **1991**, 3, 188-194.

23. Braeuchle, C.; Burland, D. M.; Bjorklund, G. C., Hydrogen Abstraction by Benzophenone Studied by Holographic Photochemistry. The Journal of Physical Chemistry **1981**, 85 (2), 123-127.

24. Lin, X.; Fukazawa, K.; Ishihara, K., Photoreactive Polymers Bearing a Zwitterionic Phosphorylcholine Group for Surface Modification of Biomaterials. *ACS Appl. Mater. Interfaces* **2015**, 7 (31), 17489-98.

25. Samuel, J. D. J. S.; Brenner, T.; Prucker, O.; Grumann, M.; Ducree, J.; Zengerle, R.; Rühe, J., Tailormade Microfluidic Devices Through Photochemical Surface Modification. Macromolecular Chemistry and Physics **2010**, 211 (2), 195-203.

26. Hu, S.; Ren, X.; Bachman, M.; Sims, C. E.; Li, G. P.; Allbritton, N. L., Surface-Directed, Graft Polymerization within Microfluidic Channels. Analytical Chemistry 2004, 76 (7), 1865-1870.

27. Virkar, A.; Ling, M.-M.; Locklin, J.; Bao, Z., Oligothiophene Based Organic Semiconductors with Cross-linkable Benzophenone Moieties. Synthetic Metals 2008, 158 (21–24), 958-963.

28. Bunte, C.; Prucker, O.; Konig, T.; Ruhe, J., Enzyme Containing Redox Polymer Networks for Biosensors or Biofuel Cells: A Photochemical Approach. Langmuir 2010, 26 (8), 6019-6027.

29. Bunte, C.; Ruhe, J., Photochemical Generation of Ferrocene-Based Redox-Polymer Networks. Macromol Rapid Comm 2009, 30 (21), 1817-1822.

30. Gao, J.; Martin, A.; Yatvin, J.; White, E.; Locklin, J., Permanently Grafted Icephobic Nanocomposites with High Abrasion Resistance. J. Mater. Chem. A 2016, 4 (30), 11719-11728.

31. Abu-Rabeah, K.; Atias, D.; Herrmann, S.; Frenkel, J.; Tavor, D.; Cosnier, S.; Marks, R. S., Characterization of Electrogenerated Polypyrrole−Benzophenone Films Coated on Poly(pyrrole-methyl metacrylate) Optic-Conductive Fibers. *Langmuir* **2009**, 25, 10384-10389.

32. Brandstetter, T.; Bohmer, S.; Prucker, O.; Bisse, E.; zur Hausen, A.; Alt-Morbe, J.; Ruhe, J., A Polymer-based DNA Biochip Platform for Human Papilloma Virus Genotyping. *J. Virol. Methods* **2010**, 163, 40-48.

33. Brisbois, E. J.; Bayliss, J.; Wu, J.; Major, T. C.; Xi, C.; Wang, S. C.; Bartlett, R. H.; Handa, H.; Meyerhoff, M. E., Optimized polymeric film-based nitric oxide delivery inhibits bacterial growth in a mouse burn wound model. Acta biomaterialia **2014**, 10, 4136-4142.

34. Pegalajar-Jurado, A.; Wold, K. A.; Joslin, J. M.; Neufeld, B. H.; Arabea, K. A.; Suazo, L. A.; McDaniel, S. L.; Bowen, R. A.; Reynolds, M. M., Nitric oxide-releasing polysaccharide

derivative exhibits 8-log reduction against Escherichia coli, Acinetobacter baumannii and Staphylococcus aureus. Journal of Controlled Release **2015**, 217, 228-234.

35. Backlund, C. J.; Worley, B. V.; Schoenfisch, M. H., Anti-biofilm Action of Nitric Oxide-Releasing Alkyl-modified Poly (amidoamine) Dendrimers Against Streptococcus mutans. Acta biomaterialia 2016, 29, 198-205.

36. Fang, F. C., Antimicrobial actions of nitric oxide. Nitric oxide : biology and chemistry / official journal of the Nitric Oxide Society 2012, 27, Supplement, S10.

37. Wang, P. G.; Xian, M.; Tang, X.; Wu, X.; Wen, Z.; Cai, T.; Janczuk, A. J., Nitric Oxide Donors: Chemical Activities and Biological Applications. *Chem. Rev.* **2002**, 102, 1091-1134.

38. Brisbois, E. J.; Handa, H.; Major, T. C.; Bartlett, R. H.; Meyerhoff, M. E., Long-term Nitric Oxide Release and Elevated Temperature Stability with S-nitroso-N-acetylpenicillamine (SNAP)-doped Elast-eon E2As polymer. *Biomaterials* **2013**, 34, 6957-66.

39. Broniowska, K. A.; Hogg, N., The Chemical Biology of S-Nitrosothiols. *Antioxidants & Redox Signaling* **2012**, 17, 969-980.

40. Singha, P.; Pant, J.; Goudie, M. J.; Workman, C. D.; Handa, H., Enhanced Antibacterial Efficacy of Nitric Oxide Releasing Thermoplastic Polyurethanes with Antifouling Hydrophilic Topcoats. Biomaterials Science 2017.

41. Brisbois, E. J.; Davis, R. P.; Jones, A. M.; Major, T. C.; Bartlett, R. H.; Meyerhoff, M. E.; Handa, H., Reduction in Thrombosis and Bacterial Adhesion with 7 Day Implantation of -Nitroso--acetylpenicillamine (SNAP)-Doped Elast-eon E2As Catheters in Sheep. *J. Mater. Chem. B Mater. Biol. Med.* **2015**, 3, 1639-1645.

42. Sundaram, H. S.; Han, X.; Nowinski, A. K.; Ella-Menye, J. R.; Wimbish, C.; Marek, P.; Senecal, K.; Jiang, S., One-Step Dip Coating of Zwitterionic Sulfobetaine Polymers on Hydrophobic and Hydrophilic Surfaces. *ACS Appl. Mater. Interfaces* **2014**, 6, 6664-71.

43. Diaz Blanco, C.; Ortner, A.; Dimitrov, R.; Navarro, A.; Mendoza, E.; Tzanov, T., Building an Antifouling Zwitterionic Coating on Urinary Catheters Using an Enzymatically Triggered Bottom-Up Approach. *ACS Appl. Mater. Interfaces* **2014**, 6, 11385-93.

44. Scatena, R.; Bottoni, P.; Pontoglio, A.; Giardina, B., Pharmacological Modulation of Nitric Oxide Release: New Pharmacological Perspectives, Potential Benefits and Risks. *Curr. Med. Chem.* **2010**, 17, 61-73.

45. Wo, Y.; Li, Z.; Brisbois, E. J.; Colletta, A.; Wu, J.; Major, T. C.; Xi, C.; Bartlett, R. H.; Matzger, A. J.; Meyerhoff, M. E., Origin of Long-Term Storage Stability and Nitric Oxide Release Behavior of CarboSil Polymer Doped with S-Nitroso-N-acetyl-d-penicillamine. *ACS Appl. Mater. Interfaces* **2015**, 7, 22218-22227.

46. Joslin, J. M.; Lantvit, S. M.; Reynolds, M. M., Nitric Oxide Releasing Tygon Materials: Studies in Donor Leaching and Localized Nitric Oxide Release at a Polymer-Buffer Interface. *ACS Appl. Mater. Interfaces* **2013**, 5, 9285-9294.

47. Privett, B. J.; Broadnax, A. D.; Bauman, S. J.; Riccio, D. A.; Schoenfisch, M. H., Examination Of Bacterial Resistance To Exogenous Nitric Oxide. Nitric Oxide: Biology And Chemistry. official journal of the Nitric Oxide Society **2012**, 26, 169-73.

48. Tong, S. Y.; Davis, J. S.; Eichenberger, E.; Holland, T. L.; Fowler, V. G., Staphylococcus aureus Infections: Epidemiology, Pathophysiology, Clinical Manifestations, And Management. Clinical microbiology reviews **2015**, 28, 603-661.

49. Ní Eidhin, D.; Perkins, S.; Francois, P.; Vaudaux, P.; Höök, M.; Foster, T. J., Clumping Factor B (Clfb), a New Surface-located Fibrinogen-Binding Adhesin of Staphylococcus aureus. Molecular Microbiology **1998**, 30, 245-257.

50. Boland, T.; Latour, R. A.; Stutzenberger, F. J., Molecular Basis of Bacterial Adhesion. In Handbook of Bacterial Adhesion, Springer: **2000**, 29-41.

CHAPTER 4

TRANSPARENT GRAFTED ZWITTERIONIC COPOLYMER COATINGS THAT EXHIBIT BOTH ANTIFOGGING AND SELF-CLEANING PROPERTIES[1]

[1]Accepted by [Liu, Q.; Locklin, J.; " Transparent Grafted Zwitterionic Copolymer Coatings That Exhibit Both Antifogging and Self-Cleaning" ACS Omega, 2018, 3 (12), 17743-17750]. Reprinted here with permission of publisher.

Abstract

In this work, we have investigated a series of zwitterionic copolymers that demonstrate outstanding antifogging and self-cleaning properties. These polymer coatings are photochemically grafted to substrates containing C-H bonds with rapid kinetics and form a robust polymer networks on plastic and alkyl-modified glass surfaces. The copolymers consist of a zwitterionic monomer, which provides high hydrophilicity, and a benzophenone moiety that produces a densely cross-linked network. The optical clarity of the substrates is not impacted by the polymer coating, and even slightly improved due to the lower refractive index of the polymer relative to glass. The antifogging and self-cleaning capabilities were determined by a series of experiments, where the optical transmittance of substrates modified with copolymer coatings was excellent under both hot and cold fogging conditions. Additionally, surfaces contaminated with oil are easily cleaned by simply submerging the coatings in water. Moreover, the coatings exhibit excellent chemical and mechanical resistance, and maintain antifogging properties after abrasion testing in the presence of either chemical detergents or common household cleaners.

Introduction

Formation of fog due to water vapor condensation on a surface as a result of a temporary change in temperature and humidity leads to many problems in practical applications, including windshields, eyeglasses, safety glasses and optical instruments.[1-5] To alleviate fog formation, there are three general strategies used to prepare antifogging films, each with its own advantages and disadvantages. One conventional approach uses photo-active inorganic nanoparticles such as TiO_2 and ZnO that become super-hydrophilic under ultraviolet (UV) light exposure.[6-9] Others include different fabrication methods such as layer-by-layer assembly or electrostatic spinning, which aim to modify the chemical environment and geometric microstructure of the surface into a nonporous or textured film, which will absorb water and facilitate the spread of water on the surface. [10-13] Both of these approaches described above require multiple steps, harsh reactants, and/or post treatments, all of which can limit practical application in everyday use.[14-15] A third approach, which involves simple deposition of hydrophilic polymer coatings on to various substrates, is a very promising candidate that provides a low cost and simple process, with high efficiency.[16-17] Nevertheless, the preparation of highly transparent and robust superhydrophilic polymer coatings still remained a challenge. For instance, there are reports of obtaining superhydrophilic coatings using spin coating[2, 18], layer-by-layer assembly[19] and polymer brushes[15, 20]. However, all these methods are difficult to scale and implement commercially.

Zwitterionic polymers have attracted attention due to their strong hydration capacity and have been widely used as biomimetic antifouling materials in marine and biomedical applications.[15, 21-22] The dipole arrangement of the water molecule in the hydration shell formed via electrostatic interactions with the charged groups of the zwitterion are close to that of free water. Therefore, adsorbed water can create a continuous or near-continuous film, minimizing

scattering events and preserving the optical transmission of the substrate.[19, 23] However, due to the high solubility of the zwitterionic polymers, these coatings are easily delaminated or dissolved in the presence of water, which is a limitation of this approach.[14] To permanently attached zwitterionic polymers thin films to a substrate, there are several reports utilizing layer by layer methods or polymer brush techniques,[15, 19-20, 24] but these still have many challenges in translation from small laboratory substrates to scale mass production. Coatings that are grafted through either chemical or photochemical crosslinking are considered to be an effective and reasonable method for modifying polymer materials on substrates through covalent bonding.[25-26]

The ability of benzophenone (BP) to act as a cross-linking agent and abstract hydrogen from a suitable hydrogen donor has been well studied and utilized in various chemical systems for many years.[27-28] BP is an ideal choice for crosslinking organic thin films, because it can be activated using mild UV light (345 – 365 nm), avoiding oxidative damage to either the polymer or substrate that can occur upon exposure to higher energy UV. The BP moiety is more chemically robust than other organic cross-linkers and reacts preferentially with C-H bonds in a wide range of different chemical environments. When irradiated with UV light, an electron from the n-orbital on the carbonyl of BP is exited to π^*-orbital to a biradical triplet excited state that can abstract a hydrogen atom from a neighboring aliphatic C-H bonds to form a new C-C bond. This triplet state also has unusually high reactivity for H atoms located alpha to electron donating heteroatoms (nitrogen and oxygen). This photoreaction has recently been used to attach thin polymer layers to metal and oxide surfaces,[29-31] along with applications ranging from organic semiconductors,[32] microfluidic devices,[33-34] hydrogels,[29, 35] and biosensors.[36-37] Because of these advantages, we have previously developed antimicrobial copolymers containing hydrophobic N-alkyl and benzophenone moiety on a polyethylenimine backbone,[38] anti-icing copolymers consisting

hexafluorobutyl, benzophenone, and nanoparticles,[39] and antifouling copolymers containing zwitterionic monomers and benzophenone.[40] All of these systems exhibit fast crosslinking kinetics and high abrasion resistance.

In this study, a zwitterionic terpolymer (2-methacryloyloxyethyl phosphorylcholine-co-butyl methacrylate-co-benzophenone, BPMPC) was synthesized and covalently grafted to alkyl-modified glass and plastic lenses with UV irradiation. After the coatings are applied, the transmittance of the substrates is well maintained regardless of coating thickness, which ranges from 50 to 300 nm in this work. These BPMPC polymer coatings exhibit excellent antifogging properties in hot-vapor and freeze-warm tests. Moreover, the self-cleaning properties were evaluated, and the results showed that the modified surface could be cleaned by a simple water rinse without surfactant or harsh abrasion. Additionally, BPMPC coating exhibited high chemical stability against household detergent and mechanical durability against abrasion with paper and cloth.

Experiment Section

Materials.

2-Methacryloyloxyethyl phosphorylcholine (MPC) and Disperse Red 1 were purchased from Sigma Aldrich (St. Louis, MO). 2,2'-azobis(2-methylpropiontirlemethylpropionitrile) (AIBN) and n-butyl methacrylate (nBMA) were purchased from Alfa-Aesar. Isobutyltrichlorosilane (iBTS) was purchased from Tokyo Chemical Industry. Tetradecane and glass slides were purchased from Fisher-Scientific. Toluidine Blue O was obtained from EMD Chemical. Iron metal powder was obtained from VWR. 4-vinylbenzophenone (BP) was synthesized according to a previously reported procedure from our group[134]. De-ionized (DI) water

(18.2 MΩ) was used for all the aqueous solution. Nitrogen gas was purchased from Airgas. All the chemicals were used as received without further purification.

Substrate Preparation and Crosslinking.

The polymer was synthesized according to our previous report.[94] Glass substrates were sonicated with deionized water, hexane, isopropanol, and acetone for 5 minutes each then dried under nitrogen, followed by plasma (Harrick Plasma PDC-32G) cleaning and treatment with iBTS in toluene (10 mmol) overnight before modification with the polymer. Polycarbonate safety glasses and eyeglasses were cleaned with DI water and ethanol then dried in air.

Spray coating was used to apply the coatings. A BPMPC/ethanol solution (2 mg mL^{-1}) was sprayed using an airbrush (Model S 62, Master Airbrush) from a distance of 10 cm onto substrates held vertically to achieve uniform coating upon drying. 1 mL solution was used for glass slides and 3 mL solution was used for eyeglasses and safety glasses. Then the glass substrates were irradiated with UV light (UVP, 254 nm, 6.5 mW cm^{-2}) for 1 min to covalently bond the BPMPC to the surface. BPMPC modified goggle and eyeglasses coated in a similar fashion before placing on a UV Crosslinker (FB-UVXL-1000, Fisher Scientific, 254nm, 2 mW cm^{-2}) for 3 min. The substrates were rinsed with sufficient ethanol to remove unattached BPMPC then dried under nitrogen.

Characterization of the polymer coatings.

According to previous study, UV-vis spectra indicated that the crosslinking occurs with rapid kinetics, and only a few seconds are needed to covalently bond BPMPC to the underlying substrates. Additionally, the reduction of C=O stretch of BP in FTIR further confirmed the

crosslinking reaction.[94] The surface wettability on glass slides was characterized by measuring the static water contact angle using a DSA 100 drop shape analysis system (KRŰSS) with a computer-controlled liquid dispensing system. 1 μL DI water droplets were deposited onto substrate, and the water contact angles were measured within 10 seconds through the analysis of photographic images.

The transmission of the coated substrates was evaluated by UV-Vis spectra, which were recorded using Cary 50 Bio Spectrophotometer (Varian), with air as reference. Since the range of visible wavelength is from 390 nm to 700 nm,[135] the UV spectra were recorded from 300 nm to 800 nm. The thickness and refractive index of the BPMPC polymer layer on the glass substrates was measured by spectroscopic ellipsometry (M-2000V J.A. Woollam) with a white light source at three incident angles (65°, 70°, and 75°). The thickness of the modified layer was measured and calculated using a Cauchy layer model.

Antifogging Test.

The antifogging property of various substrates was tested with both hot-vapor and freeze-warm methods. For the hot-vapor test, the coated glass slides, safety glasses or glasses were placed 5 cm above hot boiling water (~ 80 ℃) and held for different time periods. Videos and photographs were recorded through the entire experiments. In addition, a more aggressive evaluation was conducted by placing the safety glasses in a freezer at -20 ℃ for 30 min, and quickly exposed to a warm humid environment (~ 20 ℃, 55% relative humidity).

Self-Cleaning Experiments.

The self-cleaning properties of the BPMPC coating were evaluated using two approaches. The first method was dispensing tetradecane droplets (with disperse red 1 dye as a visual indicator) onto pure glass slides (hydrophilic), iBTS modified glass slides (hydrophobic), and BPMPC coated glass slides, followed by rinsing with DI water (with a toluidine blue dye indicator). Videos were recorded throughout the rinsing process, and photographs were taken after the water wash. Due to the low contrast of the tetradecane and background, the image was enhanced by Adobe Photoshop to achieve better resolution. The other method was trying to mimic practical contamination that occurs with common use in everyday life. The clean control and coated glass slides were contaminated with thumb prints (covered with tetradecane oil, followed by iron metal power dusting to give a clear visual of the fingerprint). Then the glass slides were immersed in DI water for 30 seconds to remove the contamination. The cleaning processes were recorded as well, and the final results were documented.

Chemical and Mechanical Durability Test.

The chemical and mechanical robustness of BPMPC coating was challenged by household cleaning products and wiping operation. (1) Glass slides were sprayed with Windex (S. C. Johnson & Son), then wiped with KimWipe (VMR) harshly for several cycles to make sure there was no residue left. (2) Eyeglasses were cleaned using White Board Cleaner (Expo), followed with KimWipe wiping. After the cleaning procedure, the glass slides and eyeglasses were placed on top of the boiling water to check their antifogging properties. Videos and photographs were taken through the hot-vapor test.

Results and Discussion

Synthesis and surface analysis of zwitterionic copolymer coatings.

According to previous work in our group, BPMPC copolymer was synthesized by radical polymerization with high yield, and the monomer ratio was confirmed by ^{1}H NMR.[40] The crosslinking kinetics are rapid and efficient with C-H containing substrates, and covalent bonds are formed between the polymer and the substrate, as shown in Scheme 4.1.

To confirm the hydrophilicity of BPMPC coating, contact angles were measured and compared. The bare glass slide is hydrophilic with a static contact angle of 53º, while iBTS modified glass is hydrophobic with a static contact angle of 95°. After spray coated with BPMPC solution and UV irradiation, a significant decrease in contact angle was detected from 95° to 50° (Figure 4.1). This contact angle is higher than other zwitterionic homopolymers reported in the literature because of the n-butylmethacrylate comonomer, which aids in substrate wetting and coating uniformity.

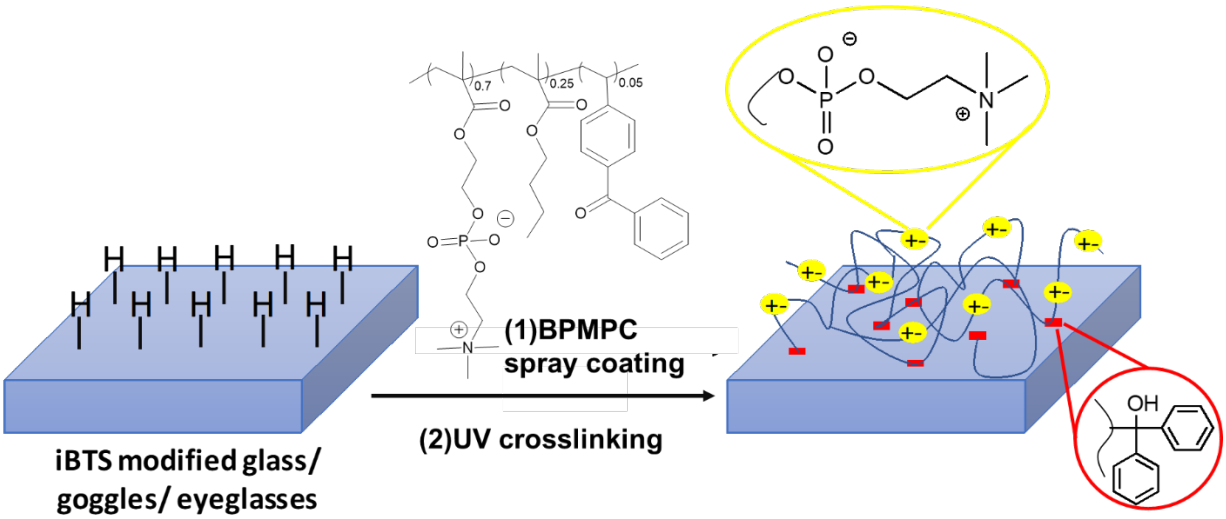

Scheme 4.1. Schematic for BPMPC crosslink to C-H containing surface under UV irradiation

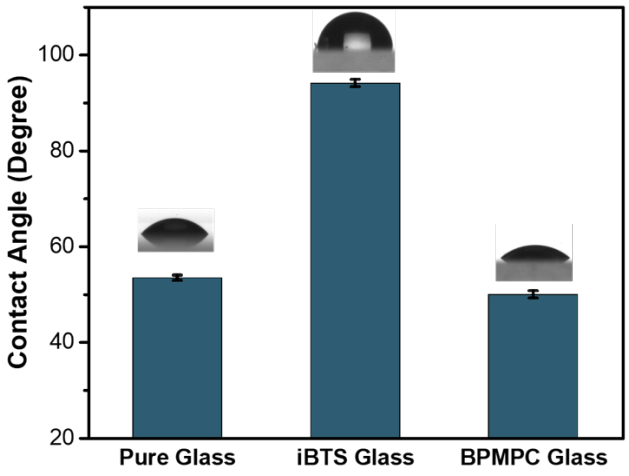

Figure 4.1. Contact angle of pure glass, iBTS modified glass and BPMPC coated glass, and digital images of water droplet respectively (top).

Transmittance.

Transmittance is one of the critical factors for the practical application of the hydrophilic coating films, especially in the fields with high requirements on safety and appearance, such as auto windshields and window glass. Figure 4.2 shows the UV-vis spectra of bare glass and BPMPC modified glass with different coating thickness and the optical photographs of coated safety glasses and eyeglasses, where the left lens was coated, and the right masked as a control. From the UV-vis spectra shown in Figure 4.2 A, the transmittance of glass did not decrease due to the BPMPC coating, ranging from 50 nm to 300 nm, which indicate BPMPC coating do not interfere with the light transmission in the visible region. The BPMPC modified glass slides have slightly higher transmission than pure glass. This might occur due to the roughness of the surface and the refractive index of the polymer. The lower refractive index of the BPMPC would benefit the optical transmittance (refractive index as measured by spectroscopic ellipsometry of BPMPC and bare

glass is 1.47 and 1.53 respectively).[110, 136] The roughness and surface topography of the coating on glass with different thickness has been examined by AFM (Figure 4.3 (A-D)). The BPMPC coatings with different thickness were smooth, as indicated by a typical root-mean-square (RMS) roughness of 2-3 nm over an area of 1 × 1 um^2, and the RMS roughness of bare glass was ~1 nm. The BPMPC top coating demonstrated similar roughness to bare glass, which would not affect the light transmittance in the visible spectra. However, the lower refractive index of BPMPC on glass promotes the destructive interference among the light rays reflected from the coating and substrate.[137] The light transmittance increases as a result of cancellation of reflection. In addition, from the optical photographs (Figure 4.2 B and 4.2 C), there was no visible difference between the modified safety glasses or eyeglasses when compared to the controls. The substrates with BPMPC coating exhibited the same excellent optical clarity.

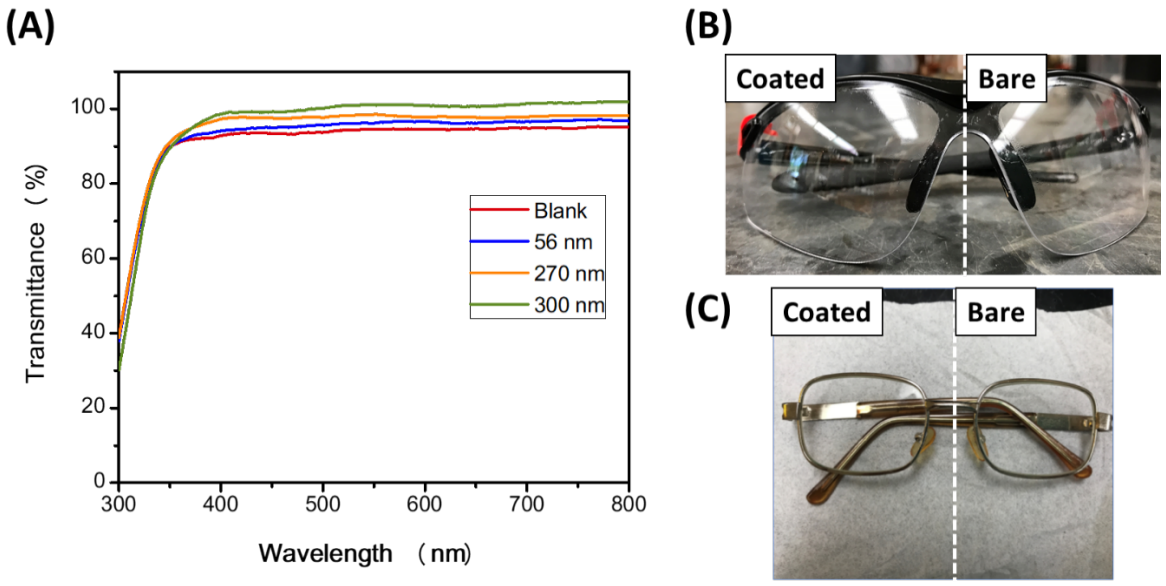

Figure 4.2. (A) UV-vis spectra of bare glass and BPMPC polymer modified glass with different coating thickness, (B) optical photograph of BPMPC coated (left side) and bare (left side) safety glasses, (C) optical photograph of BPMPC coated (right side) and bare (left side) eyeglasses.

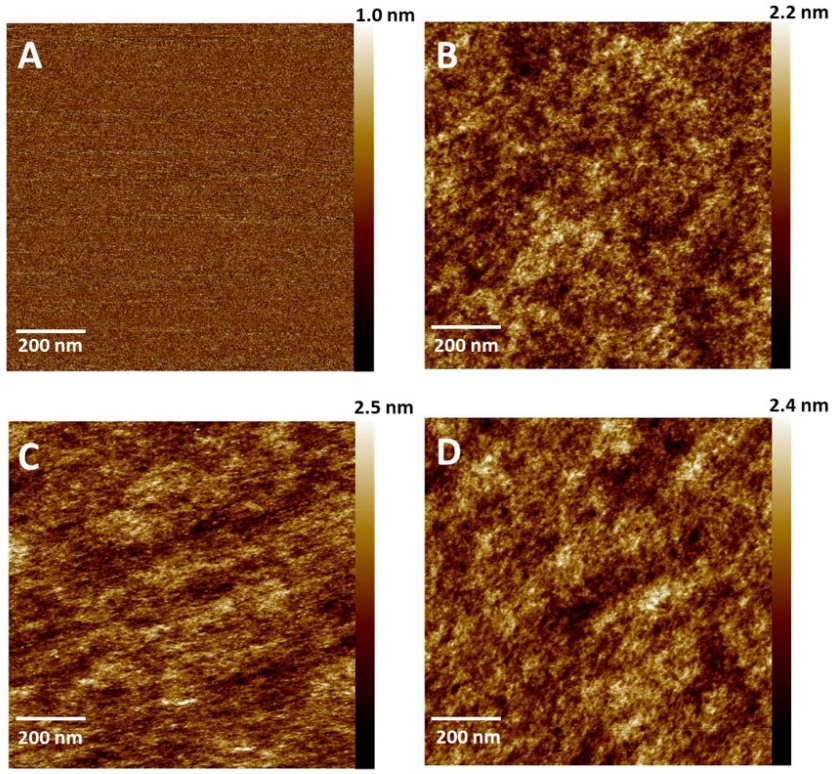

Figure 4.3. AFM topography images of (A) bare glass, (B) 60 nm, (C) 250 nm and (D) 300 nm BPMPC coatings.

Antifogging Properties.

The antifogging performance of the BPMPC coatings were demonstrated by hot-vapor and freeze-warm tests. For the glass slides, it is observed from the photographs (Figure 4.4), that condensation formed instantly on both bare glass slide (hydrophilic) and iBTS treated glass slide (hydrophobic) when placed in close contact with the boiling water vapor. With the BPMPC functionalized substrate, no condensation was observed when the slide is approaching the boiling water and after a period of time. The BPMPC modified glass maintained excellent transparency during the experiment. For the safety glasses, the left side was spray-coated with BPMPC and

cured by UV light, while the right side remained untreated. After placing the safety glasses above the boiling water, the control side (right) became opaque immediately due to the condensation, while the BPMPC modified side (left) maintained perfect clarity (Figure 4.5 A). Excess condensation can be observed toward the end of the videos due to the over-saturation of the substrate with excess condensate. The same test was conducted on the eyeglasses, and the same outcomes were observed (Figure 4.5 B). The excellent antifogging properties on these substrates and commercial samples confirmed that BPMPC could be applied to a wide variety of surfaces that are plastics or glass.

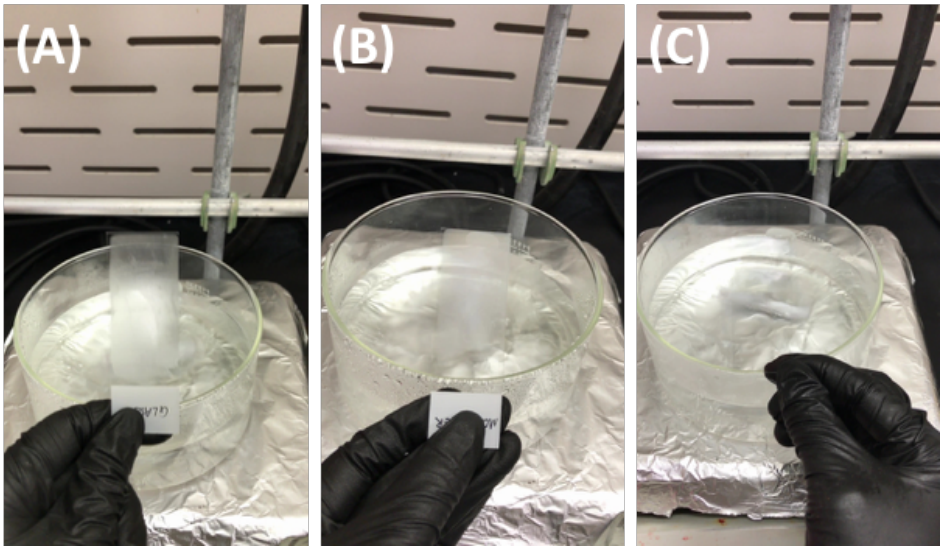

Figure 4.4. Photographs of glass slides over hot steaming water: (A) control uncoated, (B) iBTS modified and (C) BPMPC functionalized.

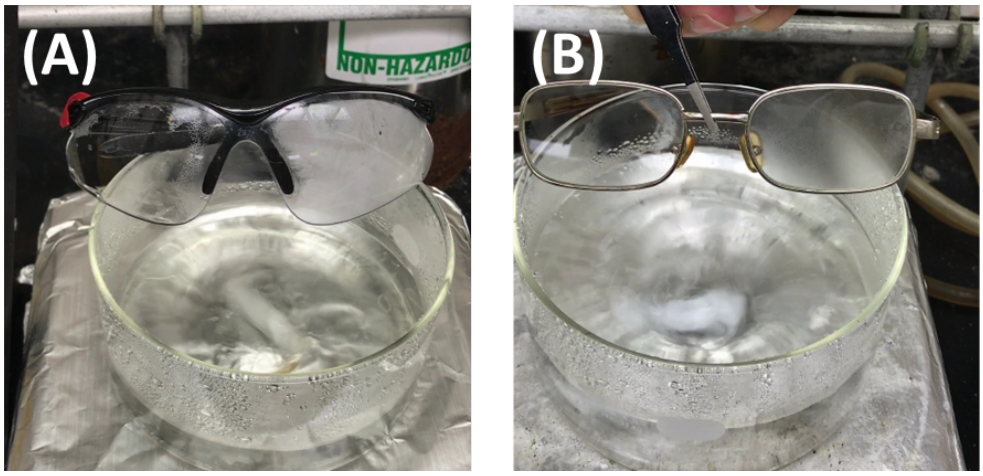

Figure 4.5. Photographs of (A) polycarbonate safety glasses and (B) eyeglasses on hot boiling water (left sides with BPMPC coating).

In the freeze-warm test, the eyewear was stored in a freezer at -20℃ for 30 min before exposed to an ambient environment (~25℃). Digital images were taken right after the sample was removed from the freezer. As shown in Figure 4.6, the uncoated safety glasses immediately fogged completely, and light scattering is easily observed. On the other hand, the coated glasses display no loss in transparency or fogging/light scattering. The results of hot-vapor and freeze-warm tests indicated that BPMPC qualifies as an antifogging material even though it is a hydrophilic coating without a contact angle close to fully wetting. This phenomena has been observed previously in coatings of semi-interpenetrating polymer networks with antifogging properties.[138, 139] Water droplets diffuse into the polymer coating, expanding the droplet basal area on the coating surface, which leads to the antifogging performance of BPMPC coating in spite of the high contact angle.

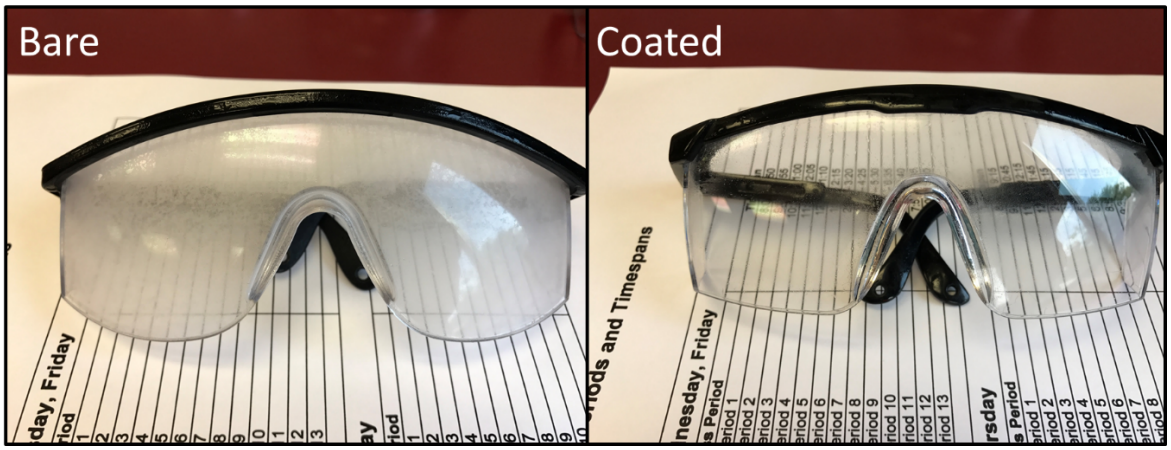

Figure 4.6. Photographs of safety glasses exposed to ambient condition (temperature ~20℃, 50% relative humidity) right after being stored at -20 ℃ for 30 min.

Self-cleaning test.

Self-cleaning coatings are generally classified into two major categories: hydrophobic and hydrophilic. Both coatings remove oil and debris by the action of water. With hydrophobic coatings, water droplets can slide and roll off the surface removing oil and debris, with hydrophilic coatings, the water spreads over the surface, which forms a water layer on the substrates that carries the dirt and impurities away.[140, 141] For BPMPC, it is anticipated that these coatings have the potential to be self-cleaning by the hydrophilic mechanism. Therefore, coated substrates were subjected to oil/grease and then immersed in water.

In the first series of experiments, the same amount of tetradecane (with dye) was placed on glass, iBTS modified glass, and BPMPC coated glass (Figure 4.7 A), then washed away by gently flowing 10 mL of H_2O over the surface. Due to the low contrast between the oil and background in the resulting image (Figure 4.7 B), we enhanced the image using Photoshop, to better discriminate the obvious remaining residue (Figure 4.7 C) on the iBTS modified (Figure 4.7 C, top slide) and control glass slide glass (Figure 4.7 C, middle slide). The gentle flow of water fails

to remove the oil contamination on either. On the other hand, the BPMPC functionalized surface has no oil residue, only a droplet of water (dyed blue), which demonstrate the self-cleaning properties. To obtain a better understanding of the mechanism behind this phenomen, we extracted several images for each substrate (Figure 4.7 D-F) from the water rinsing video. Different states and amount of water were observed on these slides. On iBTS modified glass, only a few water droplets were observed (Figure 4.7 D), which indicate the oil layer below has strong affiliation with the surface and is not displaced by water. On the control glass slide, a water stream was observed (Figure 4.7 E) due to the hydrophilicity of bare glass, which implied higher affinity between the surface and water, but this was not sufficient to remove the oil entirely. However, on BPMPC functionalized slide, the water was able to spread out on the surface and form a uniform thin layer, which can then be used to separate oil from the surface and remove it completely (Figure 4.7 F). The strong affiliation between the BPMPC coating and water leads to this result.

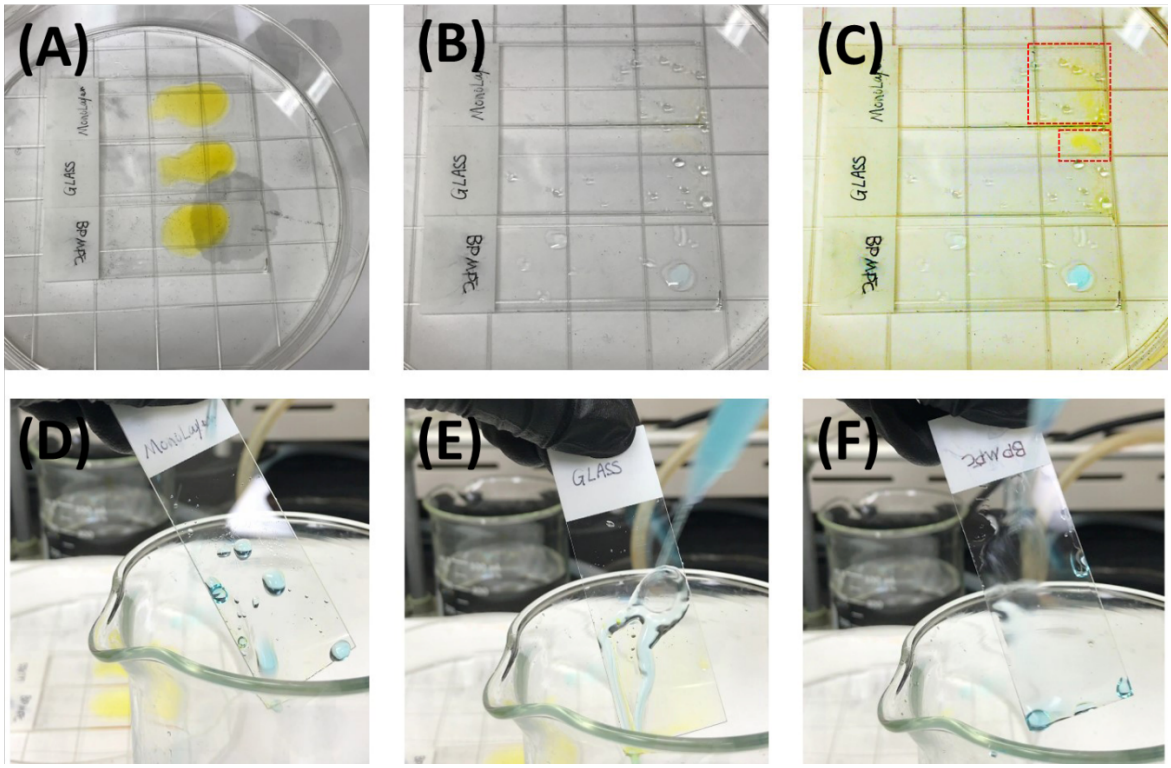

Figure 4.7. (A) Oil droplets on on iBTS modified glass (top), pure glass (middle), and BPMPC coated glass (bottom). (B) Corresponding slides after water rinse. (C) Photoshop enhanced image of (B), and the oil residues in the red box. (D)-(F) Water formation on different surfaces during the washing process, iBTS modified glass, pure glass, and BPMPC functionalized glass respectively.

In the second approach, an experiment was set up to investigate the removal of contaminations due to "greasy fingers". Water was used to remove the contaminations of greasy fingers debris (iron metal powder) attached. The fingerprints were dark and distinct on all slides (Figure 4.8 A) before cleaning. After stirring in water for 30 seconds, the fingerprint on the hydrophobic silane glass were maintained without any changes (Figure 4.8 B, top slide), which indicated that the greasy contamination remained. On the hydrophilic bare glass, a faint trace of

the fingerprint was observed (Figure 4.8 B, middle slide), which implied the contamination was partially removed. On the contrary, no trace of fingerprint was observed (Figure 4.8 B, bottom slide) on BPMPC coated surface, which exhibited outstanding self-cleaning capability. The experimental result is consistent with the hydrophilicity and hydrophobicity of all substrates. The video for the fingerprint removal is also found in the supporting information.

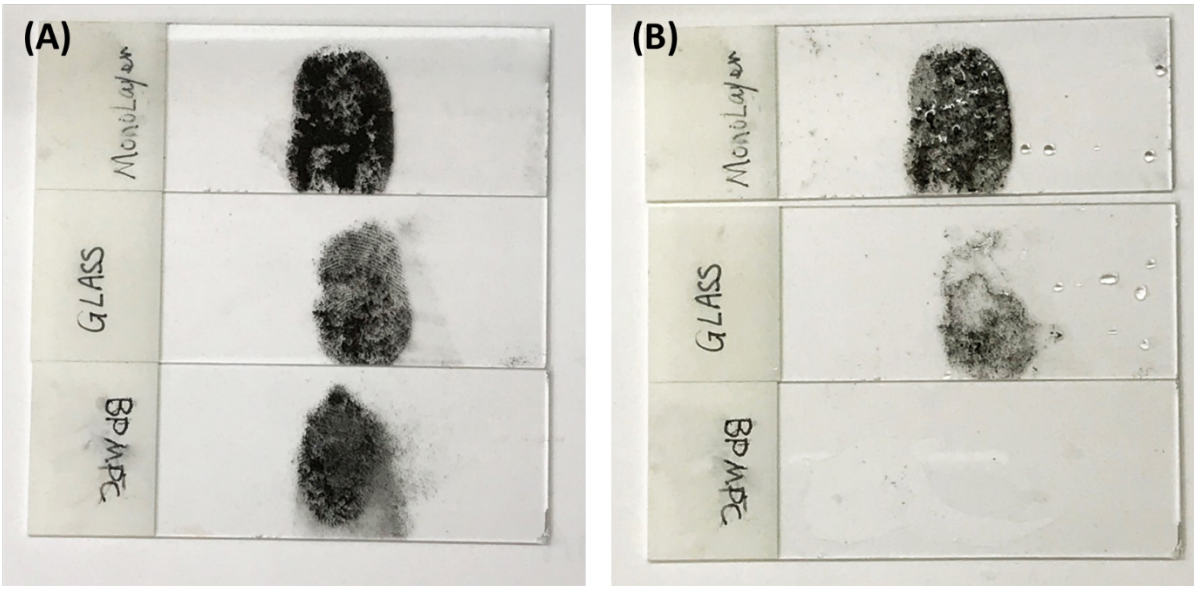

Figure 4.8. (A) Fingerprint images before water application on iBTS modified glass (top), pure glass (middle), and BPMPC coated glass (bottom). (B) Corresponding fingerprints after stirring in water solution for 30 sec.

Robust Properties.

Durability is also an essential factor in practical application of antifogging materials. The coating should survive after common cleaning methods, including water, detergent wash, and abrasion with paper towels or tissue wipe. To confirm the robustness of BPMPC coating, an excess of Windex was sprayed onto both sides of the polymer coated glass slide, then wiped harshly with

Kimwipe. There is no difference in the appearance of the glass slide after cleaning. Then, the glass slide was placed on top of the hot boiling water and no condensation was observed (Figure 4.9 A). The same procedure was conducted on a BPMPC coated glass slide without UV cross-linking, and the condensation formed instantly when coming close to the hot-vapor (Figure 4.9 B), which indicates BPMPC has been completely removed because no covalent bonds were formed without UV irradiation.

Whiteboard Cleaner (Expo) was used to examine the stability of BPMPC on eyeglasses. After spraying with enough amount of cleaner, and wiping thoroughly with a Kimwipe, both sides of the eyeglasses demonstrated excellent optical clarity and were indistinguishable from each other. However, the uncoated side formed a visible fog layer quickly while the BPMPC functionalized side showed no condensation when exposed to hot water vapor (Figure 4.9 C). The video for the antifogging behavior is also presented in the supporting information.

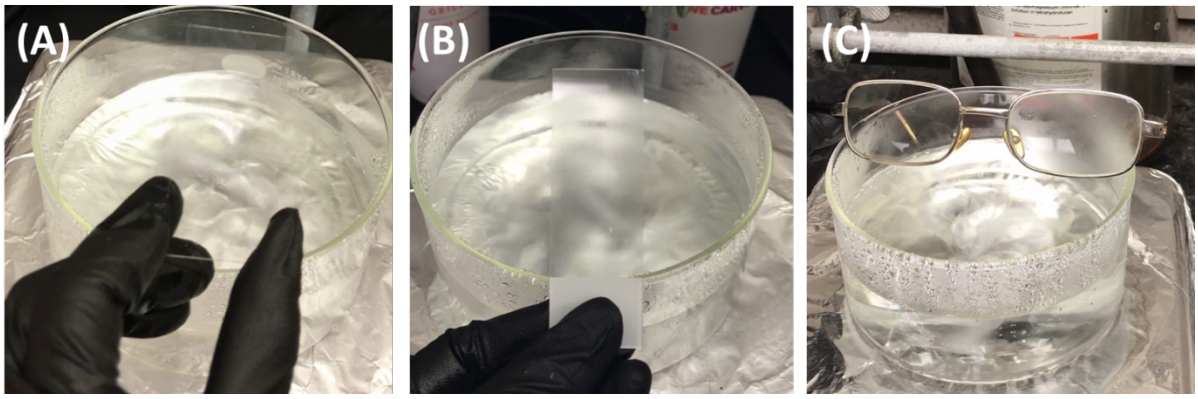

Figure 4.9. Photographs of BPMPC coated glass slides after Windex wash on hot boiling water (A) without UV curing and (B) with UV curing. (C) Photograph of eyeglasses after cleaning with Expo on hot water, BPMPC coated (left) and control (right).

Conclusion

In this research, a UV-curable antifogging and self-cleaning zwitterionic copolymer, BPMPC, was developed by a simple and straightforward radical polymerization. The polymer can be covalently grafted to various surfaces under mild UV treatment within a short period of time and does not affect the transparency of the substrates. More importantly, BPMPC coating demonstrate excellent antifogging and self-cleaning abilities on glass, eyeglasses and safety glasses. In addition, we have also challenged the BPMPC functionalized surface with household cleaning products. The surface maintained outstanding antifogging property which indicated the covalent bonds were not affected by cleaners. The facile and economical synthesis, the robust and versatile surface attachment, and the outstanding antifogging and self-cleaning abilities make it a competitive candidate for a wide array of domestic, medical and industrial coating applications.

References

1. Zhao, J.; Meyer, A.; Ma, L.; Wang, X. J.; Ming, W. H., Terpolymer-based SIPN Coating With Excellent Antifogging and Frost-resisting Properties. *RSC Adv*. **2015,** *5*, 102560-102566.

2. Chevallier, P.; Turgeon, S.; Sarra-Bournet, C.; Turcotte, R.; Laroche, G., Characterization of Multilayer Anti-Fog Coatings. *Acs Appl Mater Inter* **2011,** *3*, 750-758.

3. Petit, J.; Bonaccurso, E., General Frost Growth Mechanism on Solid Substrates with Different Stiffness. *Langmuir* **2014,** *30*, 1160-1168.

4. Wang, Y.; Li, T. Q.; Li, S. H.; Sun, J. Q., Antifogging and Frost-Resisting Polyelectrolyte Coatings Capable of Healing Scratches and Restoring Transparency. *Chem. Mater*. **2015,** *27*, 8058-8065.

5. Howarter, J. A.; Youngblood, J. P., Self-Cleaning and Next Generation Anti-Fog Surfaces and Coatings. *Macromol. Rapid Commun*. **2008,** *29*, 455-466.

6. Watanabe, T.; Nakajima, A.; Wang, R.; Minabe, M.; Koizumi, S.; Fujishima, A.; Hashimato, K., Photocatalytic Activity and Photoinduced Hydrophilicity of Titanium Dioxide Coated Glass. *2nd International Conference on Coatings on Glass, Iccg* **1999**, 374-377.

7. Wang, R.; Hashimoto, K.; Fujishima, A.; Chikuni, M.; Kojima, E.; Kitamura, A.; Shimohigoshi, M.; Watanabe, T., Light-induced Amphiphilic Surfaces. *Nature* **1997,** *388*, 431-432.

8. Fujishima, A.; Zhang, X. T.; Tryk, D. A., TiO_2 Photocatalysis and Related Surface Phenomena. *Surf. Sci. Rep*. **2008,** *63*, 515-582.

9. Lai, Y. K.; Tang, Y. X.; Gong, J. J.; Gong, D. G.; Chi, L. F.; Lin, C. J.; Chen, Z., Transparent Superhydrophobic/Superhydrophilic TiO_2-based Coatings for Self-cleaning and Anti-fogging. *J. Mater. Chem*. **2012,** *22*, 7420-7426.

10. Zhang, L. B.; Li, Y.; Sun, J. Q.; Shen, J. C., Mechanically Stable Antireflection and Antifogging Coatings Fabricated by The Layer-by-layer Deposition Process and Postcalcination. *Langmuir* **2008,** *24*, 10851-10857.

11. de Leon, A.; Advincula, R. C., Reversible Superhydrophilicity and Superhydrophobicity on a Lotus-Leaf Pattern. *Acs Appl Mater Inter* **2014,** *6*, 22666-22672.

12. Raza, A.; Ding, B.; Zainab, G.; El-Newehy, M.; Al-Deyab, S. S.; Yu, J. Y., In situ Cross-linked Superwetting Nanofibrous Membranes for Ultrafast Oil-water Separation. *J. Mater. Chem. A* **2014,** *2*, 10137-10145.

13. Zhang, L.; Zhao, N.; Xu, J., Fabrication and Application of Superhydrophilic Surfaces: A Review. *J. Adhes. Sci. Technol.* **2014,** *28*, 769-790.

14. Liang, T.; Li, H.; Lai, X.; Su, X.; Zhang, L.; Zeng, X., A Facile Approach to UV-curable Super-hydrophilic Polyacrylate Coating Film Grafted on Glass Substrate. *J. Coat. Technol. Res.* **2016,** *13*, 1115-1121.

15. Ezzat, M.; Huang, C., Zwitterionic Polymerbrush Coatings with Excellent Anti-fog and Anti-frost Properties. *RSC Adv.* **2016,** *6*, 61695-61702.

16. Wolpers, A.; Vana, P., UV Light as External Switch and Boost of Molar-Mass Control in Iodine-Mediated Polymerization. *Macromolecules* **2014,** *47*, 954-963.

17. Ge, J. P.; Lee, H.; He, L.; Kim, J.; Lu, Z. D.; Kim, H.; Goebl, J.; Kwon, S.; Yin, Y. D., Magnetochromatic Microspheres: Rotating Photonic Crystals. *J. Am. Chem. Soc.* **2009,** *131*, 15687-15694.

18. Brown, P. S.; Atkinson, O. D.; Badyal, J. P., Ultrafast Oleophobic-hydrophilic Switching Surfaces for Antifogging, Self-cleaning, and Oil-water Separation. *Acs Appl Mater Inter* **2014,** *6*, 7504-11.

19. Hyomin Lee, M. L. A., Michael F. Rubner, Robert E. Cohen, Zwitter-Wettability and Antifogging Coatings with Frost-Resisting Capabilities. *ACS Nano* **2013,** *7*, 2172-2185.

20. Howarter, J. A.; Youngblood, J. P., Self-Cleaning and Anti-Fog Surfaces via Stimuli-Responsive Polymer Brushes. *Adv. Mater.* **2007,** *19*, 3838-3843.

21. Zhang, Z.; Chen, S. F.; Chang, Y.; Jiang, S. Y., Surface Grafted Sulfobetaine Polymers via Atom Transfer Radical Polymerization as Superlow Fouling Coatings. *J. Phys. Chem. B* **2006,** *110*, 10799-10804.

22. Liu, P. S.; Domingue, E.; Ayers, D. C.; Song, J., Modification of Ti_6Al_4V Substrates with Well-defined Zwitterionic Polysulfobetaine Brushes for Improved Surface Mineralization. *Acs Appl Mater Inter* **2014,** *6*, 7141-7152.

23. Singha, P.; Locklin, J.; Handa, H., A Review of The Recent Advances in Antimicrobial Coatings for Urinary Catheters. *Acta Biomater.* **2017,** *50*, 20-40.

24. Li, C.; Li, X.; Tao, C.; Ren, L.; Zhao, Y.; Bai, S.; Yuan, X., Amphiphilic Antifogging/Anti-Icing Coatings Containing POSS-PDMAEMA-b-PSBMA. *Acs Appl Mater Inter* **2017,** *9*, 22959-22969.

25. Lin, X.; Fukazawa, K.; Ishihara, K., Photoreactive Polymers Bearing a Zwitterionic Phosphorylcholine Group for Surface Modification of Biomaterials. *Acs Appl Mater Inter* **2015,** *7*, 17489-98.

26. Ercole, F.; Davis, T. P.; Evans, R. A., Photo-responsive Systems and Biomaterials: Photochromic Polymers, Light-triggered Self-assembly, Surface Modification, Fluorescence Modulation and Beyond. *Polym. Chem.* **2010,** *1*, 37-54.

27. Dorman, G.; Prestwich, G. D., Benzophenone Photophores in Biochemistry. *Biochemistry* **1994,** *33*, 5661-5673.

28. Higuchi, H.; Yamashita, T.; Horie, K.; Mita, I., Photo-Cross-Linking Reaction of Benzophenone-Containing Polyimide and Its Model Compounds. *Chem. Mater.* **1991,** *3*, 188-194.

29. Toomey, R.; Freidank, D.; Ruhe, J., Swelling behavior of thin, surface-attached polymer networks. *Macromolecules* **2004,** *37*, 882-887.

30. Pahnke, J.; Ruhe, J., Attachment of Polymer Films to Aluminium Surfaces by Photochemically Active Monolayers of Phosphonic Acids. *Macromol. Rapid Commun.* **2004,** *25*, 1396-1401.

31. Shen, W. W.; Boxer, S. G.; Knoll, W.; Frank, C. W., Polymer-supported Lipid Bilayers on Benzophenone-modified Substrates. *Biomacromolecules* **2001,** *2*, 70-79.

32. Virkar, A.; Ling, M. M.; Locklin, J.; Bao, Z., Oligothiophene Based Organic Semiconductors with Cross-linkable Benzophenone Moieties. *Synth. Met.* **2008,** *158*, 958-963.

33. Samuel, J. D. J. S.; Brenner, T.; Prucker, O.; Grumann, M.; Ducree, J.; Zengerle, R.; Ruhe, J., Tailormade Microfluidic Devices Through Photochemical Surface Modification. *Macromol. Chem. Phys.* **2010,** *211*, 195-203.

34. Hu, S. W.; Ren, X. Q.; Bachman, M.; Sims, C. E.; Li, G. P.; Allbritton, N. L., Surface-directed, Graft Polymerization within Microfluidic Channels. *Anal. Chem.* **2004,** *76*, 1865-1870.

35. Prucker, O.; Brandstetter, T.; Ruhe, J., Surface-attached Hydrogel Coatings via C,H-insertion Crosslinking for Biomedical and Bioanalytical Applications (Review). *Biointerphases* **2018,** *13*.

36. Abu-Rabeah, K.; Atias, D.; Herrmann, S.; Frenkel, J.; Tavor, D.; Cosnier, S.; Marks, R. S., Characterization of Electrogenerated Polypyrrole-Benzophenone Films Coated on Poly(pyrrole-methyl metacrylate) Optic-Conductive Fibers. *Langmuir* **2009,** *25*, 10384-10389.

37. Brandstetter, T.; Bohmer, S.; Prucker, O.; Bisse, E.; zur Hausen, A.; Alt-Morbe, J.; Ruhe, J., A Polymer-based DNA Biochip Platform for Human Papilloma Virus Genotyping. *J. Virol. Methods* **2010,** *163*, 40-48.

38. Yatvin, J.; Gao, J.; Locklin, J., Durable Defense: Robust and Varied Attachment of Non-leaching Poly"-onium" Bactericidal Coatings to Reactive and Inert Surfaces. *Chem. Commun.* **2014,** *50*, 9433-9442.

39. Gao, J.; Martin, A.; Yatvin, J.; White, E.; Locklin, J., Permanently Grafted Icephobic Nanocomposites with High Abrasion Resistance. *J. Mater. Chem. A* **2016,** *4*, 11719-11728.

40. Liu, Q. H.; Singha, P.; Handa, H.; Locklin, J., Covalent Grafting of Antifouling Phosphorylcholine-Based Copolymers with Antimicrobial Nitric Oxide Releasing Polymers to Enhance Infection-Resistant Properties of Medical Device Coatings. *Langmuir* **2017,** *33*, 13105-13113.

41. Stephens, E. R.; Rodney, W. S., Refractive Indices of Five Selected Optical Glasses. *J. Res. Natl. Bur. Stand.* **1954,** *52*, 303-304.

42. Raut, H. K.; Ganesh, V. A.; Nair, A. S.; Ramakrishna, S., Anti-reflective Coatings: A Critical, In-depth Review. *Energ Environ. Sci.* **2011,** *4*, 3779-3804.

43. Zhao, J.; Ma, L.; Millians, W.; Wu, T. E. H.; Ming, W. H., Dual-Functional Antifogging/Antimicrobial Polymer Coating. *Acs Appl Mater Inter* **2016,** *8*, 8737-8742.

44. Zhang, T.; Yu, Q. Y.; Wang, J. J.; Wu, T., Design and Fabrication of a Renewable and Highly Transparent Multilayer Coating on Poly(lactic acid) Film Capable of UV-Shielding and Antifogging. *Ind. Eng. Chem.y Res.* **2018,** *57*, 4577-4584.

45. Liu, K. S.; Yao, X.; Jiang, L., Recent Developments in Bio-inspired Special Wettability. *Chem. Soc. Rev.* **2010,** *39*, 3240-3255.

46. Ganesh, V. A.; Raut, H. K.; Nair, A. S.; Ramakrishna, S., A Review on Self-cleaning Coatings. *J. Mater. Chem.* **2011,** *21*, 16304-16322.

47. Starr, C.; Evers, C. A.; Starr, L., *Biology: Concepts and Applications*. Thomson Brooks: **2006**.

CHAPTER 5

SELF-ASSOCIATION OF ZWITTERIONIC POLYMER COATINGS BEARING BENZOPHENONE CROSSLINKER[1]

[1]Liu, Q., Locklin, J.; To be submitted to [Langmuir]

Abstract

The application of benzophenone (BP) attracted much attention in organic chemistry, polymer and material science, even in biochemistry. The use of BP pendent groups in the polymer chain provides various possibility in creating robust chemical grafting functional coatings. The hydrogen abstraction of BP would not just occur between the polymer and the substrates, but also inside polymer networks, due to the BP photochemical properties. The chemical and physical properties of polymer coating might change under this process. For instance, the contact angle of the zwitterionic polymer bearing BP (2-methacryloyloxyethyl phosphorylcholine-co-butyl methacrylate-co-benzophenone, BPMPC) would increase significantly after irradiating under UV. The reason for this phenomenon was explained by analyzing the surface thoroughly. Additionally, the mechanism for the BPMPC coatings exhibited antifouling and antifogging properties with poor hydrophilicity was discussed.

Introduction

The development of functional surface has significant implications in tuning the chemical and physical properties of material interfaces for various applications in biotechnology, optics, electronics, and photonics.[1-5] As a result, tremendous effects have been made to produce optimal modification strategies that allow for selective and controllable covalent crosslink to achieve desired surface structure and functionality. Among all the methods, photochemical activation of C-H bonds is a particularly facile and versatile strategy for obtaining functional materials with the following advantages: (1) photochemical reactions are rapid, efficient, and environment friendly; (2) the mechanism of photochemical is well known with a number of commercially available selections; (3) the UV irradiation wavelength, intensity, time can be adjusted for further tailoring of surface properties. [2, 6-9]

Numerous photoreactive agents have been used to the functionalized surface for different applications, including azides (acryl, aroyl, aryl),[10-12] diazirine,[13] nitroanisole derivatives,[14] succinic anhydrides,[15] etc. Benzophenone (BP) and derivatives are probably the most widely studied and used in organic chemistry and material science due to their high photochemical activity, low cost, diverse application and the ease of use.[16-18] The n-π^* excitation can relax in many ways, leading to photosensitization, [2+2] cycloaddition, and most importantly, H-abstraction and radical combination, which results in covalent cross-linking.[19] This photo-reaction proceeds with reasonable efficiency in various chemical environment, even in the present of oxygen, making BP broadly used for surface modification in polymer and material science.[20-23] Additionally, BP has an excitation wavelength of 365 nm which would not destroy the polymer or living materials.

Recently, BP containing polymer has been widely used as a powerful tool to modify surface in a broad application scope. In our previous study, antimicrobial, antifouling, and

antifogging polymer coatings have been synthesized with BP pendent group, which can generate robust functional films using BP crosslinking.[24-26] Zwitterionic copolymer 2-methacryloyloxyethyl phosphorylcholine-co-butyl methacrylate-co-benzophenone (BPMPC) demonstrated outstanding antifogging and self-cleaning properties due to the high hydrophilicity of zwitterionic monomer, 2-methacryloyloxyethyl phosphorylcholine (MPC).[26] In addition, BP works as a photo-crosslinker in the copolymer to generate the covalent bonds between the functional film and substrates, which provided mechanical and chemical robustness to the coating. Although BPMPC exhibited the properties as anticipated, the water contact angle (CA) of the coating increased unexpected under UV curing from $<10^0$ to $\sim 50^0$, both 254 nm and 365 nm. The phenomena were observed with a difference ratio of MPC and n-butyl methacrylate in the copolymer, even with 90% MPC. Moreover, it is generally believed that the antifogging and self-cleaning surface must be superhydrophilic ($CA < 10^0$), but BPMPC demonstrated these abilities without required hydrophilicity.

In this chapter, we investigated the influence of BP crosslinking when presenting in a zwitterionic terpolymer, BPMPC. The increase of hydrophobicity in BPMPC after UV irradiation was explained through analyzing the surface properties of zwitterionic polymers with and without BP, including film thickness, CA, infrared spectrum and Young's modulus. Moreover, the mechanism of BPMPC demonstrating antifouling and antifogging properties with relatively poor hydrophilicity was explained by interpenetration and association releasing hypothesis.

Experiment Section

Materials.

2-Methacryloyloxyethyl phosphorylcholine (MPC) was purchased from Sigma Aldrich. 2,2'-azobis(2-methylpropiontirlemethylpropionitrile) (AIBN) and n-butyl methacrylate (nBMA) were purchased from Alfa-Aesar. Isobutyltrichlorosilane (iBTS) was purchased from Tokyo Chemical Industry. 2-methacryloyloxyethyl phosphorylcholine-co-butyl methacrylate-co-benzophenone (BPMPC) was synthesized according to a previously reported procedure from our group.[26] De-ionized (DI) water (18.2 MΩ) was used for all the aqueous solution. Nitrogen gas was purchased from Airgas. All the chemicals were used as received without further purification.

Poly (MPC-co-nBMA) synthesis.

The polymer without BP was also synthesized by radical polymerization. MPC (0.427 g, 1.48 mmol), n-BMA (84 μL, 0.53 mmol) were dissolved in 4.2 mL ethanol (total monomer concentration 1.0 mmol mL^{-1}) with initiator AIBN (0.01 mmol mL^{-1}), and the solution was poured into polymerization tube. After degassed with argon for 30 minutes, the polymerization reaction was carried out under nitrogen flow at 60℃ for 16 h. The reaction was stopped by exposing the solution to air, cooled to room temperature, and poured into ethyl ether to precipitate the polymer. The white solid was collected by vacuum filtration and dried under vacuum for 12 h. ^1H NMR (D_2O) was taken to confirm the polymer composition (Figure A7).

Silicon substrates were cut into 2 cm × 2cm size, then sonicated with deionized water, hexane, isopropanol, and acetone for 5 minutes each then dried under nitrogen, followed by plasma (Harrick Plasma PDC-32G) cleaning and treatment with iBTS in toluene (10 mmol) overnight before modification with the polymer. Polymer modified film was developed on a functionalized

silicon substrate by utilizing spin coating. Each slide used 200 μL polymer/ethanol solution (10 mg mL^{-1}) and spin at 1000 rpm for 30 seconds to generate a uniform coating.

Characterization of the polymer coatings.

The surface wettability was characterized by measuring the static water contact angle, which obtained from a DSA 100 drop shape analysis system (KRŰSS) with a computer-controlled liquid dispensing system. 1 μL DI water droplets were deposited onto substrate surfaces, and the water contact angles were recorded by the program. For the CA lower than 10^0 was treated as 10^0 due to the accuracy of the program. The thickness of the spin-coated polymer layer on the silicon substrates and CarboSil substrates were measured by M-2000V Spectroscopic Ellipsometer (J.A. Woollam co., INC.) with a white light source at three incident angles (65°, 70°, and 75°). The thickness of the modified layer was measured and calculated using a Cauchy layer model. Infrared spectroscopy studies of polymer coated films were done using a Thermo-Nicolet model 6700 spectrometer equipped with a variable angle grazing angle attenuated total reflection (GATR-ATR) accessory (Harrick Scientific). The surface modulus was collected using a PeakForce Quantitative Nanomechanical Mapping (QNM, Bruker Multimode AFM, ScanAsyst-AIR, k = 0.4 N m^{-1}, resonant frequency (f_0) = 50-90 Hz). Scan sizes were 10 μm × 10 μm.

Results and Discussion

The zwitterionic polymer (PMPCBMA) was synthesized by radical polymerization in ethanol (Scheme 5.1). The copolymer composition was confirmed by ^{1}H NMR spectroscopy (Figure A7) and consisted of 79:21 (MPC:nBMA), which roughly matched the monomer feed ratio. According to our previous study result on BPMPC, the ratio of each component is 74:18:8

(MPC:nBMA:BP). The ratio of MPC and nBMA in BPMPC (20:80) is approximately the same to PMPCBMA, with the only difference in the presence of photo crosslinker, BP.

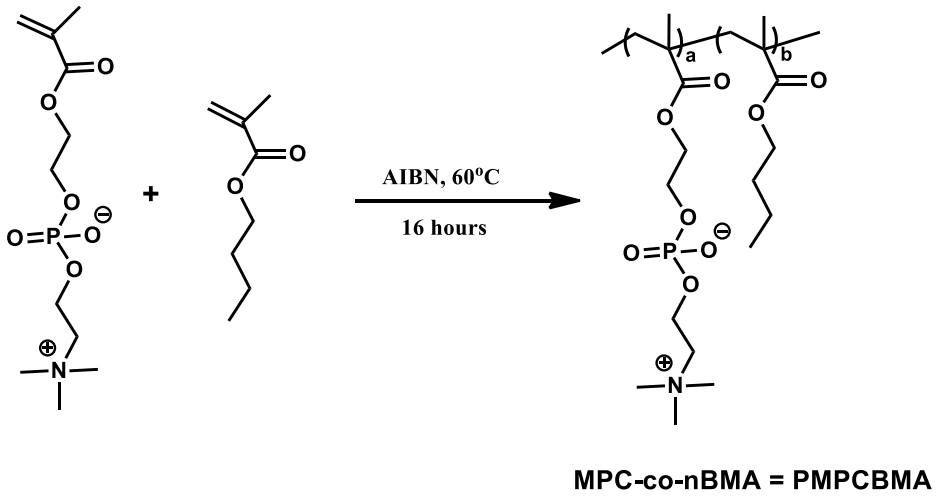

Scheme 5.1. Synthesis of PMPCBMA

The wetting property of PMPCBMA and BPMPC were investigated by DSA. Initially, the CA of PMPCBMA and BPMPC were both lower than 10^0 (Figure 5.1), which indicated the presence of 8% BP does not affect the wetting property of polymer coatings much. However, the CA of BPMPC increased from $<10^0$ to $\sim 50^0$ after 10 minutes UV irradiation (254 nm, 6.5 mW/cm^{-2}), while the CA of PMPCBMA maintained after the identical treatment. A similar result was received under difference wavelength (365 nm) UV irradiation with longer exposing time. These results suggested that the crosslinking of BP induced the increase of CA.

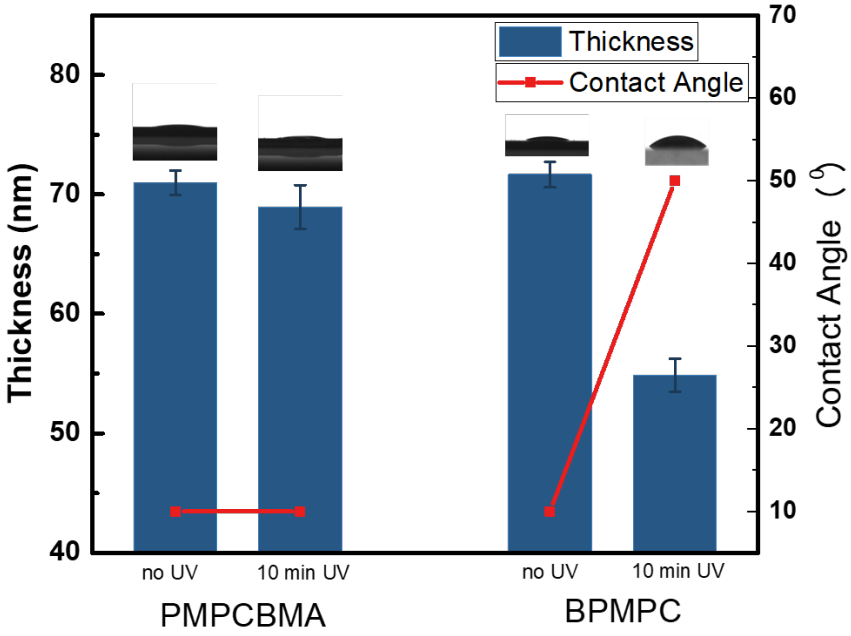

Figure 5.1. Thickness and contact angle of PMPCBMA and BPMPC coatings before and after UV irradiation.

Previous studies on zwitterionic polymer brushes, that demonstrating high contact angle, claimed that the polymer chains bearing high-dipole-moment side-groups would permanently have self-association conformation.[27-29] Electrostatic reactions between opposite charges would bring the functional groups as close as possible, which leads to the interchain and intrachain crosslinking. Additionally, the studies described the thickness of the polymer film is an essential factor for self-association. Thicker brushes (>50 nm) would promote the self-association and reduce the hydrophilicity of the surface. In our study, PMPCBMA and BPMPC both demonstrated high hydrophilicity even with a thickness around 70 nm. This phenomenon might occur due to the grafting method. “Grafting to” method is hard to achieve high graft density, which would not facilitate the self-association of the zwitterionic side chain. The self-association could also explain

why the CA increase in BPMPC. Under UV irradiation, BP is not just abstracting H atoms from the substrates, but also from the polymer backbone and other side chains. This crosslinking between the polymer chains or in the polymer chain would bring the chains closer to each other even chain collapsing, which would result in the association of zwitterionic moiety, then increase the hydrophobicity of the surface (Scheme 5.2).

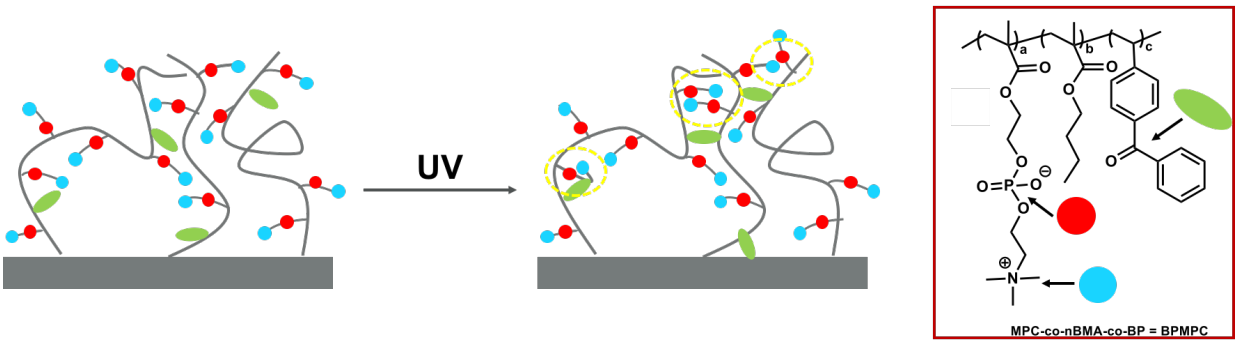

Scheme 5.2. The schematic diagram of BP crosslinking between and inside polymer chains. The self-association occurs as the chain closer to each other due to the BP crosslinking.

The thicknesses of BPMPC and PMPCBMA before and after UV were also investigated to confirm the hypothesis above. The similar initial thickness of two polymer coatings was prepared using spin coating method (Table 5.1). After UV (254 nm) irradiating for 10 min, the thickness of PMPCBMA maintained with only 2 nm reduce, which might due to the evaporation of residual solvent. However, the thickness of BPMPC significantly decreased from 71.7 nm to 54.9 nm, which suggested the formation of crosslinking between polymer chains due to BP photo-reaction.

Table 5.1. BPMPC and PMPBMA film thickness before and after UV irradiation.

Thickness	BPMPC	PMPCBMA
Initial (nm)	71.67	71.0
UV treatment (nm)	54.88	69.0

FTIR was also conducted on BPMPC, and PMPCBMA coated substrates before and after UV curing (Figure 5.2). The absorption peaks of MPC units, carbonyl group (1722 cm^{-1}) and PC group (1240, 1047, and 958 cm^{-1}), were observed in both polymer surfaces before and after UV. The peak at (1651 cm^{-1}) represents the C=O stretch of BP ketone, which was only shown in BPMPC substrates before UV treatment. A significant reduction of this peak after irradiation was observed which indicate the crosslinking of BP to the substrates and the formation of a polymer network. However, no other change was observed from IR spectra, which indicated no new bond formed except the H-abstraction and radical combination of BP triplet.

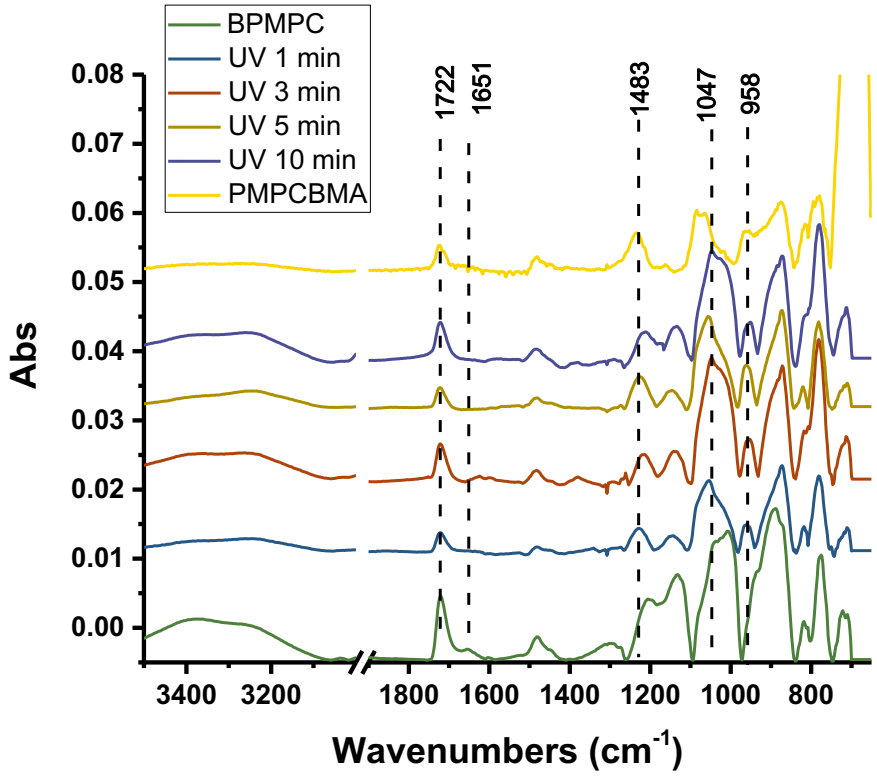

Figure 5.2. FTIR spectra of BPMPC and irradiated under UV for 1, 3, 5, and 10 min, and FTIR spectrum of PMPCBMA.

The AFM topographic and modulus images of BPMPC films after different irradiation time are shown in Figure 5.3. The moduli of BPMPC films increase with longer UV exposure, which indicated the polymer network becomes denser. As more BP reacts with surrounding alkyl groups, the side chains crosslinking is denser and more self-association between zwitterionic components, both of which lead to the increase of modulus.

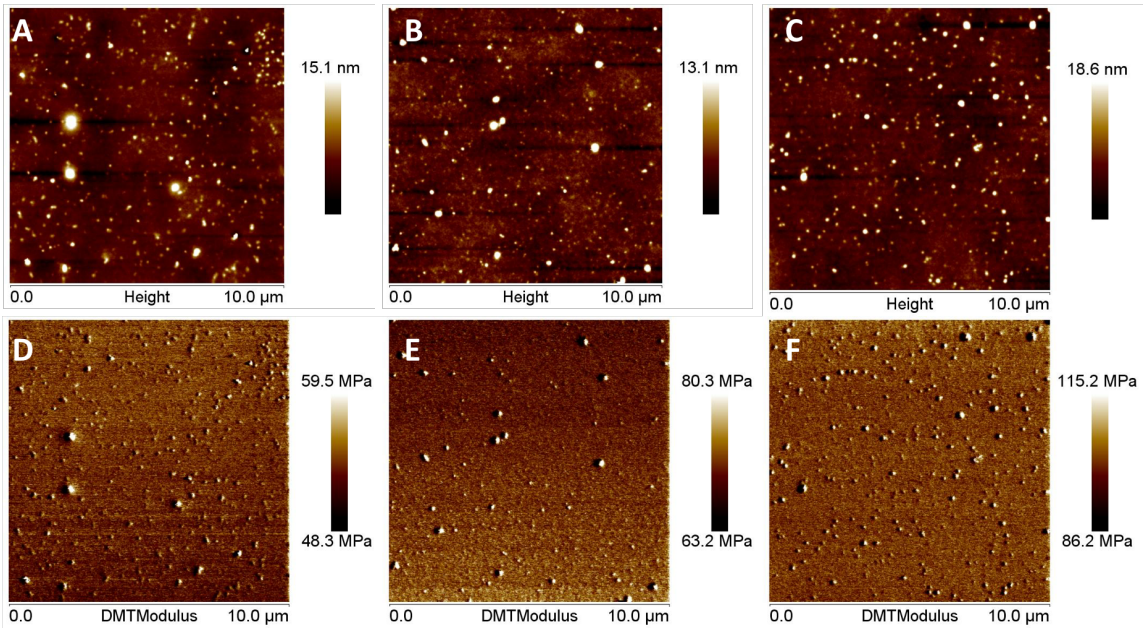

Figure 5.3. AFM topography (A-C) and DMT modulus data of BPMPC films irradiated with various time: no UV (A, D); 1 min (B, E); 5 min (C, F).

Another evidence for the presenting of self-association is the CA decease under higher temperature. The coated slides were heated up using a heat gun before measuring by DSA, and the temperatures were monitored by the infrared thermometer. From Table 5.2, a reduction in the CA was observed with the increase of surface temperature. Under higher temperature, the segment movement of polymer chains would accelerate, which can break the electrostatic connections between the opposite charges and releasing the zwitterionic side chain. This non-associated states of BPMPC at higher temperature would result in lower water CA observed.

Table 5.2. The CA of BPMPC coating under different temperature.

Temperature (°C)	Room temp.	43.8	54
CA (^{0})	47	32.6	28.5

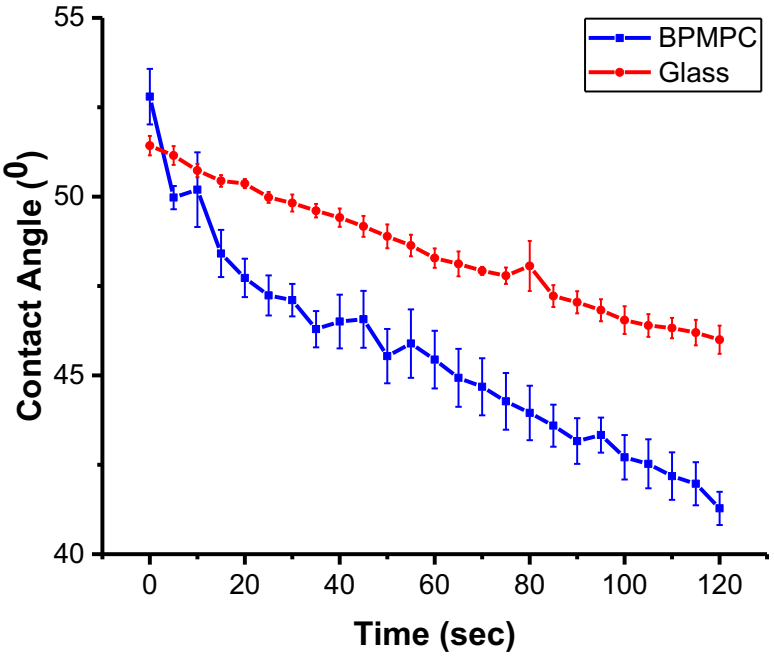

Figure 5.4. Water contact angle of BPMPC (after 1 min UV) and bare glass with time.

According to previous studies, BPMPC demonstrated antifouling and antifogging properties with relative high-water CA.[25, 26] To explain the mechanism behind this uncommon phenonmenon, the CA on BPMPC surface was monitored by DSA with elongated time, 120 seconds (Figure 5.4). The CA decease on BPMPC is much more rapidly (52^0 to 40^0) than on control glass (~ 5^0, due to water evaporation only), which can be explained by two possible mechanisms. One explanation is the water diffused into BPMPC coating, and the droplet basal area expanded on the coating surface, which is called interpenetration mechanism. The other explanation might be, in the presence of high dielectric constant (ε) solvent, like water ($\varepsilon \approx 80$),[30] the electrostatic attraction between opposite charges would reduce, which leads to the non-association of MPC

units and the decrease of CA. One or both mechanisms contribute to the antifouling and antifogging properties of BPMPC.

Conclusion

In conclusion, we have explained the reason for the water contact angle increase of the BPMPC after UV irradiation. Due to the mechanism of photo-crosslinker BP, the hydrogen abstraction would happen at any surround alkyl group, which indicates the crosslinking is not just occurred between polymer and substrates, but also inside the polymer matrix. This circumstance would induce the self-association between opposite charge groups in the zwitterionic side chain, which lead to the increase of contact angle. Moreover, the film thickness would decrease, and Young's modulus would increase with longer UV exposure. In addition, antifogging and antifouling properties of BPMPC might attribute to two possible explanation working individually or cooperatively, interpenetration mechanism and un-association mechanism.

References

1. Turgeon, A. J.; Harley, B. A.; Bailey, R. C., Benzophenone-Based Photochemical Micropatterning of Biomolecules to Create Model Substrates and Instructive Biomaterials. *Method Cell Biol* **2014,** *121*, 231-+.

2. Yang, P.; Yang, W. T., Surface Chemoselective Phototransformation of C-H Bonds on Organic Polymeric Materials and Related High-Tech Applications. *Chem Rev* **2013,** *113* (7), 5547-5594.

3. Cobley, A. J., Alternative surface modification processes in metal finishing and electronic manufacturing industries. *T I Met Finish* **2007,** *85* (6), 293-297.

4. Radu, A.; Scarmagnani, S.; Byrne, R.; Slater, C.; Lau, K. T.; Diamond, D., Photonic modulation of surface properties: a novel concept in chemical sensing. *J Phys D Appl Phys* **2007,** *40* (23), 7238-7244.

5. Dorman, G.; Prestwich, G. D., Using photolabile ligands in drug discovery and development. *Trends Biotechnol* **2000,** *18* (2), 64-77.

6. Park, E. J.; Carroll, G. T.; Turro, N. J.; Koberstein, J. T., Shedding light on surfaces-using photons to transform and pattern material surfaces. *Soft Matter* **2009,** *5* (1), 36-50.

7. Laufer, A. H.; Fahr, A., Reactions and kinetics of unsaturated C-2 hydrocarbon radicals. *Chem Rev* **2004,** *104* (6), 2813-2832.

8. Herrerias, C. I.; Yao, X. Q.; Li, Z. P.; Li, C. J., Reactions of C-H bonds in water. *Chem Rev* **2007,** *107* (6), 2546-2562.

9. Crabtree, R. H., Introduction to Selective Functionalization of C-H Bonds. *Chem Rev* **2010,** *110* (2), 575-575.

10. Khong, S. H.; Sivaramakrishnan, S.; Png, R. Q.; Wong, L. Y.; Chia, P. J.; Chua, L. L.; Ho, P. K. H., General photo-patterning of polyelectrolyte thin films via efficient ionic Bis(Fluorinated phenyl azide) photo-crosslinkers and their post-deposition modification. *Adv Funct Mater* **2007,** *17* (14), 2490-2499.

11. Nam, C. Y.; Qin, Y.; Park, Y. S.; Hlaing, H.; Lu, X. H.; Ocko, B. M.; Black, C. T.; Grubbs, R. B., Photo-Cross-Linkable Azide-Functionalized Polythiophene for Thermally Stable Bulk Heterojunction Solar Cells. *Macromolecules* **2012,** *45* (5), 2338-2347.

12. Yoo, M.; Kim, S.; Lim, J.; Kramer, E. J.; Hawker, C. J.; Kim, B. J.; Bang, J., Facile Synthesis of Thermally Stable Core-Shell Gold Nanoparticles via Photo-Cross-Linkable Polymeric Ligands. *Macromolecules* **2010,** *43* (7), 3570-3575.

13. Sinz, A., Chemical cross-linking and mass spectrometry to map three-dimensional protein structures and protein-protein interactions. *Mass Spectrom Rev* **2006,** *25* (4), 663-682.

14. Nishihira, J.; Sakai, M.; Nishi, S.; Hatanaka, Y., Identification of the Electrophilic Substrate-Binding Site of Glutathione-S-Transferase-P by Photoaffinity-Labeling. *Eur J Biochem* **1995,** *232* (1), 106-110.

15. Eisele, G.; Fouassier, J. P.; Reeb, R., Kinetics of photocrosslinking reactions of a DCPA/EA matrix in the presence of thiols and acrylates. *J Polym Sci Pol Chem* **1997,** *35* (12), 2333-2345.

16. Horie, K.; Ando, H.; Mita, I., Photochemistry in Polymer Solids .8. Mechanism of Photoreaction of Benzophenone in Polyvinyl-Alcohol). *Macromolecules* **1987,** *20* (1), 54-58.

17. Dorman, G.; Prestwich, G. D., Benzophenone Photophores in Biochemistry. *Biochemistry-Us* **1994,** *33* (19), 5661-5673.

18. Brauchle, C.; Burland, D. M.; Bjorklund, G. C., Hydrogen Abstraction by Benzophenone Studied by Holographic Photochemistry. *J Phys Chem-Us* **1981,** *85* (2), 123-127.

19. Dorman, G.; Nakannura, H.; Pulsipher, A.; Prestwich, G. D., The Life of Pi Star: Exploring the Exciting and Forbidden Worlds of the Benzophenone Photophore. *Chem Rev* **2016,** *116* (24), 15284-15398.

20. Smets, G. J.; Elhamouly, S. N.; Oh, T. J., Photochemical-Reactions on Polymers. *Pure Appl Chem* **1984,** *56* (3), 439-446.

21. Lin, A. A.; Sastri, V. R.; Tesoro, G.; Reiser, A.; Eachus, R., On the Cross-Linking Mechanism of Benzophenone-Containing Polyimides. *Macromolecules* **1988,** *21* (4), 1165-1169.

22. Shoute, L. C. T.; Huie, R. E., Reactions of triplet decafluorobenzophenone with alkenes. A laser flash photolysis study. *J Phys Chem A* **1997,** *101* (19), 3467-3471.

23. Carroll, G. T.; Triplett, L. D.; Moscatelli, A.; Koberstein, J. T.; Turro, N. J., Photogeneration of Gelatinous Networks from Pre-Existing Polymers. *J Appl Polym Sci* **2011,** *122* (1), 168-174.

24. Gao, J.; Huddleston, N. E.; White, E. M.; Pant, J.; Handa, H.; Locklin, J., Surface Grafted Antimicrobial Polymer Networks with High Abrasion Resistance. *Acs Biomater Sci Eng* **2016,** *2* (7), 1169-1179.

25. Liu, Q. H.; Singha, P.; Handa, H.; Locklin, J., Covalent Grafting of Antifouling Phosphorylcholine-Based Copolymers with Antimicrobial Nitric Oxide Releasing Polymers to Enhance Infection-Resistant Properties of Medical Device Coatings. *Langmuir* **2017,** *33* (45), 13105-13113.

26. Liu, Q. H.; Locklin, J., Transparent Grafted Zwitterionic Copolymer Coatings That Exhibit Both Antifogging and Self-Cleaning Properties. *Acs Omega* **2018,** *3* (12), 17743-17750.

27. Azzaroni, O.; Brown, A. A.; Huck, W. T. S., UCST wetting transitions of polyzwitterionic brushes driven by self-association. *Angew Chem Int Edit* **2006,** *45* (11), 1770-1774.

28. Rubinstein, M.; Dobrynin, A. V., Associations leading to formation of reversible networks and gels. *Curr Opin Colloid In* **1999,** *4* (1), 83-87.

29. Laughlin, R. G., Fundamentals of the Zwitterionic Hydrophilic Group. *Langmuir* **1991,** *7* (5), 842-847.

30. Chevalier, Y.; Leperchec, P., Intercharge Distance of Flexible Zwitterionic Molecules in Solution. *J Phys Chem-Us* **1990,** *94* (5), 1768-1774.

CHAPTER 6

CONCLUSION AND FUTURE OUTLOOK

Conclusions

In this dissertation, zwitterionic polymers bearing benzophenone (BP) pendent group was investigated thoroughly including kinetics, mechanism, and applications. In Chapter 1, a literature review of BP photo-crosslinker was presented. This includes a survey of polymer deposition methods, BP crosslink mechanism, and effecting factor for BP crosslink. Also previous works of the utilization of BP, as a photoinitiaor, photosensitizer, or anchoring group in immobilization functional films through "grafting from" or "grafting to" method was discussed with the necessary directions of the fields highlighted.

Chapter 2 demonstrated a zwitterionic antifouling polymer (BPMPC) coating covalently crosslinked to a nitric oxide-releasing polyurethane material (SNAP in Carbosil), which possess the antimicrobial ability. The combination of both materials offered a promising application in medical devices. Protein adsorption tests showed that the presenting of zwitterionic significantly reduce the adsorption of lysozyme and fibrinogen. Moreover, BPMPC coating as a top layer on CarboSil (with SNAP) does not affect the releasing of NO and the leaching of SNAP. On the contrary, the zwitterionic coating improves the NO concentration, which constant with previous study the hydrophilic coating can facilitate the NO-releasing. The bacterial killing efficiency also showed the similar improvement when the substrates coated with BPMPC. The stability

Chapter 3 is focused on an antifogging and self-cleaning zwitterionic coating (BPMPC) with mechanical and chemical robustness. Transparence is an essential factor in real-world

applications for antifogging materials, and BPMPC coating demonstrates antireflecting ability by increasing the transparency slightly due to the lower refractive index of BPPMC comparing to the glass. Antifogging ability was confirmed by hot-vapor and freeze-warm tests on glass slides, eyeglasses, and safety goggles. Additionally, this outstanding antifogging property maintained after treated with household detergent and hand wiping.

Chapter 4 discussed the factors that influence the kinetics of BP containing copolymer, which guide in designing polymer components and monomer selecting. The polarity of polymer would affect the crosslinking rate similar to the polarity of the solvent effect BP derivatives. Additionally, the length of the alkane chain plays an important role in the reaction rate. Initially, the more C-H with the longer alkane chain would improve the reaction rate. However, as the longer alkane chain, the polymer segment movement was restrained, and the crosslink rate reduced. The substituent effect also needs consideration, which the electron withdraw group would increase the rate, and the electron donating group would decrease the rate.

Chapter 5 investigated the mechanisms in BPMPC polymer, including the contact angle increase under UV irradiation and antifouling/antifogging property with such poor hydrophilicity. The crosslinking of BP inside the polymer matrix result into the self-association of the zwitterionic component, which leads to the increase of hydrophobicity of BPMPC coating.

Future Work

The work in this dissertation has provided a few strategies to modify surface with antifouling and antifogging capability rapidly and robustly using BP as photo-cross-linker. The antifouling would be applied to catheters (SNAP) and incubated in small a small animal to examine the protein adhesion and bacterial killing. Other medical device, such as implants, would also be

tested with BPMPC coating. Different coating method might be used to achieve a uniform film on the substrates, as well as solution concentration, coating thickness, UV curing time. The antifogging film would be tested on ski goggles on the field with different altitude, wind speed, temperature. Athletics would wear these ski goggles and provide feedback of the results comparing to commercial antifogging goggles. Also, this antifogging coating would be applied to army used safety glass. Not only excellent antifogging property required, but also no change in mechanical properties, including stiffness, flexibility, and bullet shattering. BP kinetics study should provide a guideline in designing BP containing polymer, more polymer can be tested to examine the validity of the t. Moreover, an equation between the rate constant and structure of the polymer might be concluded with enough data.

Final Marks

The application of BP pendent polymers has been approved expanding to antifouling, antifogging and self-cleaning fields in this study. This “graft to” method provides covalent bonds between functional polymers to organic materials, which can survive in everyday life situation. This might also offer solutions for the challenges that lots of surface immobilized functionalities are facing, especially under conditions under harsh mechanical and chemical environment. All the researches demonstrate the value of commercialization of these materials. The deep investigate into BP pendent polymer provides a guideline in polymer design, which can save lots of material and time. The crosslinking method of BP polymer, UV irradiation, is simple and applicable in many situations, which reduce the. The advantages of easy synthesis, coating, application, facial application, chemical and mechanical robustness indicated huge potential applications in medical device, agriculture, even biology.

Appendix A

NMR SPECTRA OF COMPOUNDS

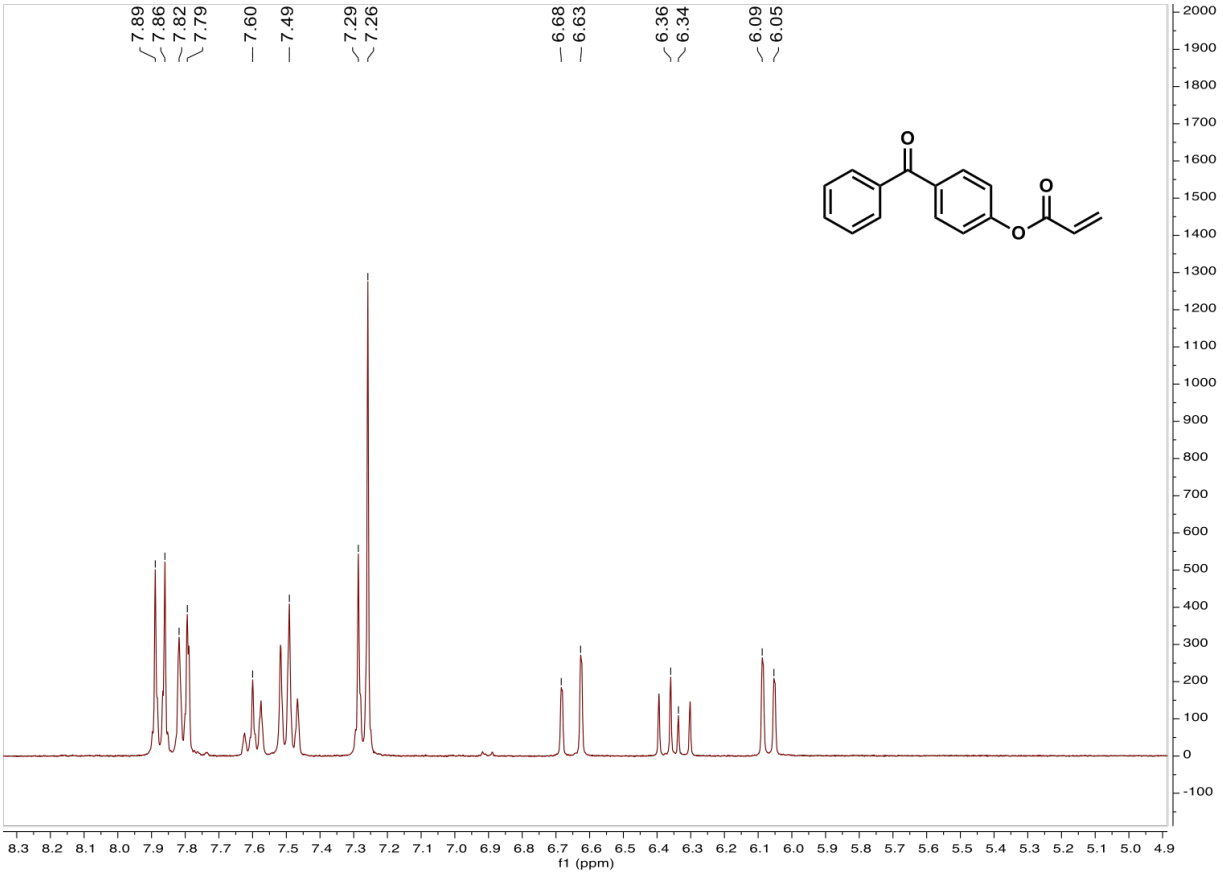

Figure A1: ^{1}H NMR of spectrum of 4-acryloylbenzophenone.

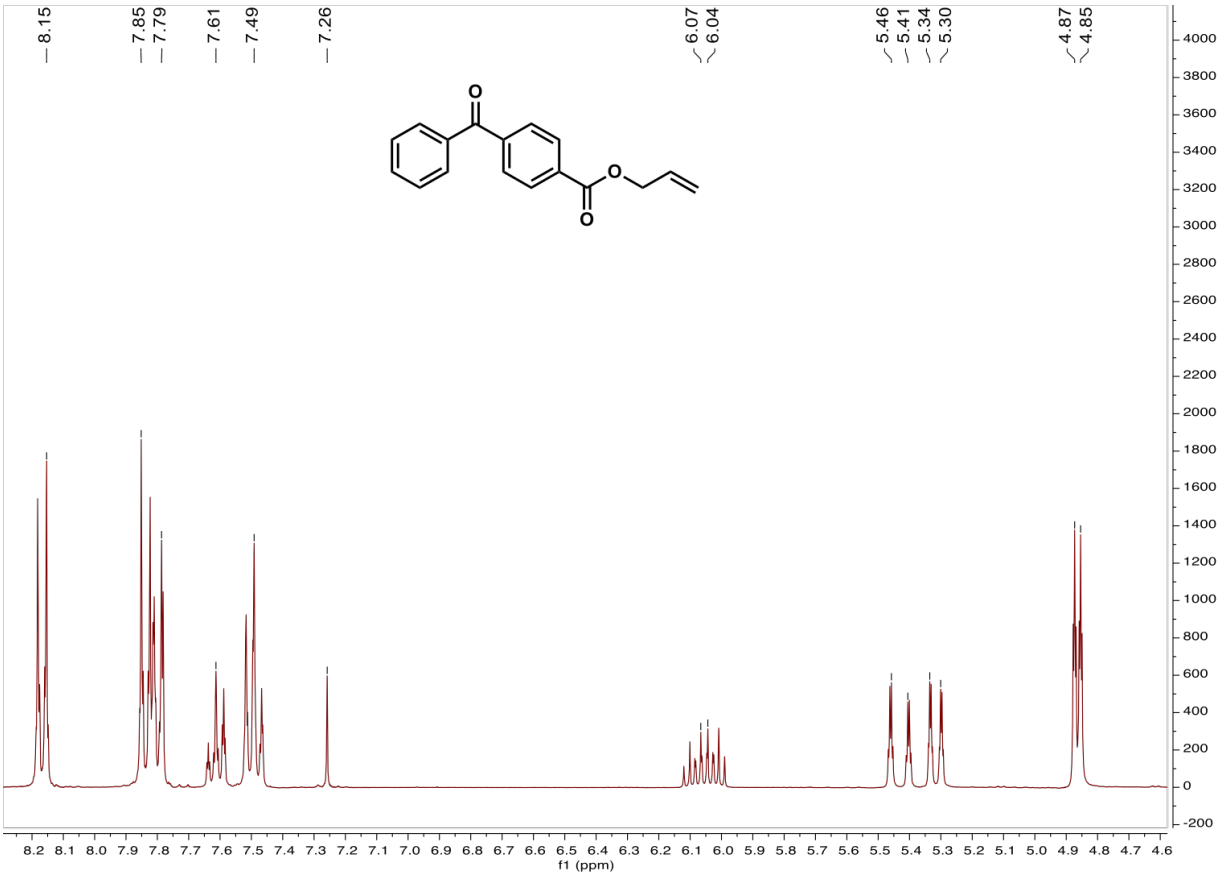

Figure A2. ^{1}H NMR of spectrum of prop-2-enyl 4-benzoylbenzonate

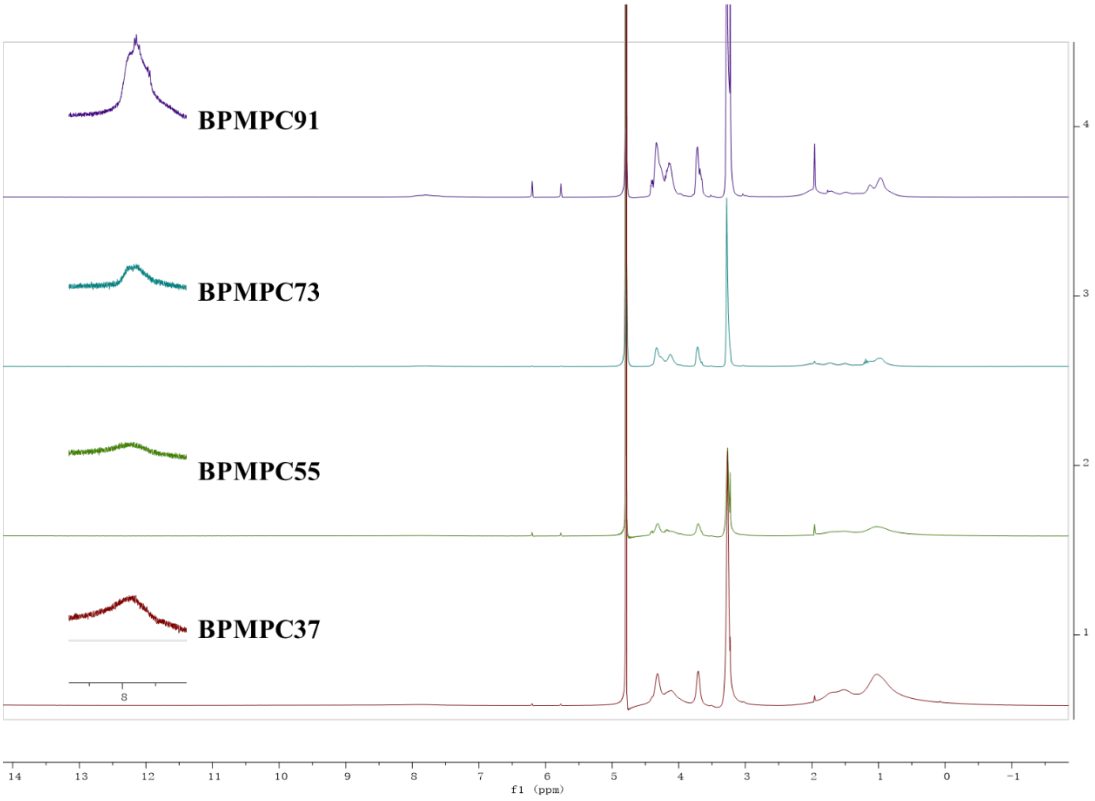

Figure A3. ^{1}H NMR of spectrum of copolymer BPMPC37, BPMPC55, BPMPC71, and BPMPC91 in D_2O (zoom in 7.5-8.5 ppm).

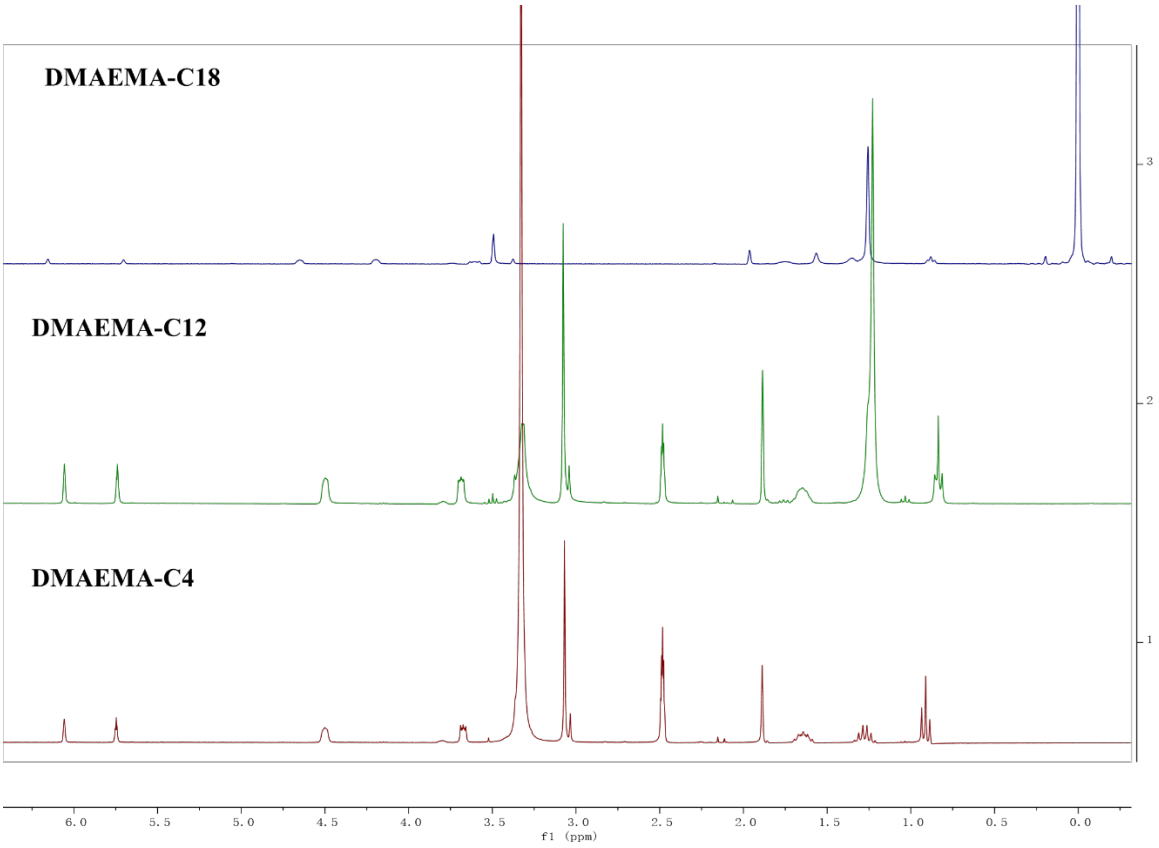

Figure A4. ^{1}H NMR of spectrum of DMAEAM-C4, C12 in DMSO-d6, and DMAEMA-C18 in $CDCl_3$

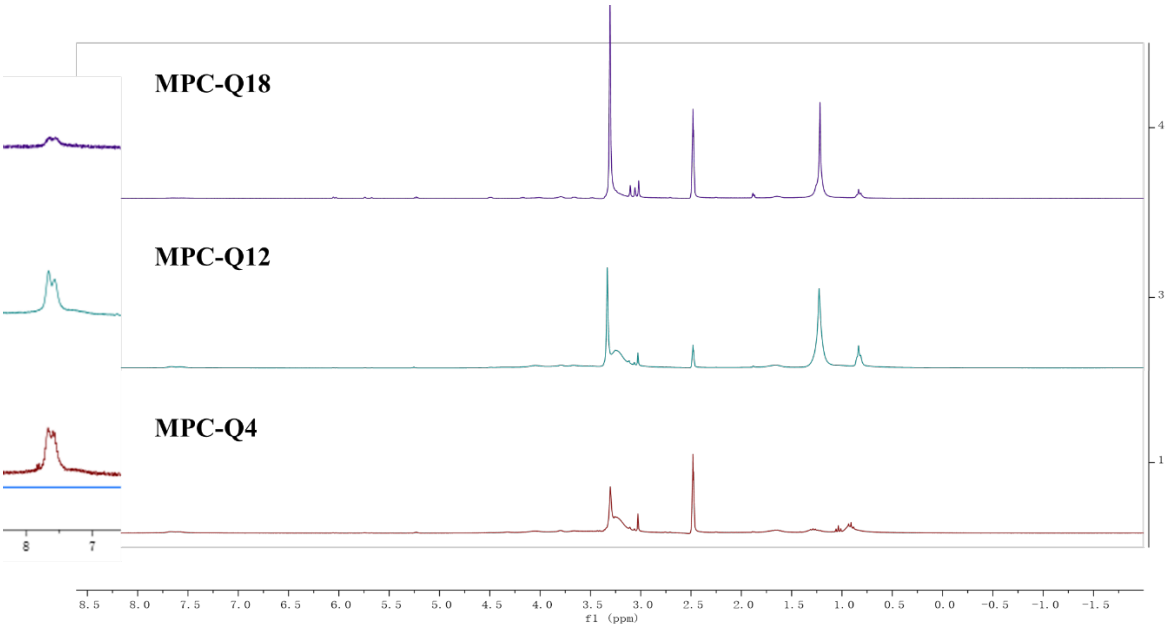

Figure A5. ^{1}H NMR of spectrum of MPC-Q4~18 in DMSO-d6

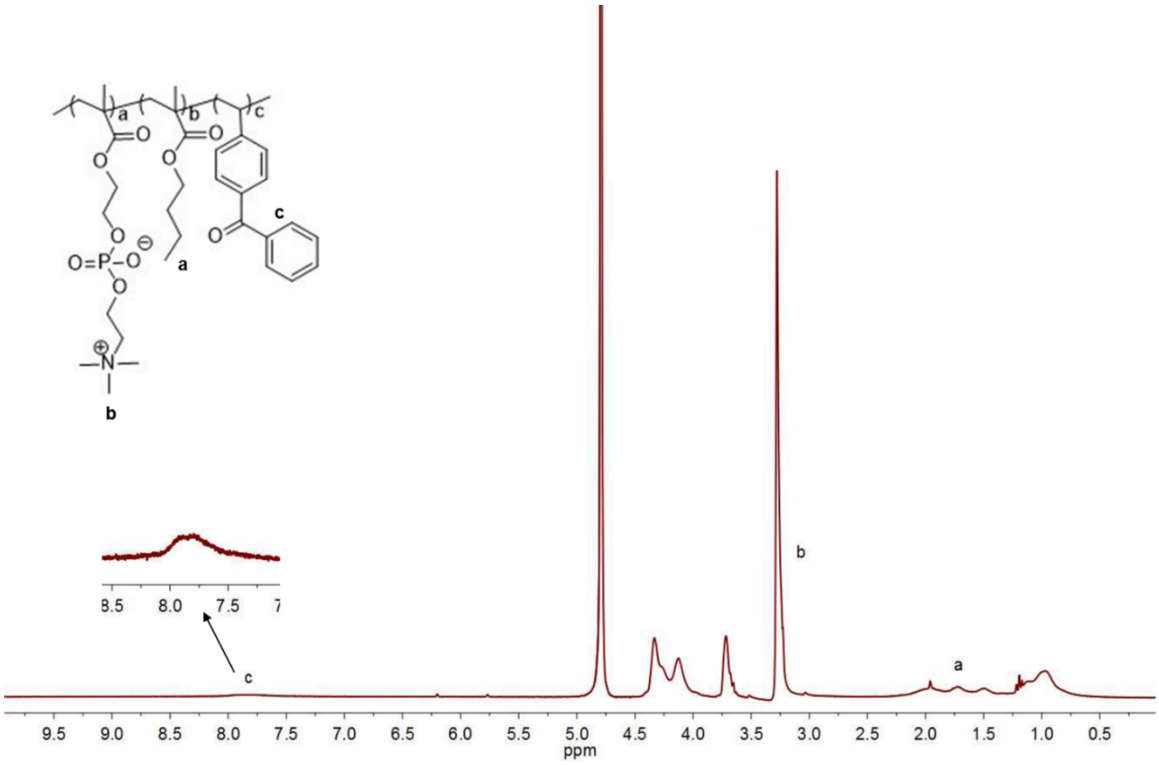

Figure A6. ^{1}H NMR of spectrum of copolymer BPMPC in D_2O

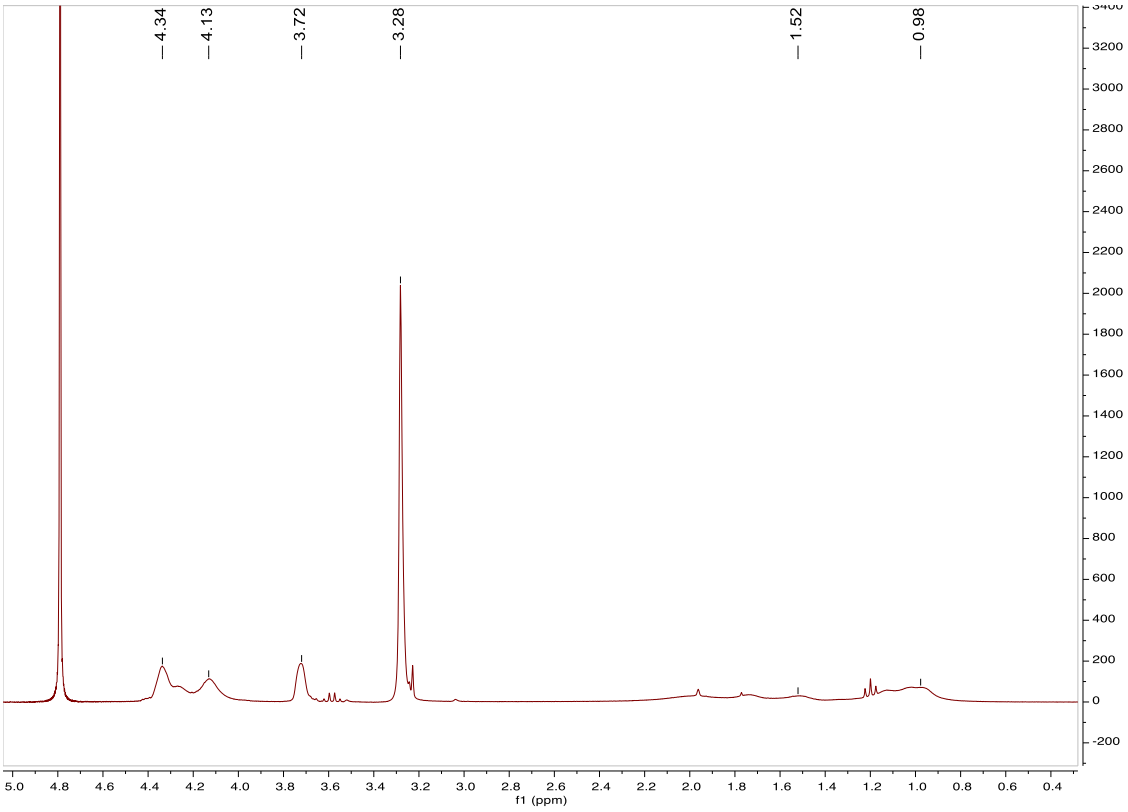

Figure A7. ^{1}H NMR of spectrum of PMPCBMA in D_2O

APPENDIX B

DSC SPECTRA OF COMPOUNDS

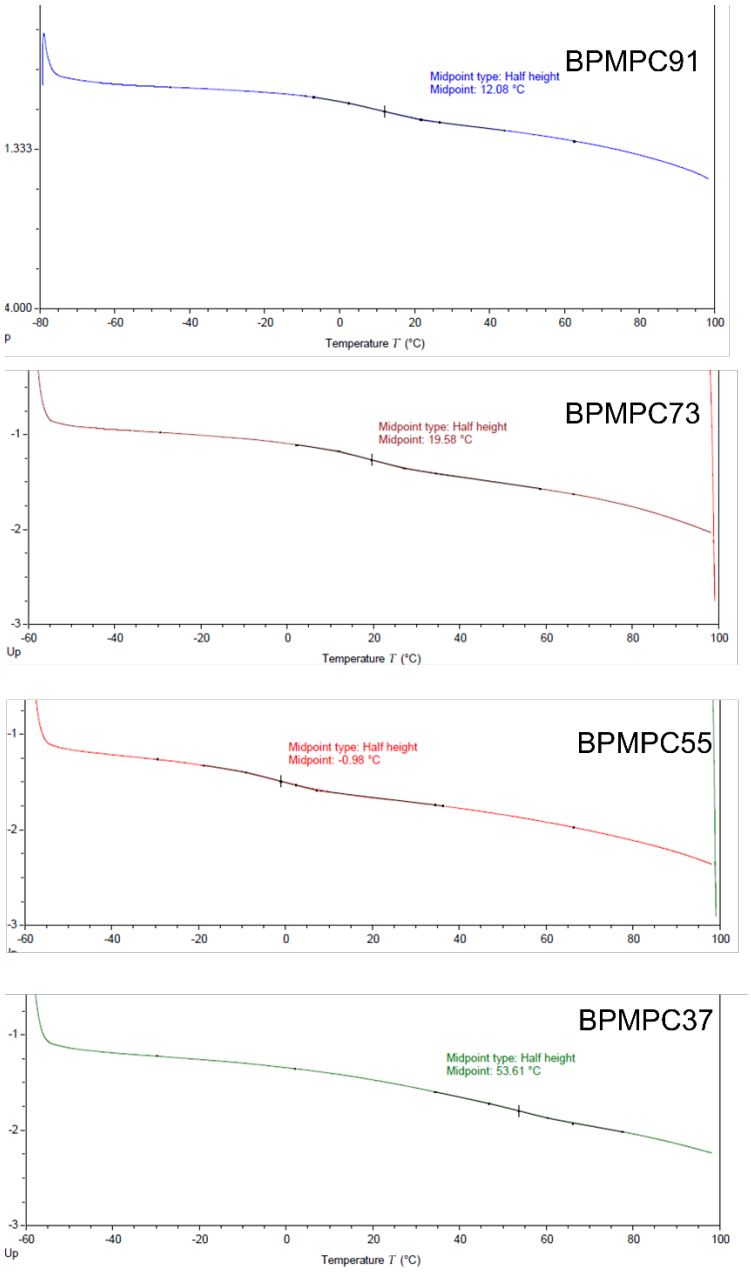

Figure B1. DSC spectra of BPMPC polymer series (-60℃ to 180℃)

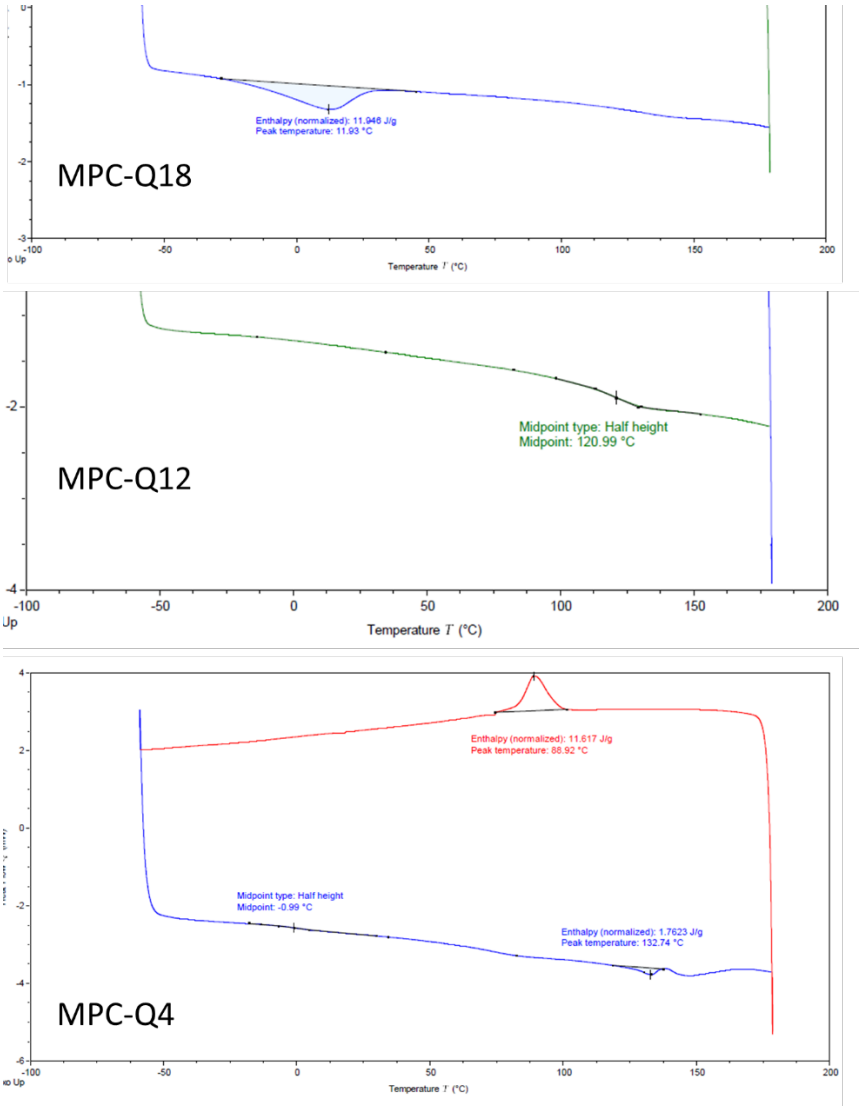

Figure B2. DSC spectra of MPC-Q4~Q12 (-60℃ to 180℃)

APPENDIX C

UV-VIS SPECTRA OF COMPOUNDS

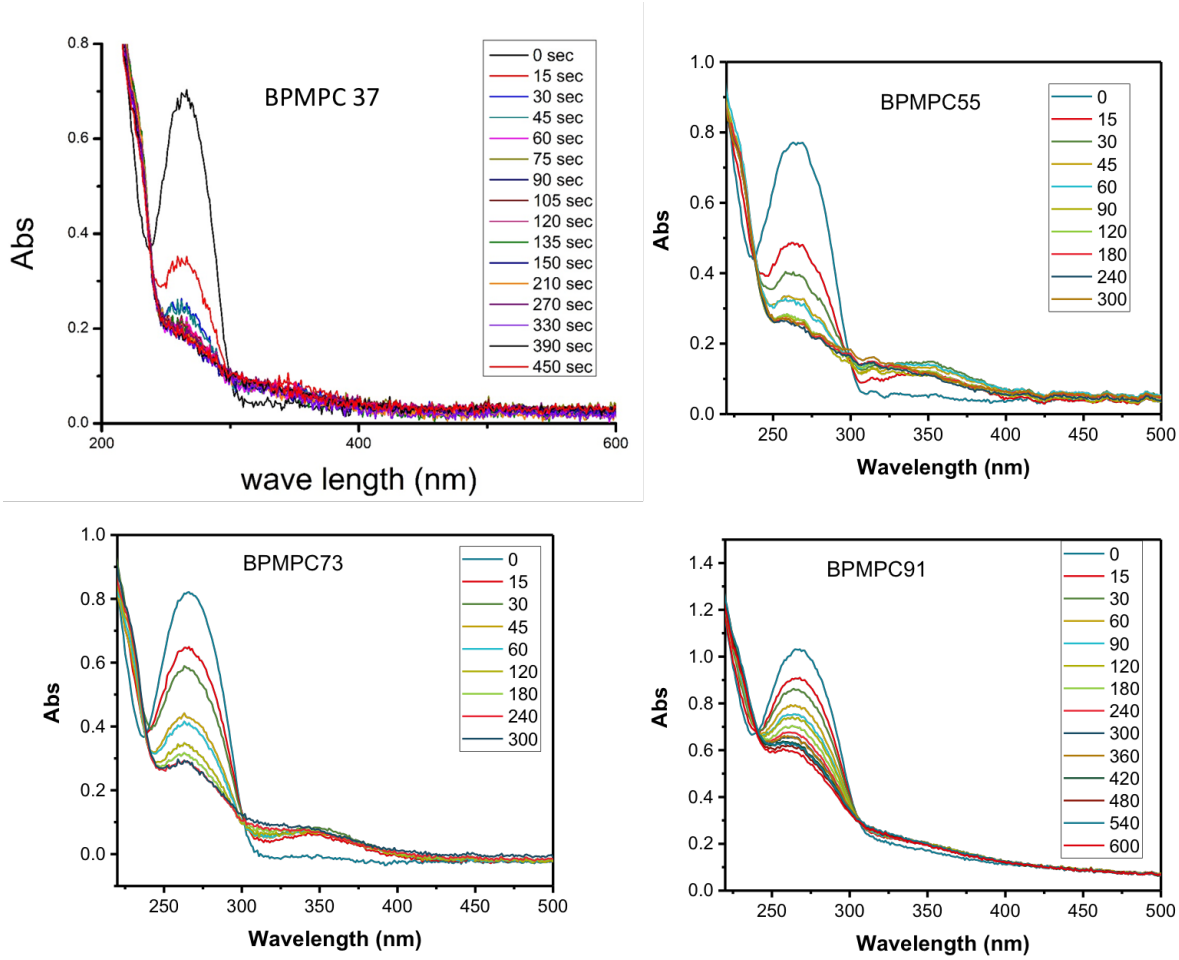

Figure C1: UV-vis spectra of BPMPC37, BPMPC55, BPMPC73, and BPMPC91 (legend units: second).

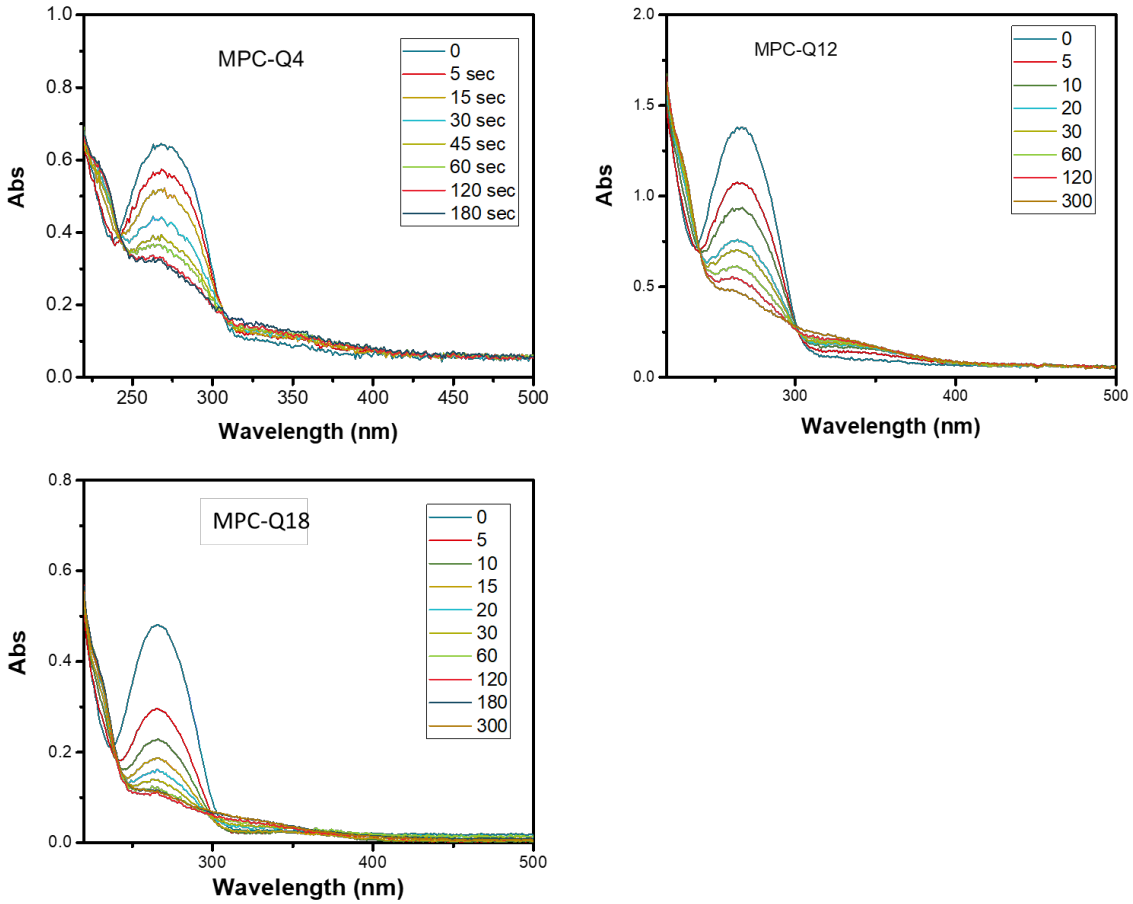

Figure C2: UV-vis spectra of BPMPC37, BPMPC55, BPMPC73, and BPMPC91.

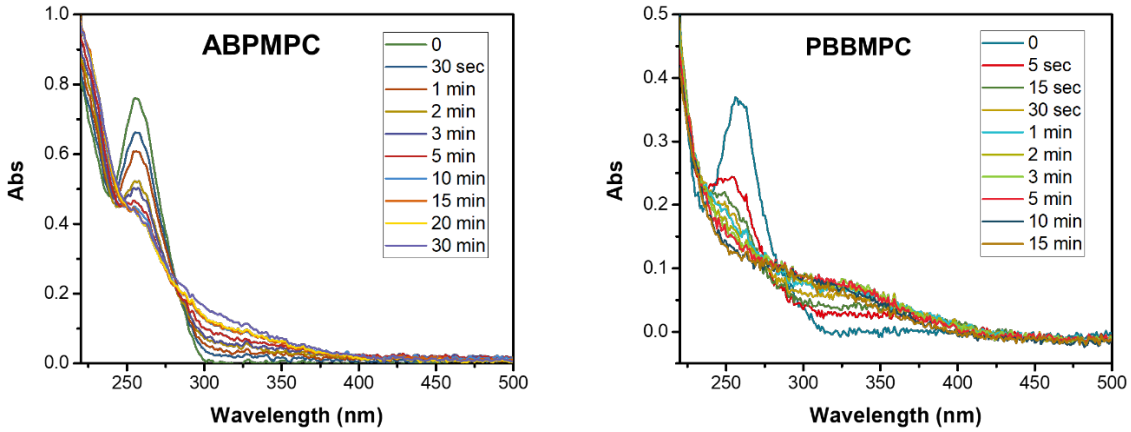

Figure C3. UV-vis spectra of ABPMPC and PBBMPC under 254 nm (6.5 mW cm^{-2}) irradiation.